The role of peripheral Nuclear Pore Complex (NPC) structures in nuclear transport and NPC architecture.

Dissertation

der Fakultät für Biologie der
Ludwig-Maximilians-Universität München

eingereicht am 29. Mai 2002 von

Tobias Christian Walther
aus München

Prüfungskommission:
Prof. Dr. R. Kahmann (Gutachter)
Prof. Dr. Th. Cremer (Gutachter), vertreten durch Prof. Dr. W. Bandlow
Prof. Dr. Ch. David
Prof. Dr. D. Eick (Protokoll)

Tag des Rigorosums: 21. August 2002

Ich versichere, dass ich meine Dissertation mit dem Titel "The role of peripheral Nuclear Pore Complex (NPC) structures in nuclear transport and NPC architecture.", selbständig, ohne unerlaubte Hilfe angefertigt und mich dabei keiner anderen als der von mir ausdrücklich bezeichneten Quellen und Hilfen bedient habe.

Die Dissertation wurde in der jetzigen oder einer ähnlichen Form noch bei keiner anderen Hochschule eingereicht und hat noch keinen sonstigen Prüfungszwecken gedient.

_____   _____
(Ort, Datum)   (Tobias Walther)

"I heard someone who had a book of Anaxagoras, as he said, out of which he read that mind was the disposer and cause of all, and I was quite delighted at the notion of this, which appeared admirable, and I said to myself: If mind is the disposer, mind will dispose all for the best, and put each particular in the best place; and I argued that if anyone desired to find out the cause of the generation or destruction or existence of anything, he must find out what state of being or suffering or doing was best for that thing, and therefore a man had only to consider the best for himself and others, and then he would also know the worse, for that the same science comprised both.(...)

What hopes I had formed, and how grievously was I disappointed! As I proceeded, I found my philosopher altogether forsaking mind or any other principle of order, but having recourse to air, and ether, and water, and other eccentricities.(...)

And I thought that I had better have recourse to ideas, and seek in them the truth of existence."

Platon, Phaedo, 97c/ 98c/100
(Plato, 1899)

Summary

Eukaryotes are characterised by compartmentalisation of the genetic information into the cell nucleus. This requires transport of molecules across the nuclear envelope. All transport is mediated by the nuclear pore complex (NPC). The vertebrate NPC consists of a 125 MDa proteinaceous pore that spans both membranes of the nuclear envelope. In addition to the symmetrical core structure, there are filaments joined to a basket structure on the nuclear side and shorter filaments on the cytoplasmic side of the NPC.

The aim of this thesis was to investigate the function of asymmetric NPC structures and nucleoporins. Nup153 and Nup214/CAN, which were previously mapped to the distal ring and the cytoplasmic filaments of the NPC, respectively, were localised close to the central NPC channel by electron microscopy. Nup358/RanBP2 was mapped to the cytoplasmic filaments. In a nuclear reconstitution assay derived from *Xenopus* egg extracts, Nup153 was required for assembly of a complete nuclear basket. In the absence of Nup153, NPCs were mobile in the nuclear membrane, which led to a clustering of the NPCs. Nup153 deficient nuclei had a defect in "classical" NLS-, but not in M9-mediated nuclear protein import. This is most likely due to less efficient cargo accumulation in the nucleus. Depletion of Nup358/RanBP2 resulted in a lack of cytoplasmic NPC filaments. This, however, had no effect on the import of either "classical" NLS or M9 containing proteins. In addition, Nup214/CAN was still present at the rim of the Nup358/RanBP2 depleted nuclei, further suggesting that it is not part of the cytoplasmic filaments. The removal of Nup214/CAN only mildly affected nuclear protein import. Nuclei that lack both Nup214/CAN and Nup358/RanBP2 import cargoes only slightly less efficient than control nuclei. Since replication is still occurring in these nuclei they are able to accumulate all necessary replication factors.

Taken together the experiments show, that the peripheral structures of the NPC are not required for its assembly. As a model for translocation through the NPC, it is suggested that import complexes move through the NPC along low affinity hydrophobic interactions. Stable interactions of import complexes with asymmetrically localised nucleoporins serve to increase their resident time in an environment of high RanGTP concentration and to therefore to facilitate their disassembly by RanGTP.

Abbreviations

ATP Adenosine-triphosphate
ATPγS Adenosine 5'-[γ-thio]triphosphate
BAF barrier-to-autointegration protein
BSA bovine serum albumin
CBC 5' mRNA cap binding complex
CDC cell devision cycle
C. elegans *Caenorhabditis elegans*
CTE constitutive transport element
DAPI 4',6-diamidino-2-phenyindole
D. melanogaster *Drosophila melanogaster*
DNA deoxyribonucleic acid
dUTP deoxy Uridine-triphosphate
E. coli *Escherichia coli*
ER endoplasmic reticulum
FEISEM field emission in-lens SEM
FRAP fluorescence recovery after photobleaching
GAP GTPase activating protein
GFP green fluorescent protein
GST Glutathione-S-transferase
GTP Guanosine-triphosphate
GTPγS Guanosine 5'-[γ-thio]triphosphate
HEAT repeat motif, shared by huntingtin, elongation factor 3, the PP65/A subunit of protein phosphatase 2A and the target of rapamycin (TOR) kinase
hnRNP heterogenous nuclear RNPs
hNup153 human Nup153 protein
HP1 heterochromatin protein 1
IBB importin β binding domain
IPTG isopropyl-β-D-thiogalactopyranoside
LBR lamin B receptor
LEM domain shared by Lap2, Emerin and Man1

mAb monoclonal antibody
NES nuclear export signal
NLS nuclear localisation signal
NPC nuclear pore complex
OD optical density
PAGE polyacrylamid gel electrophoresis
PCR polymerase chain reaction
PHAX phosphorylated adaptor of U snRNA export
PMSG pregnant mare's serum gonadotropin
U snRNA small nuclear uridine rich RNA
Ran Ras-like nuclear GTPase
RanBP Ran binding protein
Ras Rous sarcoma virus cellular oncogene
RBD Ran binding domain
RCC1 regulator of chromatin condensation
RNA ribonucleic acid
RNAi RNA interference
RNP ribonucleoprotein particles
RT-PCR reverse transcription polymerase chain reaction
RUSH RING finger motifs that bind to the uteroglobin promoter
S. cerevisiae *Saccharomyces cerevisiae*
SEM scanning electron microscopy
TEM transmission electron microscopy
TPR translocated promoter region protein
tRNA transfer RNA
U snRNA Uridine rich small nuclear RNA
WGA wheat germ agglutinin
Xenopus/X. laevis *Xenopus laevis*

TABLE OF CONTENTS

1 Introduction

1.1 The cell nucleus

The hallmark of Eukaryotes is the compartmentalisation of the genetic information in the cell nucleus.

The nucleus is surrounded by a double membrane, called the nuclear envelope. The outer nuclear membrane is continuous with and biochemically identical to the endoplasmic reticulum (ER) (Franke, 1974) (see figure 1 for an overview). The inner nuclear membrane, in contrast, contains a unique set of integral membrane proteins that are specific to the nuclear envelope. These proteins provide contact with the nuclear lamina, a network of intermediate type filaments that is thought to provide mechanical stability to the nucleus and might also be involved in the organisation of chromatin.

Figure 1: Schematic overview of the eukaryotic cell nucleus. The Nuclear envelope, the NPC, the nucleolus and different regions are marked with red boxes (modified from Alberts et al., 1994)
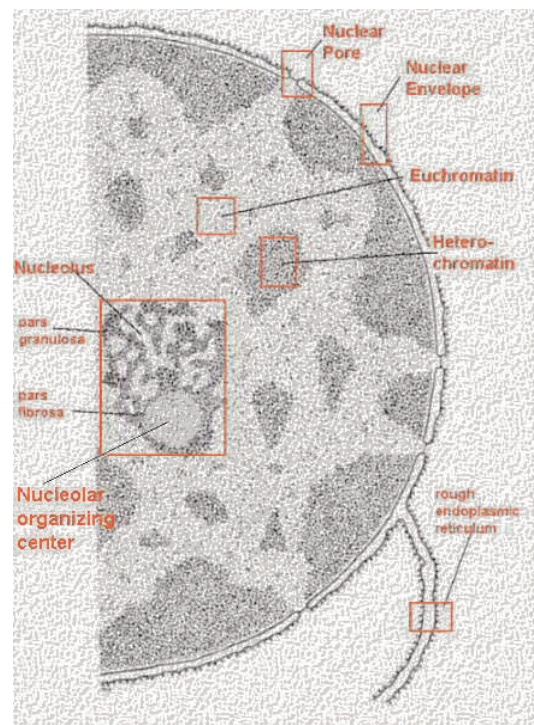
The DNA is packaged into the nucleus in the form of chromatin and recent findings show that chromosomes are stably maintained in distinct chromosome territories (Cremer and Cremer, 2001). Localisation of chromosomes in territories with respect to the nuclear envelope has been linked to the transcriptional activity of genes. Inactive genes usually are packaged in hetereochromatin, which tends to localise to the nuclear periphery,

whereas transcriptionally active genes are more often localised at the nuclear interior on the boundaries of chromosome territories (Kurz et al., 1996; for review see Cremer and Cremer, 2001). Inside the nucleus, several compartments have been implicated in specific functions of gene expression (Dundr and Misteli, 2001). The most prominent structure is the nucleolus, which is the site of ribosomal RNA transcription and ribosomal subunit assembly. The nucleolus is formed around the rRNA genes and can be divided into the fibrillar centre, the dense fibrillar compartment and the granular component. Its structural integrity is dependent on ongoing transcription of the rRNA genes (Carmo-Fonseca et al., 2000). Another example of a subnuclear compartment are the "speckles",which are thought to be directly or indirectly involved in RNA processing since SR proteins, known to be involved in pre-mRNA splicing, are highly concentrated there. Besides these, the Cajal bodies (alternatively named coiled bodies) have been shown to contain factors required for U snRNP assembly and PML bodies are enriched in transcription factors (Gall, 2000). Whether these structures assemble dynamically around sites of their proposed activity (gene expression, splicing and assembly of complexes) or whether they are permanent storage structures is still a matter of debate.

The nuclear envelope functionally separates replication, transcription and RNA processing from cytoplasmic processes such as translation and intermediary metabolism. Factors involved in nuclear processes are concentrated in the nucleus. A high concentration of the involved proteins has been shown to be crucial, for example for DNA replication (Walter et al., 1998). Compared to prokaryotes (where factors are distributed throughout the entire cell), compartmentalisation provides a plethora of possibilities for the regulation of gene expression. A variety of signalling pathways use translocation across the nuclear envelope as a key step in gene activation. The regulation of the cell cycle critically relies on the partitioning of cyclin/kinase complexes form their substrates during interphase (Yang and Kornbluth, 1999).

However, the separation of the instructive genetic information from the site of its realisation by the translation machinery necessitates an enormous capacity for regulated transport across the nuclear envelope. All this transport occurs through large macromolecular assemblies, the nuclear pore complexes (NPCs), which span both of the nuclear envelope membranes.

1.2   The structure of the nuclear envelope

Seen from the cytoplasmic side, the nuclear envelope differs from the ER only by the presence of the NPCs. The inner nuclear membrane, however, is distinguished by the presence of unique transmembrane proteins (Holmer and Worman, 2001). These proteins are generally thought to provide a connection between the nuclear envelope and either chromatin or the nuclear lamina or both. The lamin B receptor (LBR) for example, is an eight trans-membrane domain containing protein that interacts with lamins of the B-type to provide a link of the intermediate filament network with the inner nuclear envelope (Worman et al., 1988). In addition, LBR binds to heterochromatin protein 1 (HP1) and could help to organise heterochromatin to peripheral localisations in the cell nucleus via this interaction (Ye and Worman, 1996). Proteins that contain the so-called LEM domain (shared between <u>L</u>ap2, <u>E</u>merin and <u>M</u>an1) bind to the chromatin protein BAF (<u>b</u>arrier-to-<u>a</u>utointegration <u>f</u>actor) (Cai et al., 2001a; Lee et al., 2001; Shumaker et al., 2001). Examples of this class of proteins are Emerin, a protein, which has been implicated in the Emery-Dreyfuss muscular dystrophy, Man1 and the class of LAP2 proteins. LAP2β binds also to the chromosomal protein HA95 that has homology to the nuclear A-kinase anchoring protein (for review see Holmer and Worman, 2001). Together, this class of proteins could be involved in higher order chromatin organisation. Recently, Mansharamani and colleagues described a protein of the inner nuclear membrane that showed nine membrane spanning segments and an ATPase motif (Mansharamani et al., 2001). It was further demonstrated that this protein interacts with the RUSH complex, a chromatin remodelling complex of the SWI/SNF family and might therefore be a good candidate for an organiser of chromatin remodelling in the nuclear periphery.

1.3   Dynamics of the nuclear envelope during mitosis

As a prelude to the distribution of the genetic material to the two daughter cells during mitosis, the nuclear envelope breaks down in higher Eukaryotes. In a first step during prometaphase, the nuclear lamina is disassembled, a process that is thought to be mediated by the cdc2/cyclinB complex (Gerace and Blobel, 1980; Ottaviano and Gerace, 1985). At this point, the NPCs are also disassembled (see below) and therefore the

permeability barrier of the NE is lost. It has been demonstrated by transfection of GFP-tagged versions of proteins of the inner nuclear envelope, that these proteins are redistributed throughout the ER during mitosis, indicative of an absorption of the nuclear envelope into the ER (Ellenberg et al., 1997; Yang et al., 1997a). At the end of mitosis, when the nuclear envelope is being reassembled, the proteins of the inner nuclear envelope are concentrated on the surface of chromatin, possibly via their interaction with chromatin bound factors.

During all stages of the cell cycle the identity of the nuclear compartment is specified by the small GTPase Ran (Ras-like nuclear GTPase) (Clarke and Zhang, 2001; Kuersten et al., 2001). This GTPase belongs to the Ras-superfamily of GTPases and can occur in two states in the cell, bound to GTP or GDP. Due to the low intrinsic hydrolysis rate of the protein and the low dissociation constant of either GDP or GTP from Ran, both states are stable in the cell. When aided by the only known nucleotide exchange factor RCC1, however, the nucleotide is dissociated, allowing rebinding of Ran to GTP, which is more abundant in the cell (Bischoff and Ponstingl, 1991). Since a fraction of RCC1 is bound to chromatin during the whole cell cycle the concentration of RanGTP is high around the chromatin at all times (Ohtsubo et al., 1989; Hetzer et al., 2000; Kalab et al., 2002;). This situation is pronounced in interphase where the nuclear compartment is enclosed by the nuclear membrane. In the cytoplasm, the GTP on Ran is hydrolysed by the combined action of the Ran GTPase activating protein, RanGAP, and the assisting proteins RanBP1 and RanBP2, and therefore the level of RanGTP is low (Becker et al., 1995; Bischoff et al., 1994; Bischoff et al., 1995). The GTP bound form is the active form of Ran in all processes that have been characterised to be dependent on Ran so far. During interphase, it regulates nucleocytoplasmic transport (see below; Görlich and Kutay, 1999; Mattaj and Englmeier, 1998), during mitosis it mediates the chromatin effect on the mitotic spindle and the reformation of the nuclear envelope at the end of mitosis. For spindle formation it has been demonstrated that RanGTP acts by releasing a microtubule nucleating activity, the Tpx2 protein. This protein is inactive when bound to importin α and β and Ran releases it from this inhibition (Gruss et al., 2001). In addition, it is known from *in vitro* experiments that Ran is crucial for the organisation of the spindle and maturation of the

centrosomes, but target proteins for these functions remain to be identified (Carazo-Salas et al., 2001; Wilde et al., 2001).

Similarly, no targets for Ran during the reassembly of the nuclear envelope after mitosis are known yet. As far as the mechanism of assembly of the nuclear membranes is concerned, it is only known that the Ran system is required for fusion of the nuclear membrane and that, in addition, the AAA-ATPase p97 is also necessary for this process (Hetzer et al., 2000; Zhang and Clarke, 2000; Hetzer et al., 2001; Zhang and Clarke, 2001). This ATPase has been shown to act in a variety of processes (Patel and Latterich, 1998) and acts in nuclear membrane fusion together with its specific adapter complexes consisting of the proteins Ufd1/Npl4 for the initial fusion events and the p47 protein for the subsequent fusions resulting in nuclear growth (Hetzer et al., 2001).

1.4   <u>Nucleocytoplasmic transport - the soluble phase</u>

During interphase, the Ran system determines the identity of the nucleus by regulating nucleocytoplasmic transport of molecules. There are several classes of pathways of nucleocytoplasmic transport that can be distinguished by the factors they require. A first class is characterised by the requirement of proteins of the family of importin β like transport receptors for cargo transport. A second class are proteins whose import is apparently independent of the Ran system, such as the U1A protein, and export of cellular mRNAs can be distinguished as a third class.

1.4.1   <u>Protein and RNA transport mediated by transport receptors of the importin β family</u>

Importin β-like transport receptors mediate both the import and the export of proteins (see figure 2 for an overview). For both cases, the pathways are signal-dependent and receptor-mediated. The M9 nuclear localisation sequence, that was first identified in hnRNPA1, for example is directly bound by transportin in the cytoplasm, then the complex translocates through the NPC. Subsequently, in the nucleus, transportin binds to RanGTP and thereby the cargo molecule is released (Pollard et al., 1996). There are several modifications to this basic principle. Importin β itself uses at least two classes of

adaptors, importin α and Snurportin 1, via which it binds its cargos. In this pathway, the so called "classical" basic nuclear localisation signal (NLS) is bound by importin α, which in turn is bound by importin β via its conserved importin β binding domain (IBB). Again this complex is translocated through the NPC and disassembled on the nuclear side by binding of RanGTP (reviewed in Mattaj and Englmeier, 1998). In vertebrates, there are several importin α proteins, thereby increasing the spectrum of substrate specificity for the importin β pathway. The other adaptor, Snurportin 1, binds to the tri-methylated cap-structure of mature U snRNPs and thereby mediates re-import of this class of RNPs into the nucleus, together with the Sm-core protein complex (Huber et al., 1998; Huber et al., 2002).
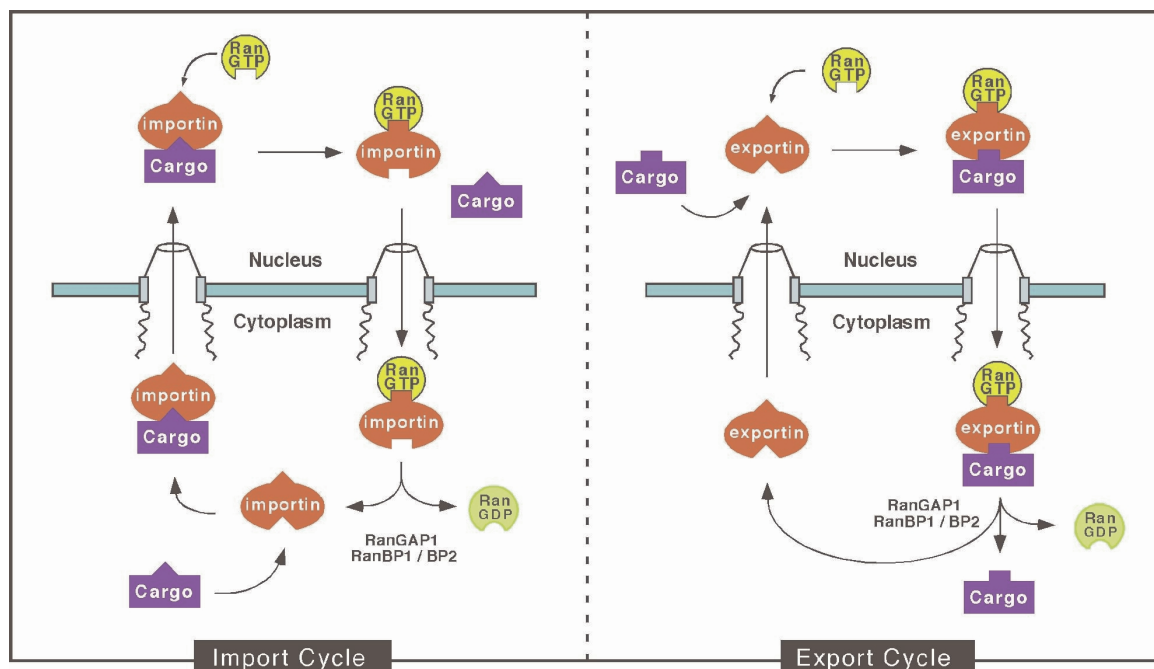
Figure2: Schematic overview of nuclear import and export mediated by the receptors of the importin β family.

Not only protein and RNA import can be mediated by importin β-like transport receptors, but also export of both classes of molecules. Conversely to the situation in protein import, exportin-1, also called Crm1, binds to its cargo, leucine rich nuclear export signal (NES) containing proteins, together with RanGTP in the nucleus. After translocation of this export complex to the cytoplasm, the GTP on Ran is hydrolysed with the help of

RanGAP and RanBP1 or 2 and the complex disassembles, thereby releasing the cargo (Fornerod et al., 1997a). The receptors can be recycled into the nucleus thereafter. Since nuclear export leads to a net flux of Ran out of the nucleus, a transport receptor for RanGDP, called NTF2, completes the cycle by taking Ran back to the nucleus (Ribbeck et al., 1998).

Examples for export of RNA from the nucleus by members of the importin β family are export of tRNA and nascent U snRNAs. tRNAs are exported by a rather simple mechanism in which the RNA is directly recognised by its receptor, exportin-t, and is then exported as a trimeric complex with RanGTP (Arts et al., 1998a; Arts et al., 1998b; Kutay et al., 1998). U snRNAs, however, follow a more complex pathway utilising an adaptor molecule, PHAX, which bridges the interaction of exportin-1 with CBC and the 5' cap structure of the RNA. In addition, the assembly and disassembly of the resulting hexameric complex with Ran is regulated by phosphorylation of PHAX in the nucleus. Dephosphorylation of PHAX destabilises the complex after it arrives in the cytoplasm and together with GTP hydrolysis on Ran mediates cargo release (Ohno et al., 2000). The probably most complex RNP that is exported from the nucleus, the 60S subunit of the ribosome may also use exportin-1. This process has been studied most extensively in yeast, where genetic screens have identified conditional mutants that accumulate precursors of ribosomal subunits in the nucleus. One of the mutants obtained was an allele of a Rpl10, a gene encoding a protein of the large ribosomal subunit. This has in turn been shown to bind to Nmd3p, which in this cases serves as an adaptor to exportin-1, which is proposed to mediate the export of the 60S particle (for review see Aitchison and Rout, 2000).

These last examples illustrates the wide variety and diversity of cargos that can be recognised and transported via the importin β family members of receptors. The receptors themselves can also act in multiple ways and fulfil several functions. Two examples are Msn5p, a receptor that works bidirectionally and mediates import and export of different cargoes (Kaffman et al., 1998; Yoshida and Blobel, 2001) and the function of importin β and importin α, the receptors for basic NLSs, during mitosis (Gruss et al., 2001; Nachury et al., 2001).

In recent years, structural analyses of the components of the Ran system has greatly advanced our understanding of the mechanisms of nucleocytoplasmic transport. Several structures of importin β family members have been obtained by X-ray diffraction of crystals and showed that the proteins have a repeat structure consisting of 19 HEAT repeats, each motif of 40 amino acids being structured as a hairpin motif made up from two helices connected by a sharp turn motif (Chook and Blobel, 1999; Cingolani et al., 1999; Vetter et al., 1999a). These repeats are structurally similar to the armadillo repeats found in the importin α adaptor and they can be overlaid, which suggests an evolutionary relationship between the two proteins (Conti et al., 1998). The overall structure of importin β is like a corkscrew. The protein can be divided into a N-terminal and a C-terminal half, which adopt similar tertiary structures. The C-terminus of importin β wraps around the acidic IBB domain of importin α and makes intimate contacts, burying 42% of the IBB solvent accessible surface. The N-terminus of importin β contacts RanGTP. Extrapolating from the structures of transportin bound to RanGTP, the N-terminal half of importin β bound to RanGTP and importin β to IBB, it can be predicted that RanGTP displaces the acidic loop and thereby mediates cargo release. The mechanism of GTP/GDP exchange and hydrolysis has also been investigated by structure determination of complexes. Several structures of RCC1 with or without Ran have shown that the reaction mechanism of exchange occurs via a displacement of the P loop of Ran, which contributes a major part of the binding energy for the nucleotide (Renault et al., 2001; Renault et al., 1998). Recently, a complex between a RanBP domain, RanGAP and Ran has been solved. Like the previously reported structure of RanGTP and RanBP, this structure shows that RanBP1 helps hydrolysis by displacing a C-terminal extension and an acidic helix, which otherwise folds back onto the surface of Ran. Removing this helix allows for RanGAP binding. Unlike the GAPs of other GTPases, RanGAP does not provide an arginine residue ("arginine-finger") to the catalytic centre, but seems to facilitate hydrolysis solely by stabilising the RanGTPase in an active conformation (Vetter et al., 1999b; Seewald et al., 2002).

1.4.2 <u>Unconventional protein import pathways</u>

A second class of proteins, which apparently does not require the Ran system, seems to be much smaller and the mechanism of their transport has not been characterised to the molecular detail. Representatives of this class of proteins include the U1A protein, which is incorporated into the U1 snRNP, U2B", which is part of the mature U2 snRNP and the hnRNP K protein, which possesses a KNS motif that confers shuttling of the protein between the nucleus and the cytoplasm. These proteins might either directly access the NPC without a receptor and therefore be able to translocate or use so far unknown receptors (Hetzer and Mattaj, 2000; Michael et al., 1997). Neither the mechanism of this translocation nor of the accumulation of this class of proteins in the nucleus or its energy requirement are understood so far. Yet another pathway is examplified by the Vpr protein that is encoded by the human immunodeficiency virus 1 (Jenkins et al., 1998). However, this protein has been demonstrated to rupture the nuclear envelope and therefore probably does not represent a physiologically relevant transport pathway (de Noronha et al., 2001).

1.4.3 <u>mRNA export</u>

The transport pathway of the third class of cargos, messenger RNAs (mRNAs), is mediated by a distinct set of proteins and seems not to directly require the Ran system. Although there has been huge progress in the understanding of the mechanism of mRNA transport in the recent years, many of the molecular details of this process remain to be clarified. mRNAs are the most diverse set of cargos, varying in composition, length and abundance and are exported from the nucleus as complexes with proteins, hnRNPs (Cole, 2000; Conti and Izaurralde, 2001; Reed and Magni, 2001). In the past, several laboratories have conducted successful genetic screens in the yeast *Saccharomyces cerevisiae* to identify mutants that accumulate polyA+ RNA in the nucleus. An additional line of research used the giant oocytes of the African clawed frog, *Xenopus laevis*, which allow injection of radiolabelled RNAs or proteins in either the nucleus or the cytoplasm. After an incubation period, the transport of molecules between the two compartments can be analysed by dissecting the oocyte manually and determination of the amount of radiolabelled molecules that were redistributed. This was used for example to characterise the different pathways of RNA from the nucleus (Jarmolowski et al., 1994).

From studies on NMD (nonsense mediated decay), a model emerged in which the processing of hnRNA to mRNA, in particular splicing, leaves a mark on the RNA that targets it for nuclear export (for review see Schell et al., 2002). Alternatively and not mutually exclusively, unspliced RNAs could be actively retained in the nucleus. Recently, a complex of proteins has been described that could serve as such a mark that targets mRNA for export. It is deposited roughly 24 nucleotides upstream of the exon-exon junction (Le Hir et al., 2000; Le Hir et al., 2001). Furthermore, it was shown that a RNA-helicase, UAP65, is required to load the Ref/ALY protein onto RNA and that this in turn leads to the recruitment of the mRNA export factor TAP (Luo et al., 2001; Strasser and Hurt, 2001; Reed and Hurt, 2002). Together with its binding partner p15, TAP has been shown to interact with some proteins of the NPC and is therefore thought to play a key role in translocation (Bachi et al., 2000). The simian retrovirus type D utilises TAP for exporting its pre-spliced genomic RNA. In the normal cellular context, an unspliced mRNA would not be exported from the nucleus. This virus, however, contains a sequence, the constitutive transport element (CTE) that binds to TAP directly and thereby mediates the export of unspliced RNA. In competition experiments in *Xenopus* oocytes, the CTE sequence was able to compete for the export of a mRNA injected into the nucleus, indicating that TAP is part of the cellular mRNA export pathway (Saavedra et al., 1997; Gruter et al., 1998). This machinery has also, at least in part, been conserved throughout evolution, since the yeast homologue of TAP, Mex67p has been demonstrated to play a role in mRNA export (Segref et al., 1997). Whereas for TAP the function in mRNA export is becoming more clear, the role of other factors that have been implicated in this process is not understood. Both yeast screens and biochemical interaction analyses have implicated RAE1/yGle2 in mRNA export, but what exactly the involvement is remains elusive (see for example Pritchard et al., 1999). The same is true for Dbp5, a DEAD-box helicase, that is bound to the NPC on its cytoplasmic side (Snay-Hodge et al., 1998; Tseng et al., 1998; Schmitt et al., 1999). In addition, the role of several shuttling hnRNP proteins is not clear, neither is the role of hnRNP proteins that remain in the nucleus. This latter group could mediate retention of incompletely processed RNAs (for review see Mattaj and Englmeier, 1998).

1.5   <u>The Nuclear Pore Complex (NPC)</u>

All transport into and out of the nucleus occurs through the nuclear pore complex (NPC). This macromolecular assembly of 125 MDa in vertebrates and 65 MDa in yeast mediates the enormous flow of molecules between the nucleus and cytoplasm in a selective, bi-directional, diverse and high throughput manner. From real-time measurements of flux into the nucleus in a permeabilised cell system it has been estimated that a single NPC can translocate roughly 500 receptor/cargo complexes per second (Ribbeck and Görlich, 2001).

1.5.1   <u>Structure and composition of the NPC</u>

Ultrastructural analyses of the NPC using transmission electron (Akey, 1989; Akey and Radermacher, 1993; Hinshaw, 1994; Yang et al., 1998), scanning electron (Jarnik and Aebi, 1991; Ris, 1991; Goldberg and Allen, 1993; Ris and Malecki, 1993; Goldberg and Allen, 1996; Ris, 1997) and atomic force (Rakowska et al., 1998; Stoffler et al., 1999b) microscopy has shown the vertebrate NPC to be a ~65 nm deep, 8-fold symmetrical, plugged channel, decorated on each side with eight filaments attached to a coaxial ring that project away from the nuclear envelope (see figure 3 for a schematic overview).
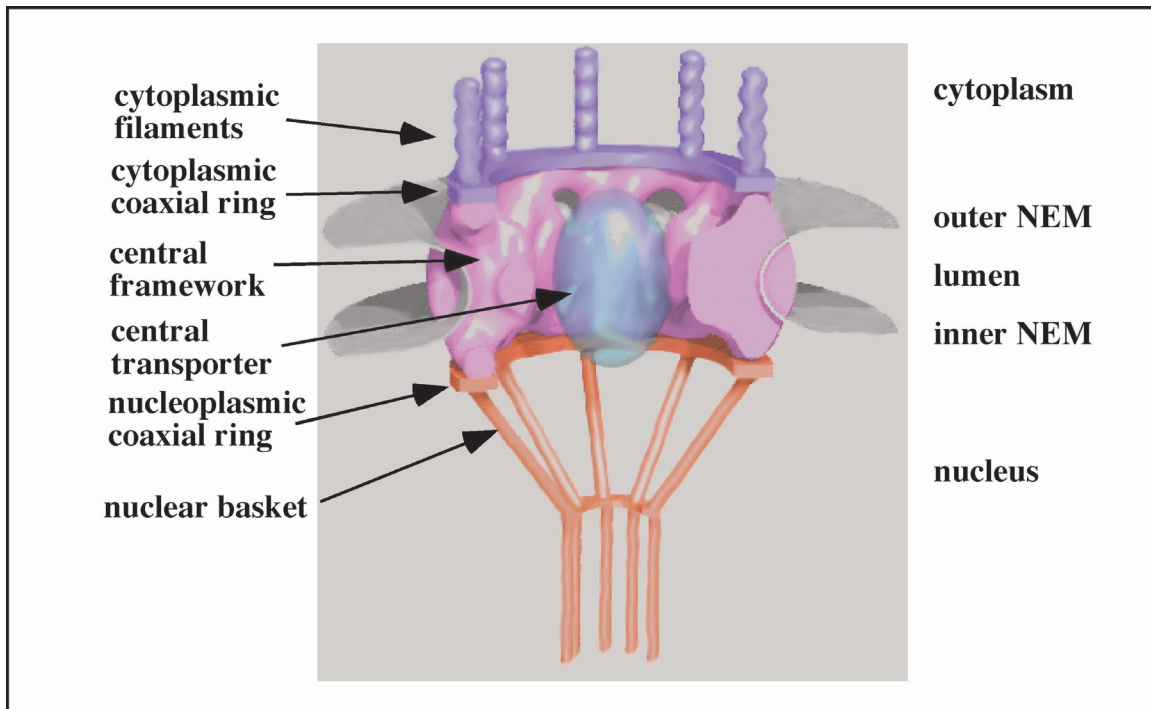
Figure 3: Three dimensional structure of the vertebrate NPC. (modified from Pante and Aebi, 1996b).

The longer filaments on the nuclear face have a diameter of 3-6 nm and join together at their distal ends to form a so-called "nuclear basket" or "fishtrap" around 100 nm away from the midplane of the nuclear envelope (Goldberg and Allen, 1993; Ris and Malecki, 1993; Goldberg and Allen, 1996; Ris, 1997).

In contrast, the filaments on the cytoplasmic side are shorter (~35-50 nm) and have free distal ends (Goldberg and Allen, 1993; Jarnik and Aebi, 1991). EM analysis of nuclear import of NLS-conjugated gold was found to involve multiple stages that were subsequently referred to as energy independent "docking" of import complexes to the NPC and translocation through the NPC into the nucleus (Feldherr et al., 1984; Newmeyer and Forbes, 1988; Richardson et al., 1988). Since the import complexes were enriched at the cytoplasmic filaments, it was assumed that this binding had an important function for nuclear protein uptake (Newmeyer and Forbes, 1988; Richardson et al., 1988; Rutherford et al., 1997) (see also 1.5.5). This hypothesis was further strengthened by the cloning of the giant nucleoporin Nup358/RanBP2 that is localised to the filaments. Antibodies against the protein could block protein import (Yokoyama et al., 1995).

In comparison to the vertebrate version, the yeast NPC is smaller and has roughly half the mass. In order to fit this mass into the 15% smaller NPC (in linear dimensions), it has been suggested that the yeast NPC has a more compact organisation. In spite of these differences, the overall structure seems to be conserved throughout evolution (Yang et al., 1998).

In parallel to structural studies, extensive molecular analysis of both the yeast and the vertebrate NPC has been carried out and broadly three different classes of protein components of the NPC, called nucleoporins, have been characterised (for review see Doye and Hurt, 1997; Ryan and Wente, 2000). The first class contains proteins that show repeated motifs containing Phenylalanine-Glycine (FG) dipeptide sequences. These nucleoporins can be further subdivided into a class having GLFG-containing repeats, like Nup98 in vertebrates and yNup116p in yeast, and a class with FXFG-containing repeats (letters indicate amino acids and X represents any amino acid). The latter class is highly heterogenous and varies in localisation, size and the other domains of their members. Usually in this class of proteins, the sequence SXFG is also found in the repeat region. The number of FG repeats varies greatly among nucleoporins: Nup153 contains approximately 30 FXFG repeats (depending on species) and RanBP2/Nup358, has roughly 18 repeats. On the other hand, proteins that, due to their non-exclusive localisation to the NPC could also be regarded as transport factors, like RanBP3, contain only 4 repeats. The early analysis of this class of proteins has been greatly helped by the isolation of monoclonal antibodies, like mAb 414 or QE5, that recognise a subset of these proteins via their FG repeats (Davis and Blobel, 1987; Pante et al., 1994).

In yeast, a proteomic approach identified ca. 30 proteins that both co-fractionated with and co-localised to the NPC in EM and fluorescence microscopy and can be viewed as a rather complete NPC inventory. Protein A-tagged versions of these proteins have been mapped to subdomains of the NPC revealing that most nucleoporins are localised symmetrically on both sides of the NPC. Five nucleoporins (yNup159p, yNup82p, yNup42p, yNup1p and yNup60p), however, were exclusively localised to one of the faces of the NPC. Sequence identities between yeast nucleoporins and their vertebrate homologues are in general very low (Rout et al., 2000). For some yeast nucleoporins homologues can nevertheless be found (like yeast Nsp1p and vertebrate p62), for others,

like yNup159p a vertebrate homologue can be assigned based on the presence of shared domains, similar localisation within the NPC and interaction with other nucleoporins. However, there are also nucleoporins for which there seems to be no homologue in yeast, like Nup358/RanBP2 and Nup153, even though functionally similar nucleoporins might exist. Conversely, for some yeast nucleoporins, like Pom34p no vertebrate homologue is known to date.

Within the NPC several nucleoporin subcomplexes have been characterised. These seem to constitute the "building blocks" of the NPC. Often, those subcomplexes are stable during the cell cycle and therefore can also be isolated more easily from mitotic or meiotic extracts. The first nucleoporin subcomplex that was identified is the p62 complex consisting of p62 and its partners p58, p54 and p52 (in yeast yNsp1p and yNup49p, yNup57p, Nic96p) (Davis and Blobel, 1987; Finlay et al., 1987; Grandi et al., 1993; Grandi et al., 1995). Often, nucleoporins also occur in more than one subcomplex. p62 for example, in addition to the mentioned complex, also forms a complex with the exclusively cytoplasmically oriented nucleoporins Nup214/CAN and Nup88 (yNup159p and yNup82) (Bastos et al., 1997; Fornerod et al., 1997b; Hurwitz et al., 1998). Again, the composition of these subcomplexes seems to have been conserved during evolution between yeast and vertebrates.

1.5.2   Dynamics of the NPC during cell cycle

During the cell cycle, new NPCs are inserted during S phase and insertion can also be observed after stimulation of quiescent cells (Maul, 1977; Maul et al., 1972; Maul et al., 1971). Later in the cell cycle, during prophase, the nuclear pore complexes are completely disassembled. This process is thought to be mediated by reversible phosphorylation by a yet unidentified kinase (Macaulay et al., 1995). The transmembrane proteins redistribute within the mitotic ER membrane network, possibly within NE specific membrane domains (Ellenberg et al., 1997; Yang et al., 1997a). The other nucleoporins become soluble within the cytoplasm either as monomers or subcomplexes (e.g. p62 complex) or homo-oligomers (Nup153). After mitosis, as soon as the nuclear

envelope is recruited to the chromatin, the nucleoporins are sequentially recruited back to form NPCs. This sequential recruitment occurs, with a few exceptions, starting with nucleoporins located on the nucleoplasmic side, to nucleoporins of the cytoplasmic side, which are recruited late in the reassembly process. This sequence of recruitment of nucleoporins, which has been determined using fluorescence microscopy of GFP-tagged nucleoporins and immunolocalisation, correlates with maturation of the NPCs as seen in scanning electron microscopy studies (Sheehan et al., 1988; Goldberg et al., 1996; Bodoor et al., 1999; Haraguchi et al., 2000).

In *S.cerevisiae* the situation is different, since this endomycete has a "closed" mitosis, meaning that the nuclear envelope never completely breaks down and spindle formation and chromosome segregation take place within the nucleus. In this organism the insertion of NPCs into the nuclear envelope occurs continuously during the cell cycle (Winey et al., 1997).

1.5.3   Asymmetrically localised nucleoporins:Nup153

As mentioned above, there are several nucleoporins in vertebrates, which are exclusively localised to one of the faces of the NPC. At the beginning of this study only one nucleoporin was known to be exclusively localised to the nucleoplasmic side (Sukegawa and Blobel, 1993). This nucleoporin, Nup153, was thought to be a constituent of the terminal ring of the nuclear basket structure (Pante et al., 1994). Nup153 has no apparent yeast homologue, but has been implicated in various aspects of NPC function. It has been suggested that Nup153 might link to either the nuclear lamina, the Tpr-containing intranuclear filaments or both (Bastos et al., 1996; Cordes et al., 1993). Support for the former hypothesis was obtained initially by over-expressing Nup153 in mammalian cell culture, where, among other phenotypes, the formation of lamina-containing intranuclear membrane arrays was observed (Cordes et al., 1993). Subsequently, an interaction between Lamin LIII, the major form of B-type lamin in *Xenopus* egg extracts, and Nup153 was reported (Smythe et al., 2000).

The primary structure of Nup153 can be divided into three parts (see figure 4): the N-terminus is unique in sequence and contains a so called M9 import signal that interacts with transportin and overlaps with the region that is required in transfection assays for

targeting of the protein into the nucleus (Enarson et al., 1998). A second, partly overlapping region, which was shown to mediate the recruitment to the NPC was later found to interact with another set of nucleoporins, the Nup160 complex (Vasu et al., 2001). The middle domain contains 4-5 zinc finger motifs (depending on species), which bind to RanGDP and which are homologous to motifs found in another asymmetrically cytoplasmic nucleoporin, Nup358/RanBP2 (Nakielny et al., 1999). The C-terminus harbours roughly 30 scattered FXFG repeats. These have been suggested to mediate the observed interaction of this domain with various transport receptors of the importin β family. In addition, this domain interacts with the adaptor molecule importin α (Moroianu et al., 1997).
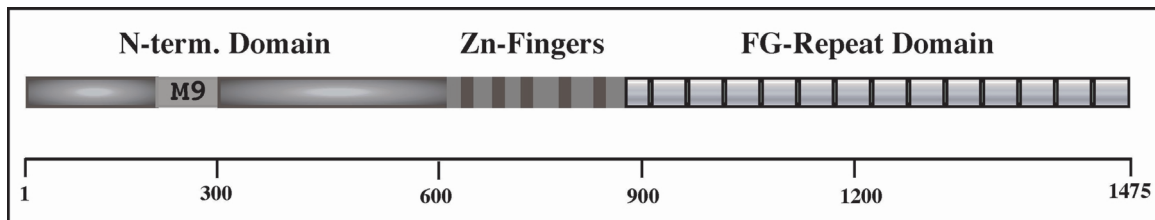
Figure 4: Primary structure of Nup153. Black bars indicate the 5 Zn-fingers of the *Xenopus* protein. Thin bars represent the FXFG repeats in the C-terminus.

Functionally, Nup153 has been implicated in diverse transport pathways through the NPC. Injection of antibodies against Nup153 into the nucleus of *Xenopus* oocyte nuclei inhibited the export of radioactively labelled RNA substrates, representing the different export pathways for mRNA and U snRNA. However, the export of tRNA was not inhibited (Ullman et al., 1999). Over-expression of the C-terminal portion of the protein in cultured somatic cells affected mRNA export, while the addition of this fragment to an *in vitro* import assay inhibited importin α/β mediated, but not transportin mediated, protein import (Shah and Forbes, 1998). These studies were suggestive of a role for the C-terminus in transport events but could also be explained by a titration of importin β or other transport receptors in the reaction via their binding to the nucleoporin fragment. In agreement with this latter hypothesis, Shah et al. reported an unusually stable interaction between Nup153 and importin β in *Xenopus* egg extracts (Shah et al., 1998).

In vitro, Nup153 also interacts with homopolymeric RNAs and with DNA via its zinc finger domains (Sukegawa and Blobel, 1993; Ullman et al., 1999; Dimaano et al., 2001). The functional significance of these interactions or of the proposed binding of RanGDP to the same region is not yet clear.

1.5.4 Asymmetrically localised nucleoporins: Nup214/CAN

The nucleoporins localised to the cytoplasmic face have been implicated in a variety of transport routes. In vertebrates, there are three proteins known to be localised exclusively to the cytoplasmic side of the NPC: Nup214/CAN, which is in a nucleoporin subcomplex with the also exclusively cytoplasmic Nup88, and the largest known nucleoporin Nup358/RanBP2 (see below).

Nup214/CAN was initially cloned as one part of a genomic translocation to the SET or DEK proteins and this rearrangement was implicated in the development of acute myeloid leukaemia. Only later, Nup214/CAN was recognised as a nucleoporin (Kraemer et al., 1994; Fornerod et al., 1995). The causal relationship between these translocations and the pathology is not clear, nor is it understood for a similar translocation between another repeat containing nucleoporin, Nup98, and the HOXA9 transcription factor, which also cause leukaemia (Borrow et al., 1996; Nakamura et al., 1996; Wong et al., 1999; Kroon et al., 2001). It has been suggested, however, that the nucleoporin part proteins provides an artificial activation domain fused to a DNA binding domain of HOXA9 or another nuclei acid binding protein. This could then lead to mis-expression of oncogenes, especially in fast proliferating cells like leukocytes.

The primary sequence of Nup214/CAN can be divided into two parts. In the N-terminal two thirds of the human protein, there are 11 scattered FXF repeats and in the C-terminal third 35 closely spaced FXFG repeats are found (see figure 5 for an overview). Furthermore, Nup214/CAN contains central regions that have a high probability to form a coiled-coil and a leucine zipper. These two regions have been shown to be important for targeting of the nucleoporin to the NPC (Fornerod et al., 1995).
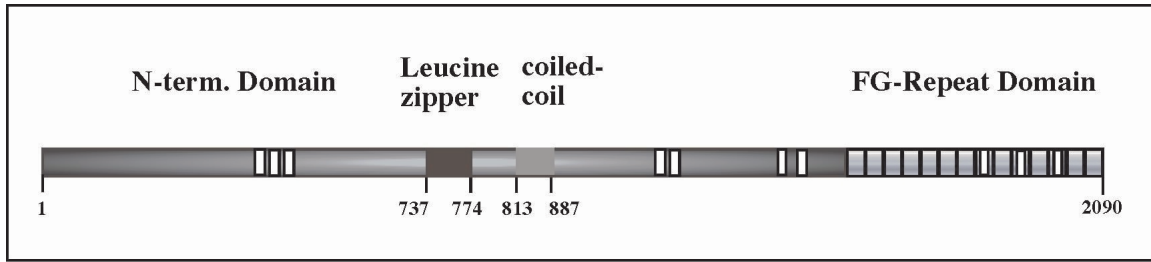
Figure 5: Primary structure of Nup214/CAN. FXF repeats are indicated by white boxes. Thin bars represent ca. 35 FXFG repeats in the C-terminus.

Based on immunogold electron microscopy studies, Nup214/CAN is commonly referred to as a component of the cytoplasmic filaments (Kraemer et al., 1994; Pante et al., 1994). Nup214/CAN has been genetically depleted in a mouse knock-out experiment. Nup214/CAN -/- embryos die at day 4 *in utero* and derived embryonic stem cells are not viable either. More detailed analysis has shown that after depletion of the maternal contribution of Nup214/CAN, the cells arrest in G2 phase of the cell cycle, are impaired in canonical NLS-mediated protein uptake into the nucleus and accumulate polyadenylated RNAs in the nucleus. The depleted cells did not, however, show an abnormal morphology of the nuclear envelope or the NPCs (van Deursen et al., 1996).

Several proteins have been found to interact with Nup214/CAN. The nucleoporin Nup88 (alternatively named Nup84) has been shown to be in a stable subcomplex with Nup214/CAN. Functional data on this nucleoporin was recently obtained in *Drosophila*, where a mutation in Nup88, called *members only*, leads to a specific transport defect for the *dorsal* protein (Uv et al., 2000).

In yeast, the Nup159p protein contains domains similar to Nup214/CAN, albeit arranged in a different order. Nup159p has recently been demonstrated to be part of an analogous subcomplex that contains both the yeast homologue of the vertebrate Nup88, Nup82p, and the homologue of vertebrate p62, Nsp1p. Furthermore, the same studies provided evidence for a link to the yeast GLFG nucleoporin Nup116p (Bailer et al., 2000; Ho et al., 2000). Mutations in yNup159 and the interacting nucleoporins result in misdistribution of the NPCs within the nuclear envelope and mutants display an accumulation of polyadenylated mRNA in the nucleus (Belgareh et al., 1998; Hurwitz et al., 1998). In addition to the interactions with other components of the NPC, a number of interactions with transport factors have also been reported. Nup214/CAN has been shown

to co-purify with the human homologue of Crm1, which is a member of the importin β family of transport receptors (Fornerod et al., 1997b). Following this observation, it was demonstrated that Crm1 is the nuclear export receptor for proteins containing leucine rich NESs (Fornerod et al., 1997a). The export receptor for cellular mRNAs, TAP, also interacts via its C-terminus, with Nup214/CAN (Bachi et al., 2000). In addition, Dbp5, a DEAD box RNA helicase that has also been implicated in nuclear mRNA export, is targeted to the NPC by binding an N-terminal region of Nup214/CAN and this interaction is conserved between yeast and human (Schmitt et al., 1999).

1.5.5 Asymmetrically localised nucleoporins: Nup358/RanBP2

Nup358/RanBP2 is the largest nucleoporin described so far and is located exclusively on the cytoplasmic side of the NPC (Wilken et al., 1995; Wu et al., 1995; Yokoyama et al., 1995). It consists of 3224 amino acids and a variety of functional domains have been characterised (see figure 6).
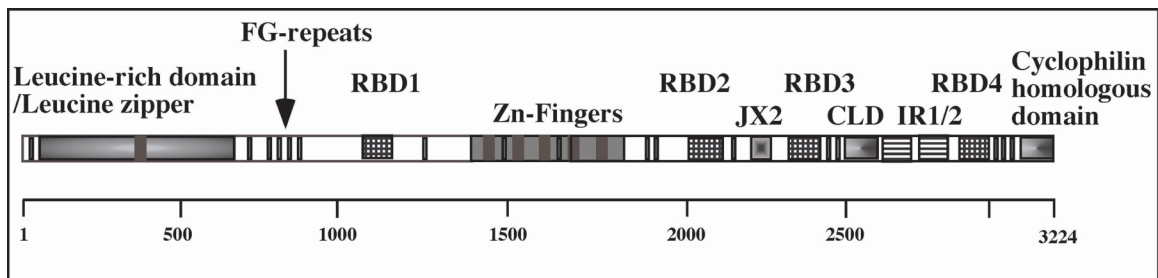
Figure 6: Primary structure of Nup358/RanBP2. Black bars represent Zn-fingers; Thin bars indicate the scattered FXFG repeats. The 4 Ran binding domains (RBD) are indicated as striped boxes. JX2, kinesin binding domain; CLD, cyclophilin-like domain; IR1/2 internal repeat 1 and 2.

The N-terminus of the protein harbours a leucine-rich repeat region (LRR) and, within it, a leucine zipper can be predicted. Futhermore, four Ran-binding domains (RBD), which bind RanGTP, can be found. Nup358/RanBP2 shares this motif with the soluble RanBP1 and RanBP3 proteins. A RBD is required for efficient hydrolysis of the GTP by Ran (see above) and the essential function of this domain for nucleocytoplasmic transport is reflected in its evolutionary conservation. Whereas the yeast *S.cerevisiae* does not have a clear homologue of Nup358/RanBP2, it contains the RanBP1 homologue Yrb1p. The

nematode *C.elegans* and the insect *D.melanogaster* only have a gene homologous to Nup358/RanBP2. It has been proposed that the targeting of SUMO-modified RanGAP to two internal repeats in the C-terminus of Nup358/RanBP2 (located between RBD3 and RBD4) facilitates GTP hydrolysis by Ran (Matunis et al., 1996; Mahajan et al., 1997; Matunis et al., 1998). SUMO is a small ubiquitin-like protein that modifies nuclear proteins. The notable exceptions to this generalisation are Nup358/RanBP2 and RanGAP, which are cytoplasmic. The reaction leading to the modification by SUMO is thought to follow the same paradigm as ubiquitination. In this model, SUMO is first bound to an E1 enzyme to generate an activated thioester. This thioester is then transferred to an E2 enzyme, which either directly or with the help of an E3 ligase transfers SUMO to the target protein. At each of these steps, additional specificity towards a subset of targets is achieved. An E2 enzyme for the sumoylation reaction, Ubc9, is targeted to a region of Nup358/RanBP2 that is overlapping with the binding site for RanGAP (Saitoh et al., 1998). Recently, it has been shown that Nup358/RanBP2 itself acts as an E3 ligase in the sumoylation reaction (Pichler et al., 2002).

Between domains RBD1 and RBD2, Nup358/RanBP2 harbours a Zn-finger domain, which shows homology to the Zn-fingers of Nup153 and has been reported to bind RanGDP specifically (Yaseen and Blobel, 1999b). In addition, the same portion of the protein was also shown to bind Crm1, the receptor for protein export from the nucleus (Singh et al., 1999). Furthermore, importin β has been shown to interact with the RBDs of Nup358/RanBP2 *in vitro* in the presence of either RanGTP or RanGDP. Since the addition of importin α and NLS containing cargo proteins stimulated RanGAP mediated GTP hydrolysis, it was suggested that hydrolysis of GTP as the last step of receptor export from the nucleus is coupled to the next round of cargo import on Nup358/RanBP2 (Yaseen and Blobel, 1999a).

Further C-terminally, between RBD3 and RBD4, a cyclophilin-like domain was found to interact with components of the 19S regulatory subcomplex of the proteasome (Ferreira et al., 1998). An even more conserved cyclophilin domain is found at the extreme C-terminus of the protein. Studies of this domain hinted to additional functions of Nup358/RanBP2 in neuronal tissues. The cyclophilins have prolyl-isomerase activity and the C-terminal domain of Nup358/RanBP2 is involved in the interconversion of red opsin

isoforms in the eye (Ferreira et al., 1996; Ferreira et al., 1997). Further evidence pointing to a brain-specific function of Nup358/RanBP2 is the recent observation that a domain between the second and third RBD interacts with the kinesin subunits KIF5B and KIF5C in brain tissue (Cai et al., 2001b).

Taken together, this multitude of protein interactions with Nup358/RanBP2 suggest that this protein has the role of a scaffold, coordinating both transport events at the NPC and being employed in a tissue specific fashion to coordinate other processes.

Although there is a lot of biochemical data available on the binding partners of Nup358/RanBP2 , the function of the protein is only beginning to be understood. Besides the recent description of an E3 activity of Nup358/RanBP2, injection of antibodies into cultured cells suggested a function in protein import (Yokoyama et al., 1995). This observation has later been rationalised by the finding that importin β is targeted to the cytoplasmic filaments in a RanGTP specific manner (Delphin et al., 1997). In the same study, also the structure of Nup358/RanBP2 was investigated by electron microscopy of negatively stained protein preparations purified from rat liver nuclear envelopes. Nup358/RanBP2 was visible in the form of a roughly 35 nm long filamentous structure. Together with its localisation on the cytoplasmic filaments, this led to the suggestion that it is a major component on the cytoplasmic filaments of the NPC. It was further hypothesised that the binding of importin β to Nup358/RanBP2 would reflect the initial docking step of cargo complexes that was described earlier and that this would be an important step in protein translocation through the NPC.

1.6 <u>Experimental systems to study nucleocytoplasmic transport and the NPC</u>

Several experimental approaches have been successfully applied to study translocation of molecules across the nuclear envelope. Genetic analyses of both the NPC and soluble factors involved in transport in a few model organisms, most notably the yeast *S.cerevisiae*, have helped to identify the genes involved and also helped to dissect the different transport pathways. For the NPC, screens for synthetic lethality between genes turned out to be particularly useful for the identification of subcomplexes (Fabre and Hurt, 1997). Recently, this analysis has been augmented by purification, micro-sequencing and localisation of the components of the NPC (Rout et al., 2000). A genetic approach also yielded major insights into the function of vertebrate nucleoporins. Due to amount of time and resources necessary to generate targeted mouse strains, however, only a few nucleoporins have been analysed in this way (van Deursen et al., 1996; Wu et al., 2001).

In addition, cell biological approaches have yielded important contributions to the understanding of nucleocytoplasmic transport. The large size of *Xenopus* oocytes, roughly 1 mm in diameter, make this system amenable for microinjection of labelled probes into either the nucleus or the cytoplasm, dissection of the two compartments and analysis of transport between them. This system was used for example to differentiate the different export pathways of RNAs and the characterisation of protein export from the nucleus (Fornerod et al., 1997a; Jarmolowski et al., 1994). In addition, the employment of fluorescent proteins in cell culture allows a characterisation of the proteins in their natural context by light microscopy. An example for the successful application of this technology is the description of nucleoporin dynamics during interphase and mitosis (Belgareh et al., 2001; Bodoor et al., 1999; Daigle et al., 2001).

One problem inherent to both genetic as well as cell biological systems is that the analysis is limited by constraints of viability of the organism or cells used. This has made loss-of-function analysis of esssential nuclear transport factors difficult or impossible. In addition, the pleiotropic and indirect effects of mutations in NPC components and transport mediators have complicated the interpretation of phenotypes resulting from

genetic experiments. In the light of this, biochemical approaches have been more than complementary. Besides the characterisation of protein-protein interactions between transport receptors and nucleoporins, the development of an *in vitro* system for protein import based on permeabilised cells was very successful. In this assay system, the plasma membrane of cells is permeabilised and cytosolic proteins are washed away. The nuclear import of labelled proteins can afterwards be reconstituted by addition of cell extracts or recombinant proteins, and in this way transport receptors and components of the Ran system were identified (Adam and Adam, 1994; Adam and Gerace, 1991; Adam et al., 1992; Görlich et al., 1995a; Görlich and Laskey, 1995; Görlich et al., 1994; Görlich et al., 1995b). The disadvantage of this biochemical system is that it relies on the integrity of the nuclear envelope in the permeabilised cells and therefore does not allow the characterisation of insoluble proteins, like for example the components of the NPC.

This disadvantage can be overcome by using nuclei reconstituted in *Xenopus* egg extract. Eggs of oviparous species accumulate an enormous amount of protein, lipids and carbohydrates for the first cell divisions, which occur without transcriptional activity in the zygote nucleus. Extracts prepared from eggs of *Xenopus laevis* for example use these components and assemble either a functional nucleus or a mitotic spindle around exogenously added chromatin, depending on their cell cycle state. Since eggs of this species are normally arrested at metaphase of meiosis II, extracts prepared form them are in a mitotic state. However, the addition of calcium promotes exit from mitosis and the extract is arrested in interphase in the absence of new protein synthesis. Readdition of either cyclin B or a mitotic extract will again reconvert the extract, and thus the added chromatin, into a mitotic state. In this way, several cell cycles can be recapitulated, which has proven very useful for research on mitotic processes (for review see Desai et al., 1999; Newmeyer and Wilson, 1991). The function of individual proteins can be studied in this system by removing them from the extract by immunodepletion prior to nuclear formation. Using this method, nuclei can be generated that lack specific nucleoporins and the effect of this on the NPC structure and nucleocytoplasmic transport can be investigated (Finlay and Forbes, 1990; Finlay et al., 1991; Powers et al., 1995; Grandi et al., 1997).

2 <u>**Aim of the project**</u>

This PhD project had the goal to characterise the function of the peripheral, asymmetrically localised nucleoporins in nucleocytoplasmic transport, the architecture of the NPC and its assembly. There are three major reasons for choosing those nucleoporins. First, the peripheral localisation of these nucleoporins within the NPC makes it unlikely that removal of these proteins will affect its overall structure, making results easier to interpret. Second, previous data suggested that the known asymmetrically localised nucleoporins Nup153, Nup214/RanBP2 and Nup214/CAN were all important for transport across the NPC. Third, their exclusive localisation to only one side of the NPC, together with their reportedly stable interactions with transport receptors (that is not commonly seen for all nucleoporins), made them likely to be involved in the mechanism of NPC translocation, a process that was very poorly understood when this project was initiated.

For the analyses of these nucleoporins, their localisation within the NPC was first mapped more precisely by a combination of electron microscopical techniques. Subsequently, a nuclear reconstitution system was employed, following the work of Forbes and coworkers (Finlay and Forbes, 1990; Finlay et al., 1991; Powers et al., 1995; Grandi et al., 1997). The function of the nucleoporins was then studied after their depletion from the system, generating a genuine loss-of-function situation. The reconstituted nuclei lacking one specific nucleoporin were analysed using a variety of light microscopic, biochemical and electron microscopic techniques to gain insight into the function of the depleted nucleoporin in NPC architecture, assembly, and nucleocytoplasmic transport.

3 Results

3.1 Nup153, a nucleoporin exclusively localised to the nucleoplasmic side of the NPC

3.1.1 Localisation of Nup153 within the NPC

Three studies have previously examined the localisation of Nup153 within the NPC. While all studies agreed that Nup153 was on the nucleoplasmic side of the NPC, the reported localisations differed in detail (Cordes et al., 1993; Sukegawa and Blobel, 1993; Pante et al., 1994; see also 4.2.1). In order to obtain more information and resolve the conflicting reports, we reinvestigated the localisation of Nup153 by different electron microscopic techniques. To this end, an antibody specific for the *Xenopus* Nup153 protein was raised.
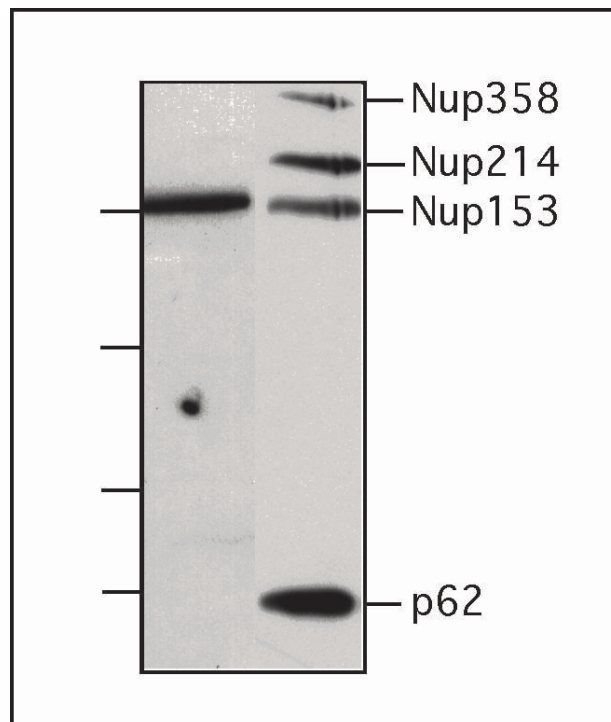

Figure 7: Specificity of the antibody against Nup153. Soluble proteins from 4-5 *Xenopus* eggswere separated by SDS-PAGE and used for immunodetection by mAb414 (right lane) or anti-Nup153 antibody (left lane). Positions of marker proteins of 175, 115, 80, 65 kD are given on the left margin, position of nucleoporins reactive with mAb414 are indicated on the right margin.

31

For this, a cDNA sequence corresponding to the N-terminal 149 amino acids was cloned by RT-PCR and expressed in *E. coli* (see Materials and Methods). Rabbits were immunised with the protein fragment and serum was obtained. Affinity purification on an antigen column yielded antibodies that recognised a single band on Western blots that was superimposable with the Nup153 band seen using the well-characterised mAb414 (Davis and Blobel, 1987; see figure 7). This commercially available antibody directed against FG-repeat containing nucleoporins recognises 5 proteins in *Xenopus* egg extracts: Nup358/RanBP2 and Nup214/CAN, Nup153, a weak unidentified band of 97 kD and, most strongly, p62.

The affinity purified antibodies were subsequently used for immunolocalisation of Nup153 within the NPC. Several techniques were employed to determine the exact position of Nup153 on manually dissected *Xenopus* oocyte nuclear envelopes after immunogold staining. In order to gain high resolution in the plane of the nuclear envelope, a surface imaging technique, scanning electron microscopy (SEM) was employed. For this, an instrument with field emission of electrons and in-lens detection of secondary electrons generated by the coated specimen was used (FEISEM). The position of the electron dense gold particles was determined by recording a backscatter image and overlaying it with the topography image (see Materials and Methods).

In order to gain more resolution in the dimension perpendicular to the NPC, 70 nm sections of *Xenopus* envelopes were labelled and viewed with a transmission electron microscope (TEM).

For SEM, the manually dissected nuclear envelopes were placed on a silicon chip, prefixed and then labelled with primary anti-Nup153 antibody and subsequently with gold conjugated secondary antibody. After post-fixation, dehydration and coating with chromium, several images were recorded. Figure 8 A shows a representative image of two single NPCs obtained by SEM (topography image) and the overlayed backscatter image false-coloured in yellow. The 10 nm gold particles that are coupled to secondary antibodies recognising the anti-Nup153 antibodies can be seen as yellow points. No significant gold labelling was observed on the cytoplasmic side of the NPC (data not shown).
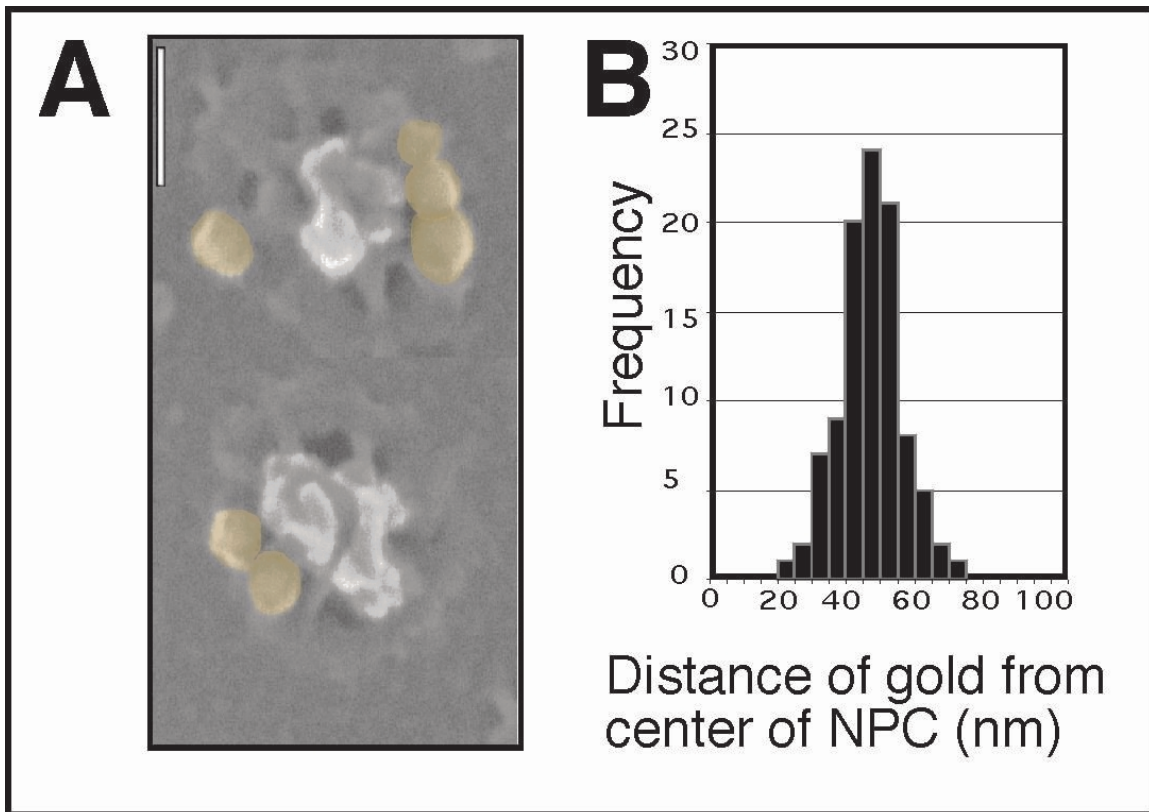
Figure 8: Localisation of Nup153 within the NPC determined by SEM. (**A**) Representative image of two NPCs viewed from the nuclear side. Yellow dots indicate the position of the gold particles detected in the backscatter image. Bar = 100 nm (**B**) Distance distribution of gold particles relative to the centre of the NPC (in nm).

The position of the gold particles was measured relative to the centre of the NPC on several similar pictures and the data obtained was statistically analysed. For 100 gold particles analysed, the mean distances from the centre of the NPC was 47 nm and the standard deviation for this data set was 8.8 nm. Figure 8 B shows the distribution of gold particles from the centre of the NPC represented in classes. Control experiments using only the secondary gold conjugated antibody gave no significant labelling of the nuclear envelope (data not shown).

For TEM analyses, the oocyte nuclear envelope samples were fixed after antibody labelling and stained with Osmium tetroxide, dehydrated and then embedded in epoxy resin. 70 nm sections were prepared and images of midsections through the NPC were imaged. A typical cross section through the nuclear envelope and four NPCs is shown in figure 9 A. The distance of the gold particles from the mid-plane of the nuclear envelope

was measured and determined to be 44.6 nm (see distribution in figure 9 B). The standard deviation was 13.9 nm. Again, no labelling of the cytoplasmic side of the nuclear envelope was observed, nor was there any gold labelling when only the secondary gold-conjugated antibody was used (data not shown). In order to ensure that the two different electron microscopic techniques yielded comparable results, the distance of the gold particles from the centre of the NPC was also measured in the TEM experiments.
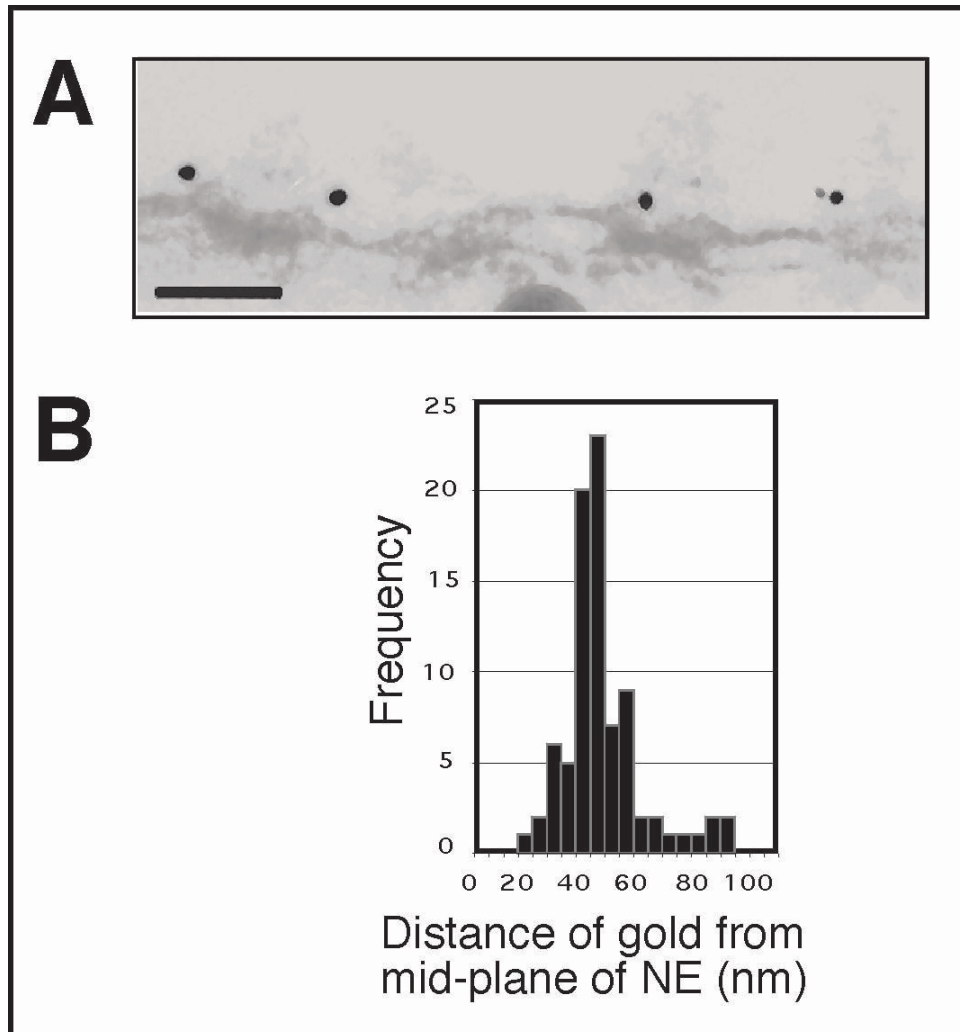
Figure 9: Localisation of Nup153 within the NPC determined by TEM. (**A**) Representative image of a stretch of the nuclear envelope viewed from the side. The 10 nm gold particles can be seen as black dots. Bar = 100 nm (**B**) Distance distribution of gold from the midplane of the nuclear envelope (in nm).

Pictures of central sections were selected and the mean radial position of the gold from the centre of the NPC was measured to be 49.15 nm with a standard deviation of 14 nm. Statistical analyses using a Mann-Whitney *U* test showed that there was no significant difference to the data obtained by FEISEM imaging (P = 0.4149). Therefore, the two data sets can be incorporated into a common model for the localisation of Nup153 within the NPC, which suggests that Nup153 is most likely located on, or near the nucleoplasmic coaxial ring and adjacent to the nuclear envelope. Alternatively, Nup153 might be part of the nuclear basket filaments with the localised N-terminal epitope being located close to the nuclear envelope.

A crystal structure of the transport receptor importin β together with an FXFG peptide revealed that this peptide can be 2 nm in length. Given the roughly 30 FG repeats in Nup153, the protein could extend over 60 nm, making it possible that the protein extends from the nuclear coaxial ring (close to the nuclear envelope) to the proximal distal ring of the nuclear basket. To investigate this possibility, the nuclear envelopes were treated with a combination of 2 mM EDTA and 500 mM KCl prior to immunolabelling. This treatment resulted in a removal of the basket filaments of the NPC.
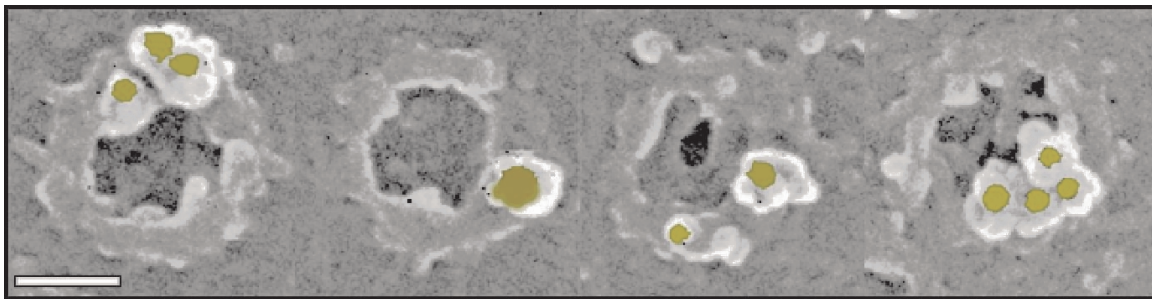
Figure 10: Gallery of salt washed NPCs seen from the nuclear side by SEM. Positions of gold particles are derived from overlaying the backscatter image and are shown in yellow. Bar = 100 nm.

If Nup153 were part of these filaments, the level of labelling with antibodies against Nup153 would be expected to disappear or at least to be reduced . As seen in figure 10, the opposite effect was observed (see figure 8 for comparison). The labelling efficiency increased by 2-3 fold per NPC, indicating a better accessibility of the epitope. This result

strongly suggests that Nup153 is part of the nuclear coaxial ring of the NPC (see figure 11 for a model of the relative position of Nup153).
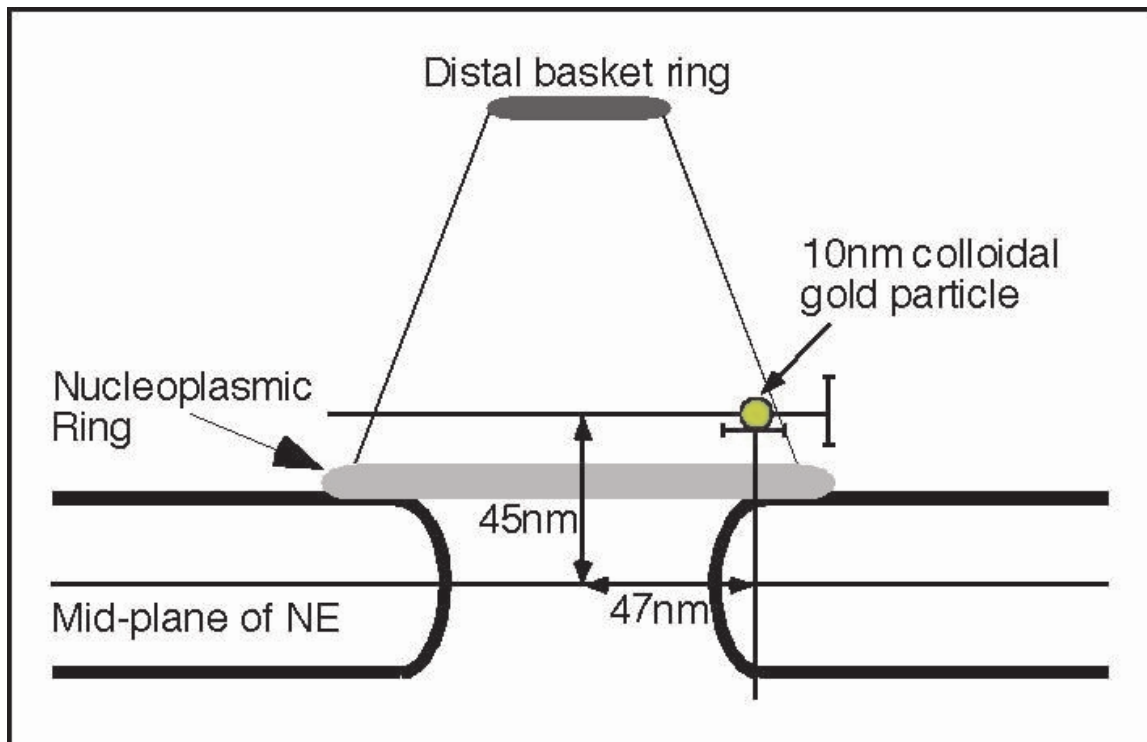
Figure 11: Model for the localisation of Nup153 within the NPC. The position of the gold particles is indicated by a yellow circle. Bars indicate the standard deviation of the measurements.

3.1.2 Development and characterisation of a nuclear reconstitution system to study the function of nucleoporins

Structural information is important and can provide an insight into the potential function of a protein or of a protein complex. Ultimately, however, functional assays are required to elucidate the function a protein. To investigate nuclear functions *in vitro*, an extract system derived from *Xenopus* egg extracts has been successfully used. DNA replication, nuclear architecture and also nucleoporins have been studied in nuclei assembled in such extarcts (see introduction).

To investigate the function of peripheral nucleoporins, the nuclear formation assay derived from *Xenopus* egg extracts was first characterised in detail. Routinely, eggs were collected from female *Xenopus* frogs that were primed by injection of PMSG and induced

to lay eggs by injection of human chorionic gonadotrophin 4-10 days later. The collected eggs were dejellied, activated by calcium to release the metaphase block and then crushed by centrifugation. The resulting low speed extract supported nuclear formation around exogenously added chromatin. As a source for this, *Xenopus* sperm head chromatin was routinely used. For storage and better reproducibility, the extracts were further separated into a soluble fraction, a membrane fraction and glycogen by high-speed centrifugation at 200 000 g (see Materials and Methods). The cytosolic soluble fraction together with membranes, glycogen and energy can form nuclei around chromatin (see Materials and Methods).

Previously there was a conflict in the literature concerning the state of the membranes involved nuclear postmitotic assembly. Whereas studies in cell culture systems reported a resorption of nuclear membranes into the ER network during prometaphase and later in the cell cycle a "wrapping" of chromatin by the ER network (Ellenberg et al., 1997; Yang et al., 1997a; Daigle et al., 2001), data using nuclear reconstitution systems suggested that specific vesicles with nuclear membranes bind to chromatin and fuse to give rise to the nuclear envelope (Imai et al., 1997; Drummond et al., 1999; Sasagawa et al., 1999). To resolve this apparent discrepancy, the nuclear formation process was characterised in more detail using membranes pre-labelled with a fluorescent dye. Figure 12 shows different time points during the assembly reaction where chromatin at the different discernible stages of the assembly process can be seen.

In a first step, the sperm head chromatin is decondensed and remodelled (figure 12, 10 min time point). In this process, nucleoplasmin mediates the removal of the protamines, which are then replaced by the canonical histones (Philpott et al., 1991).

In a second stage, vesicles dock to the chromatin surface. Upon fusion of the vesicles an ER-like network intermediate structure is formed, similar to the ER network that is observed in living cells (figure 12, 20 min time point). The formation of this network requires energy and can be inhibited by either ATPγS or GTPγS (data not shown). Further studies have shown that this reflects at least in part the requirement for the action of both the GTPase Ran and the ATPase p97. (Hetzer et al. 2000; Hetzer et al., 2001).

In a next step, the nuclear membrane is sealed, the nuclei start to import nucleophilic proteins and grow (figure 12, 60 min time point and data not shown). The exact time

point of the insertion of functional NPCs is not known, but nucleoporins can be detected very early during the assembly process. The monoclonal mAb414, which is thought to mainly recognise native p62, first stains small dots on the chromatin surface and after fusion stains the whole membrane network (figure 12, lower panel). Again this is similar to the observations made *in vivo* by immunofluorescence and following GFP-tagged transfected nucleoporins (Bodoor et al., 1999; Haraguchi et al., 2000; Daigle et al., 2001). The nuclei that formed *in vitro* were not only surrounded by a closed membrane, but also specifically imported NLS-containing proteins and contained markers for the nuclear envelope, like for instance the nuclear lamina (see below, figure 14).
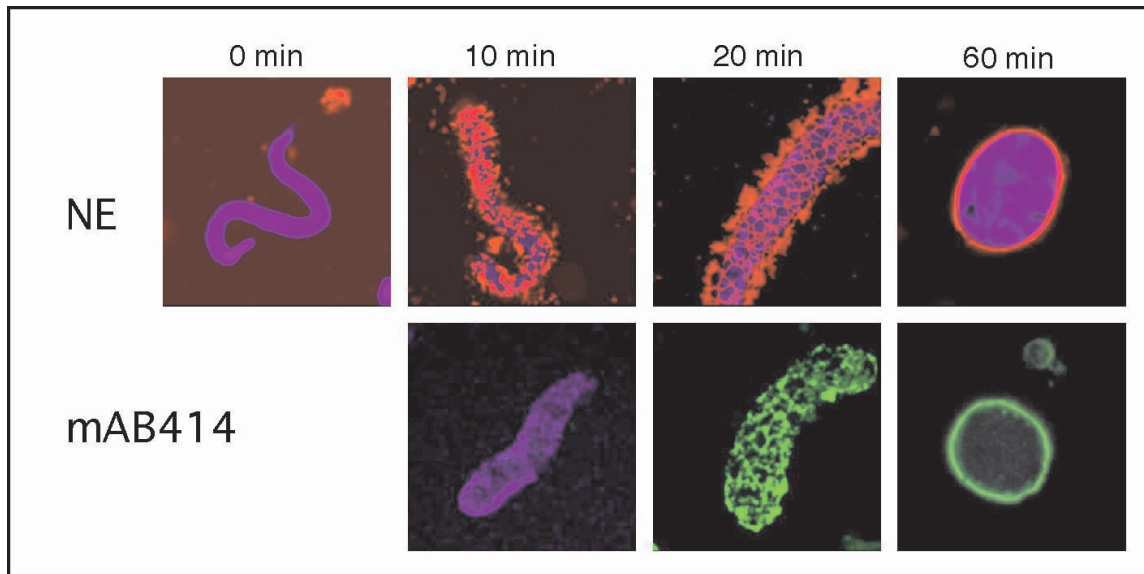
Figure 12: Time course of nuclear assembly in *Xenopus* egg extracts. Chromatin is visualised with DAPI and shown in blue. Membranes are stained with $DiOC_{18}$ in red (upper panel) and NPCs with the monoclonal mAb414, which is detected using an Alexa 488 secondary antibody.

Thus, nuclear assembly *in vitro* follows a similar pathway like observed in living cells, including an ER network-like stage. The apparant discrepancy in the literature therefore most likely results form vesiculation of such a network duting the preparation. It remains to be seen whether the observed enrichment of chromatin binding vesicles in certain density fractions reflects the existance of nuclear membrane subdomains in the mitotic ER.

Taken together, these results show that the nuclei formed *in vitro* from *Xenopus* egg extracts were functional and recapitulate postmitotic assembly and nuclear transport. For

this reason, they seemed well suited to study of individual nucleoporins in nuclear architecture, NPC structure and NPC function.

3.1.3   Depletion of Nup153 from synthetic nuclei

The goal of this study was the elucidation of the role of peripheral nucleoporins in NPC architecture and nuclear transport. The *in vitro* reconstitution of nuclei provided a useful system to study Nup153. Nup153 was immunodepleted from the extract, nuclei were assembled in the depleted extracts and investigated for potential defects in NPC architecture and nucleocytoplasmic transport. For the reconstitution of synthetic nuclei several components are required: a cytosolic soluble fraction, a membrane fraction, sperm head chromatin, glycogen and an energy regenerating system. In order to be able to remove Nup153 from the reconstitution system, it was first determined by Western blot (using the monoclonal mAb414) in which of these components Nup153 can be detected. Figure 13 (lanes 4, 5 and 6) shows that the only source of Nup153 in the nuclear constitution assay is the soluble cytosolic fraction. The energy regenerating system and glycogen consist of pure commercially available reagents and were therefore not tested (see Materials und Methods). As a next step the cytosolic fraction was immunodepleted of Nup153. To this end, affinity purified polyclonal antibody against the N-terminus of *Xenopus* Nup153 (see above 3.1.1) was bound and cross-linked in saturating amounts to sepharose beads. Then freshly prepared extracts were incubated with an equal amount of resin in the cold for 30 min. Since this treatment left trace amounts of Nup153 in the extract it was repeated and this completely removed Nup153 (see figure 13 lane 8). The depletion of Nup153 seemed to be specific since the nucleoporins Nup358/RanBP2, Nup214/CAN and p62 were not depleted in the same extract (figure 13, lane 8). As a control for unspecific depletion or inactivation of the extract, the same amount of cytosol was treated in the same way with sepharose cross linked to non-immune rabbit antibodies and this did not lead to any significant reduction of Nup153 or any other of the detected nucleoporins (figure 13, lane 6).
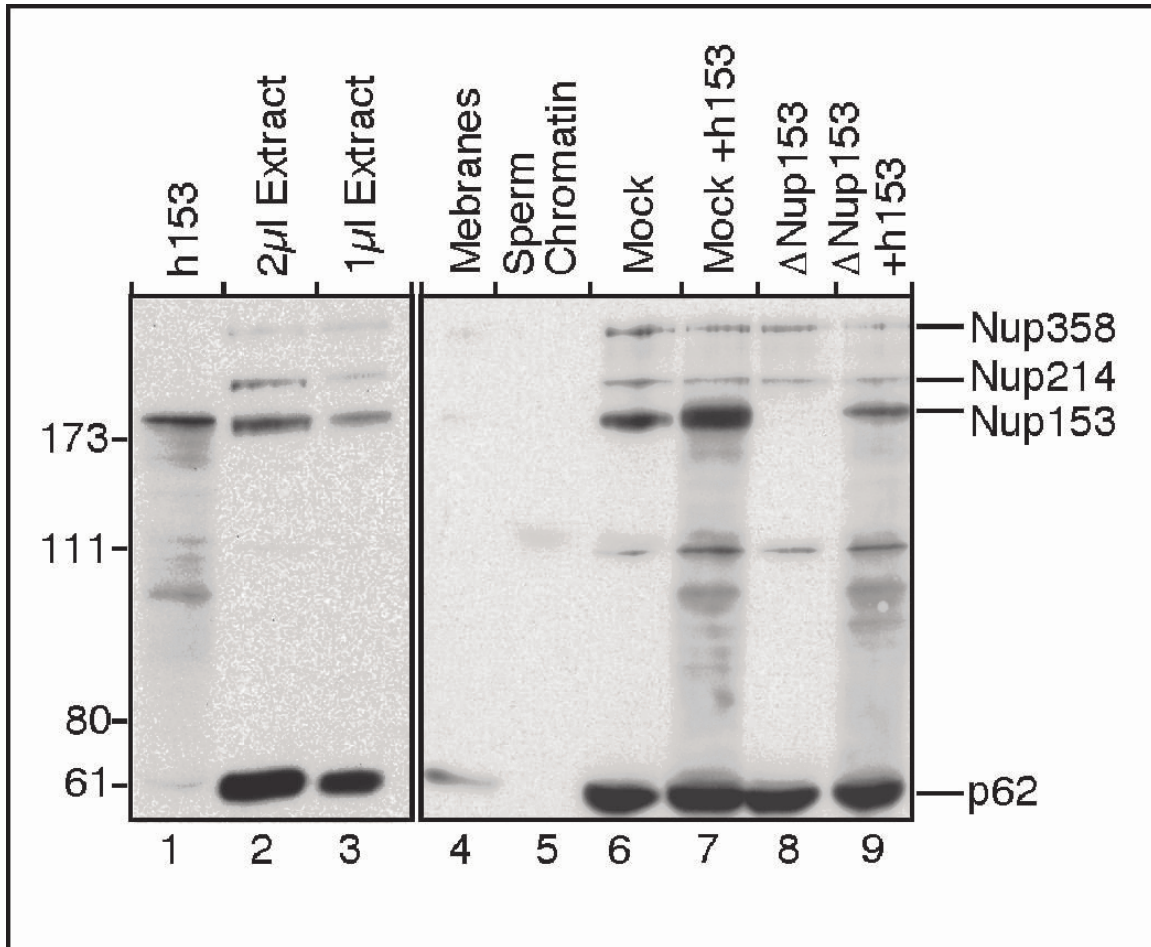
Figure 13: Western blot analysis of depleted *Xenopus* egg extracts and recombinant hNup153. Left panel: 1 μl of recombinant Nup153 (lane 1) is compared with 2 and 1 μl of undepleted *Xenopus* egg cytosol fraction (lanes 2 and 3). Right panel: 2 μl of *Xenopus* egg membrane fraction (lane4), 2 μl of sperm chromatin (lane 5), 1μl of either mock or Nup153 depleted extracts without (lane 6 and 8) or with the addition of hNup153 at the beginning of the reaction (lane 7 and 9). Position of molecular weight markers is indicated on the left. Position of the mAb414 reactive nucleoporins is shown on the right.

To exclude that trace amounts of Nup153 in the depleted extracts were concentrated on chromatin during the assembly reaction, nuclei were formed in mock or Nup153 depleted extracts and Nup153 was visualised by immunofluorescence. Figure 14 shows that Nup153 was efficiently removed from nuclei assembled in depleted extracts whereas the nuclear lamina remained intact.
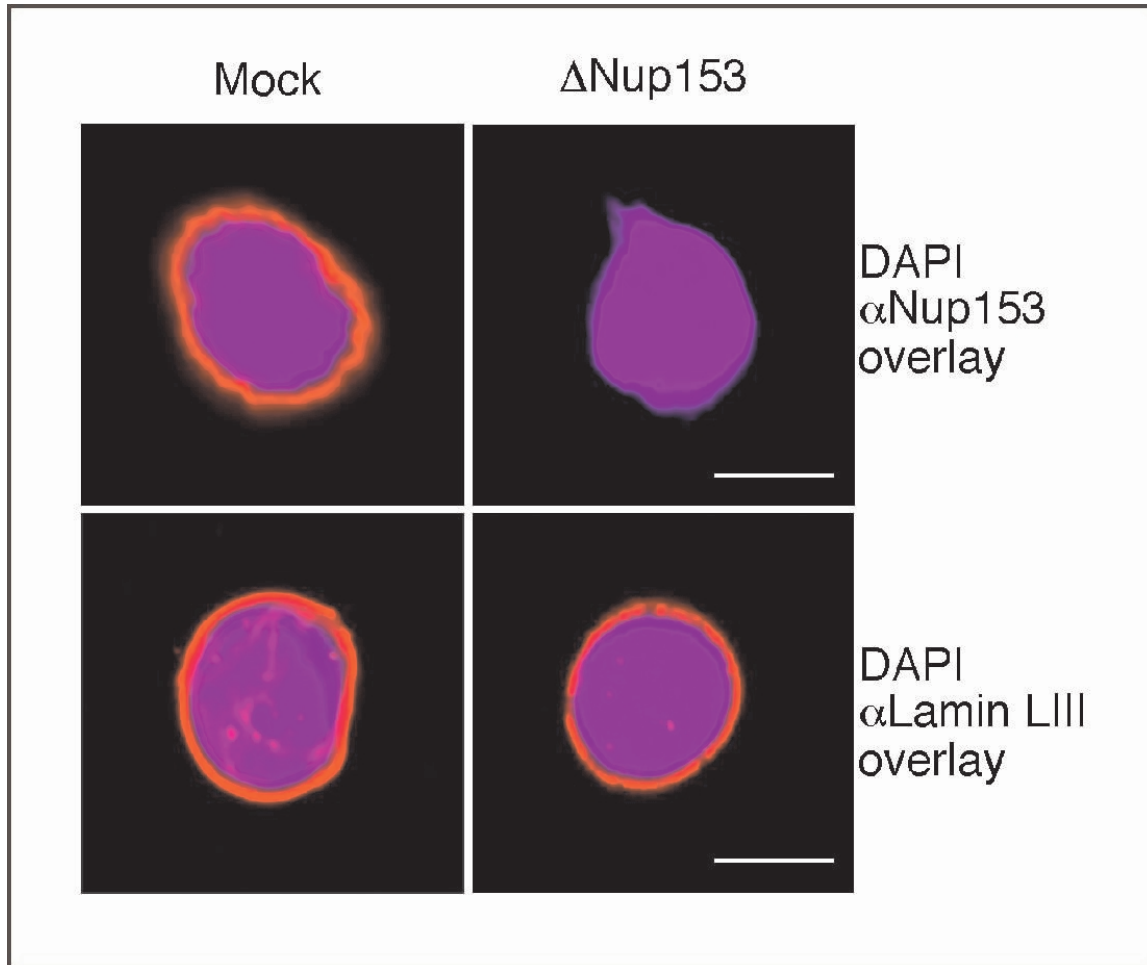
Figure 14: Immunofluorescence of nuclei assembled in mock (left) or Nup153 depleted (right) extracts using either specific Nup153 antibodies (αNup153) or the monoclonal antibody S49 (αLamin LIII) against lamins (Lourim and Krohne, 1993; Lourim and Krohne, 1998). Bar =10 μm.

In order to be able to further test the specificity of the depletion during the characterisation of the resulting defects, recombinant Nup153 was added back to the depleted extracts. Since the N-terminus of *Xenopus* Nup153 has not been sequenced to date and since we were unable to express the truncated *Xenopus* Nup153 fragment in any expression system tested, human Nup153 (hNup153), expressed as a GST fusion protein in *E. coli* was used for this purpose. The amount of recombinant hNup153 added back and its stability during the assembly reaction was tested by Western blot analysis of an aliquot removed at the end of nuclear assembly reaction (figure 13, 1, 7 and 9).

3.1.4 Depletion of Nup153 from the NPC leads to clustering of NPCs

The next step in the functional characterisation of Nup153 was the analysis of the phenotype of the depleted nuclei. During the initial observations it was realised that, unlike in mock-depleted nuclei, NPCs are not uniformly distributed over the surface of the synthetic nuclei reconstituted in Nup153 depleted extracts. To analyse this misdistribution, immunofluorescence was performed using either mAb414 or an antibody against Nup214/CAN on synthetic nuclei reconstituted in mock or Nup153 depleted extract and stacks of confocal sections were recorded. The resulting images were used for deconvolution and three-dimensional reconstruction. Projections of these reconstitutions demonstrated that the nucleoporins were not uniformly distributed in the absence of Nup153 (figure 15). This phenomenon is reminiscent of, but apparently less severe than, the clustering phenotype in a class of yeast nucleoporin mutants (Fabre and Hurt, 1997).
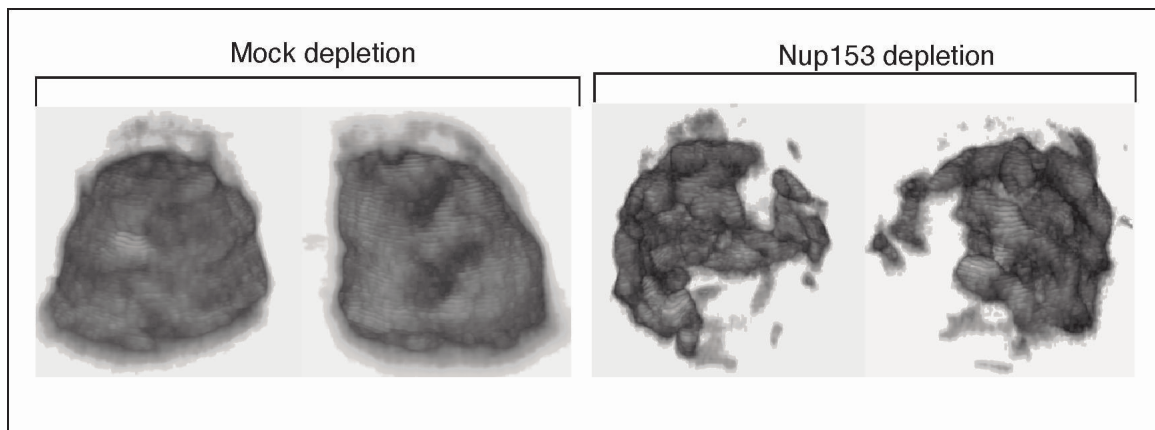
Figure 15: Clustering of NPCs in Nup153 deficient nuclei. Projections of 3D reconstructions from confocal images of immunofluorescence using anti-CAN antibodies and Alexa 488 conjugated secondary antibody. Left hand images are rotated 90° compared with right hand images.

In optical cross sections through the nuclei, this clustering appeared as a broken line. In order to get a quantitative impression of the defect, several optical cross sections were recorded and two parameters reflecting the degree of clustering were measured. First, the percentage of nuclear envelope that was not covered by nucleoporin signal was measured

and secondly the number of gaps within the nuclear envelope was counted. Representative images that were used for the quantification are shown in figure 16 B.
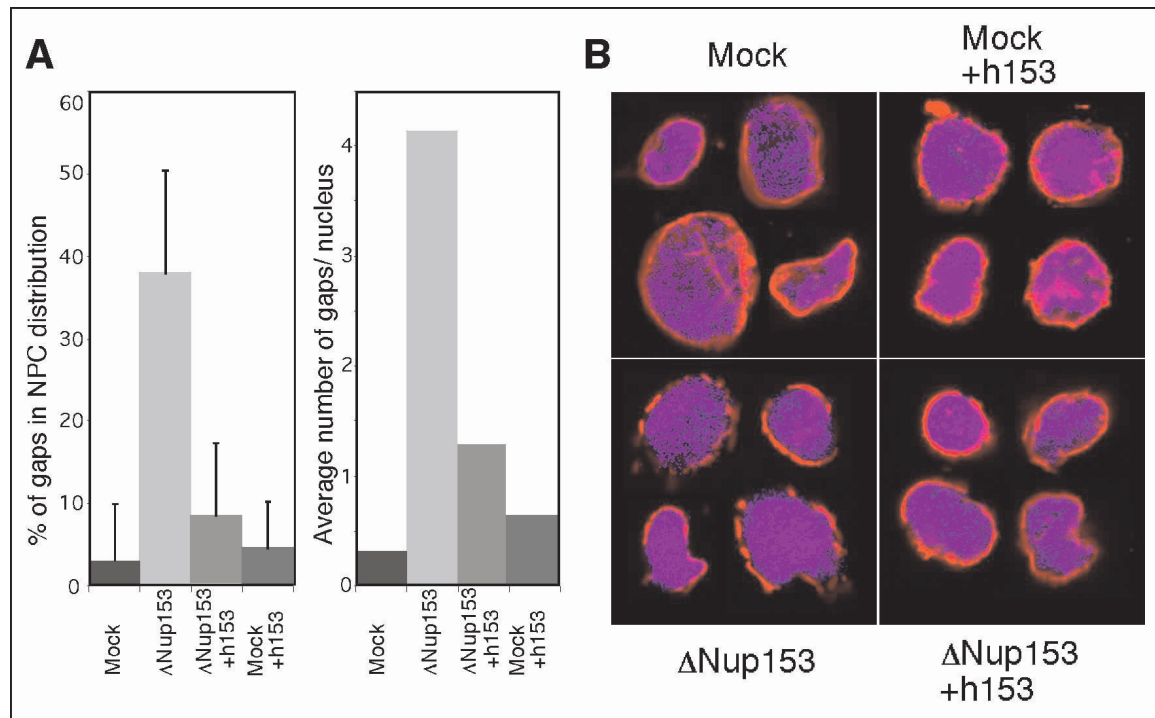
Figure 16: Quantification of NPC clustering in Nup153 deficient nuclei. Nuclei were assembled in mock or Nup153 depleted (ΔNup153) *Xenopus* egg extracts in the presence (+h153) or absence of recombinant human Nup153 and immunostained with mAb414 and an Alexa 546 conjugated secondary antibody. Optical midsections were recorded and the nuclear envelopes were analysed for discontinuities. (**A**) Both the percentage of nuclear envelope length without NPCs (A, left panel) and the number gaps in the nucleoporin signal was determined (A, right panel). (**B**) Representative images of midsections that were used for quantification. DNA is stained by DAPI and shown in blue; the immunofluorescence signal in red.

As shown in figure 16 A, the depletion of Nup153 resulted in almost 40% of the nuclear envelope not being covered by NPCs, whereas 97% was covered in mock depleted nuclei. In contrast, when recombinant hNup153 was added to the reaction this phenotype could be reversed almost completely, to 91%, thereby demonstrating that the effect of the depletion on NPC distribution was specific to Nup153. A similar result was obtained when the number of gaps in the nuclear envelope signal of mAb414 was counted. Only a minor fraction of nuclei assembled in mock-depleted extracts showed any gap in their rim staining (average = 0.3; n = 21; figure 16 A). In contrast, an average of 4.1 gaps per

optical section were counted in nuclei depleted of Nup153 (n = 18; figure 16 A). Again, this effect was almost completely reversible (average of gaps = 0.6; n = 18) by the addition of recombinant hNup153 (figure 16). The addition of the same amount of hNup153 to mock depleted nuclei had no significant effect (figure 16).

3.1.5 Depletion of Nup153 leads to a loss of several nucleoporins from the nuclear basket

In order to gain understanding of the molecular basis of the non-uniform distribution of NPCs within the nuclear envelope in Nup153 depleted nuclei, the incorporation of other components of the nuclear basket and associated proteins was investigated. Nuclei assembled in mock or Nup153 depleted extracts were stained by immunofluorescence with antibodies specific for Nup93, Nup98 and Tpr. Confocal midsections were recorded using the same microscope settings within an experiment. Nup93 and Nup98 have been localised to the nuclear basket of the NPC (Grandi et al., 1997; Radu et al., 1995) and Tpr has been detected on both the nuclear basket distal ring and the adjacent intranuclear filament network (Cordes et al., 1993; Cordes et al., 1997b; Frosst et al., 2002). All three proteins, Nup93, Nup98 and Tpr, gave a rim staining in normal nuclei but were not detectable on the nuclear envelope of nuclei reconstituted from Nup153 depleted extract (more than 100 nuclei were analysed ; figure 17). Western blot analysis showed however that the proteins were not co-depleted from the extract together with Nup153 and their loss could be completely reversed by the re-addition of recombinant hNup153 to the nuclear assembly reaction (figure 17 and data not shown).
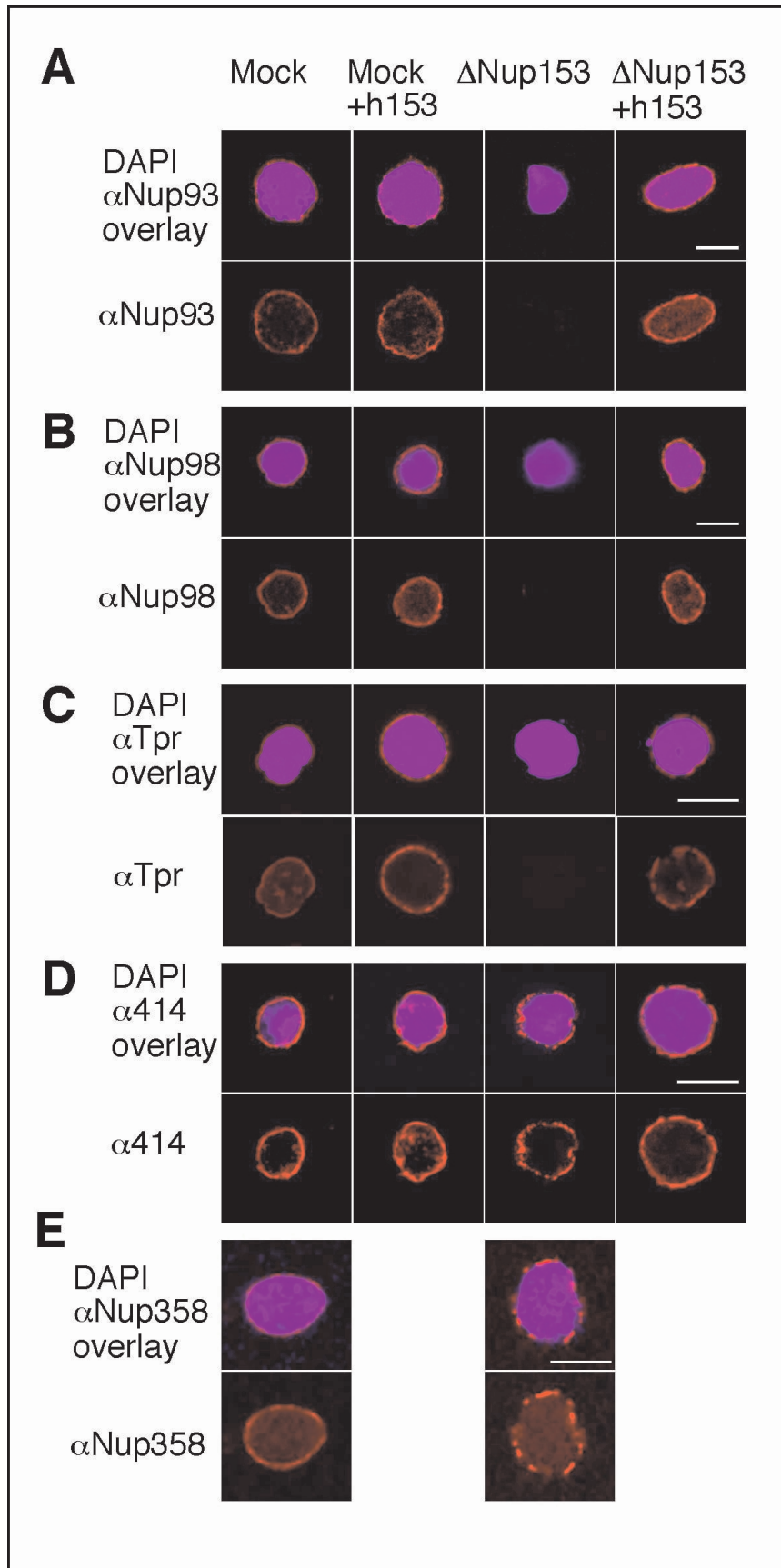
Figure 17: Nuclei deficient in Nup153 lack several other nucleoporins. Nuclei were assembled in mock depleted (Mock) or Nup153 depleted (ΔNup153) extracts in the presence (+h153) or absence of recombinant human Nup153 as indicated. The nuclei were immunostained with antibodies against Nup93 (**A**), Nup98 (**B**), Tpr (**C**), the monoclonal mAb414 (**D**) and Nup358/RanBP2 (**E**) and detected with a secondary antibody labelled with Alexa 546 (red). DNA was stained with DAPI and is shown in blue. Bar = 10 μm.

A previous report investigated the role of the nuclear lamina for NPC structure and assembly. The addition of a dominant negative lamin fragment prevented the assembly of a correct lamina and also led to a loss of Nup153 from the NPC. Under this condition, Nup93 was not lost from the NPC (Smythe et al., 2000). At the moment it is impossible to resolve the apparent discrepancy between this data and the results obtained here after depletion of Nup153, but it could be due to the different experimental conditions used. The most obvious difference is that in the case of the addition of the dominant negative lamin fragment, Nup153 was still present whereas it is completely removed in the experiments presented here.

The absence of all Nup93, Nup98 and Tpr from the NPC indicates that Nup153 is required or the correct formation or maintenance of the nuclear basket structure and further suggests that in Nup153 depleted nuclei this NPC substructure is missing.

To test whether nucleoporins on the cytoplasmic side or in the central channel of the NPC are also affected by the depletion of Nup153, additional immunofluorescence experiments were conducted. The monoclonal antibody mAb414 mainly recognises the nucleoporins of the p62 complex, that are part of the central transporter, but also Nup153 and the cytoplasmically localised proteins Nup214/CAN and Nup358/RanBP2. The labelling intensity of the nuclear rim in immunofluorescence experiments with this antibody appeared only slightly reduced (figure 17) and showed the NPC clustering phenotype described above. The cytoplasmic nucleoporins Nup358/RanBP2 and Nup214/CAN were also present at normal levels in Nup153 depleted nuclei as judged by immunofluorescence experiments (figure 17 and data not shown). This showed that the depletion of Nup153 did not lead to a general defect in NPC architecture but to a specific assembly defect in the nuclear basket. This was further supported by imaging the cytoplasmic face of NPCs of either mock depleted or Nup153 depleted nuclei by

FEISEM, which showed no discernible difference between the two conditions (data not shown). In addition, other structural features of the synthetic nuclei, like the nuclear lamina were also not affected by the depletion of Nup153 from the reconstitution system (see figure 14).

3.1.6 Loss of Nup153 leads to increased mobility of NPCs within the nuclear envelope

Analyses of the nucleoporin composition of depleted nuclei showed that the NPCs without Nup153 either do not assemble a nuclear basket or assemble one that is substantially incomplete. In addition, immunofluorescence showed that the NPCs were misdistributed in the absence of Nup153. Together, this suggested that the normal anchoring of NPCs within the nuclear envelope was altered in nuclei assembled in Nup153 depleted extracts. In order to test this hypothesis, the mobility of NPCs in the nuclear envelope was directly investigated using fluorescence recovery after photobleaching (FRAP). FRAP experiments in eukaryotic cells have shown that NPCs are stably anchored within the NPC and only a few nucleoporins are more mobile between NPCs (Zolotukhin and Felber, 1999; Daigle et al., 2001; Griffis et al., 2002).

In an analogous experiment, the NPCs of both mock and Nup153 depleted nuclei were labelled with the lectin wheat germ agglutinin coupled to the fluorescent dye Oregon Orange 488 (WGA*). WGA has been shown to specifically recognise a subset of nucleoporins via their O-linked N-acetylglucosamine modification (Finlay et al., 1987). The assembled nuclei were spun onto a coverslip, free WGA* was removed and a stripe was bleached in the rim signal, reflecting the NPCs. When the rim of nuclei assembled from mock-depleted extracts were bleached no significant recovery of fluorescence was observed in 40 min (figure 18 A). This demonstrated that the NPCs were immobile and that the bound WGA* did not dissociate from the NPCs and rebind to others during the time course of the experiment. In contrast, when a similar stripe was bleached in the NPC rim signal of a nucleus reconstituted from Nup153 depleted extracts, there was significant recovery of fluorescence (figure 18 A).
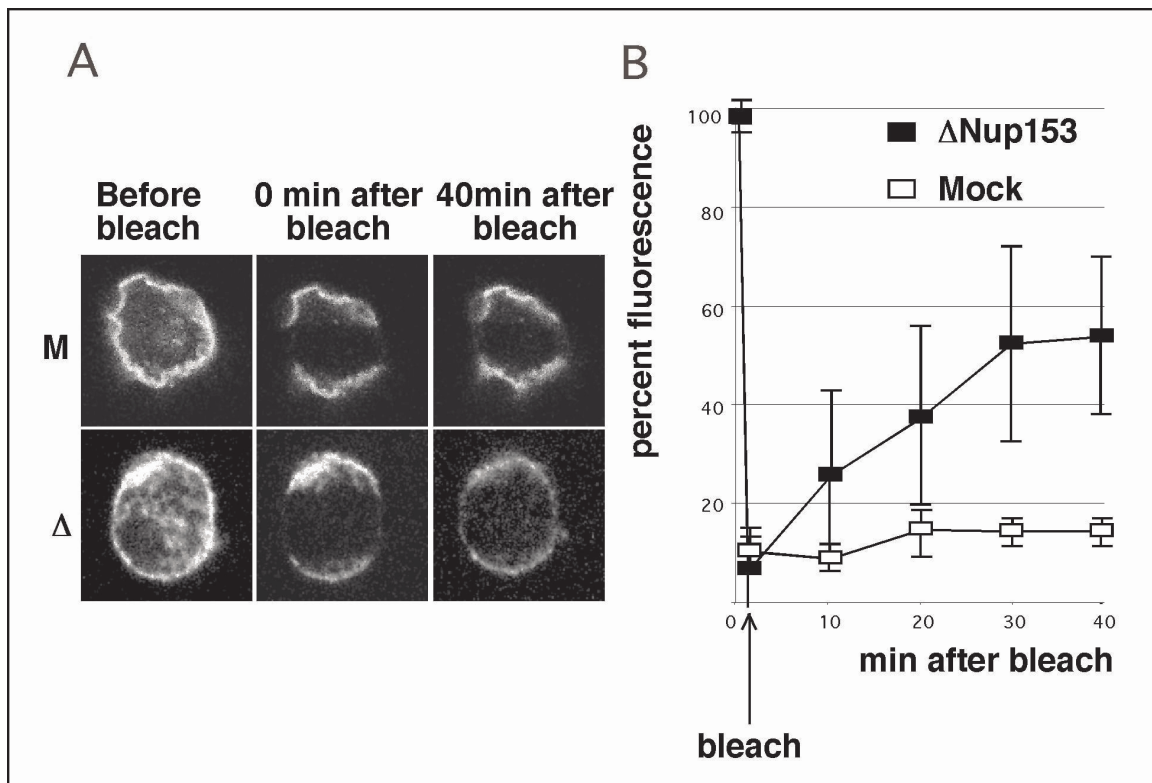
Figure 18: NPCs are mobile within the nuclear envelope in the absence of Nup153. (**A**) Representative series of fluorescence images after photobleaching (FRAP) of nuclei assembled *in vitro*. Mock (M) or Nup153 depleted (Δ) nuclei are shown. (**B**) Quantitation of FRAP from three independent experiments using mock (open squares) or Nup153 depleted nuclei (solid squares).

The recovery of fluorescence from three independent experiments was quantified and this confirmed the visual impression. 50% of the initial NPC fluorescence intensity was regained in the bleached stripe of Nup153 depleted nuclei after 30 min, whereas there was no significant recovery in mock-depleted nuclei (figure 18 B). This showed that the NPCs are mobile within the nuclear envelope in the absence of Nup153.

3.1.7 Nup153 is required for basic NLS but not M9 mediated nuclear protein import

In addition to the function of Nup153 in NPC architecture, its role in protein transport into the nucleus was investigated. Two pathways of protein translocation were studied using two different model substrates. For the first pathway, bovine serum albumin (BSA)

was coupled to the basic nuclear localisation signal from the Simian Virus 40 (SV40) large T antigen and fluorescently labelled with Alexa 488 (Palacios et al., 1996). This substrate binds the importin α/β heterodimer that mediates its translocation through the NPC. Since BSA alone is already bigger than the size exclusion limit of the NPC (roughly 60 kDa), this substrate did not diffuse into the nucleus. Nor was it actively imported in the presence of WGA, a dominant negative importin β fragment (ΔN44) or at 4 °C (Palacios et al., 1996 and data not shown). Routinely, the integrity of the nuclei that were analysed was also ensured by addition of labelled BSA cross-linked to a peptide with the reverse NLS sequence and this substrate was excluded from intact nuclei.
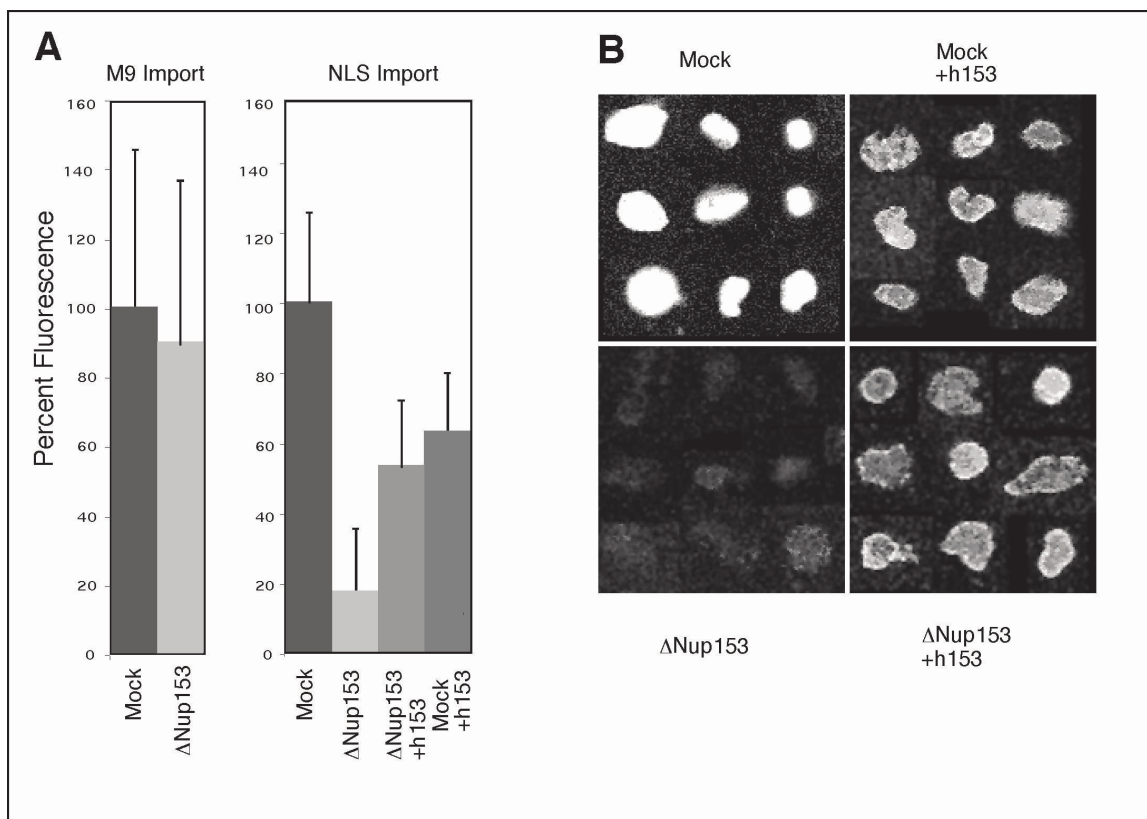
Figure 19: Nup153 deficient nuclei display a selective protein import defect. Nuclei were assembled in either mock or Nup153 (ΔNup153) depleted extracts in the presence of absence of recombinant human Nup153 (+hNup153).(**A**) Quantitation of import of fluorescently labelled NPC-M9 (left panel) and fluorescently labelled BSA-NLS (right panel) into assembled nuclei. (**B**) Representative images of BSA-NLS import into nuclei as analysed in (A).

The second model substrate was a fusion between the core domain of nucleoplasmin and the M9 import signal of hnRNPA1. This signal is recognised by the transportin import receptor and this mediates import of the complex (Pollard et al., 1996). The nucleoplasmin core domain forms very stable pentamers and therefore, this substrate is also too big to passively diffuse into the nucleus (Englmeier et al., 1999). Both substrates accumulate in nuclei assembled in undepleted or mock depleted extracts and import can easily be quantified by measuring the intranuclear fluorescence levels by confocal microscopy (see figure 19). When the M9-nucleoplasmin core substrate was added to nuclei lacking Nup153, the M9 substrate was accumulated to the same level as in nuclei assembled in mock-depleted extracts. However, the import of the BSA-NLS substrate was strongly reduced, to maximally 15-20% of the level of mock-depleted nuclei (figure 19 A). Figure 19 B shows representative images of nuclei reconstituted from mock and Nup153 depleted nuclei after the import reaction. It can be seen that both the intranuclear signal and the nuclear envelope rim signal, indicative of import complex docking to the NPC, were strongly reduced indicating that it was not a block in NPC translocation that led to a build-up of intermediates at the NPC. The defect of import of classical NLS-containing substrates was not due to a codepletion of any component of the Ran system or the receptors importin α or importin β with Nup153 as judged by Western blot (data not shown). Addition of recombinant hNup153 to mock depleted nuclei lead to a reduction of imported substrate to 70%, most likely due to the presence of C-terminal fragments of hNup153 in the preparation that have been reported to act in a dominant negative way to inhibit importin β mediated protein import (Shah and Forbes, 1998). Importantly however, when hNup153 was added to the Nup153 depleted extracts, the import of the labelled BSA-NLS into the nuclei reconstituted in these extracts was restored to almost the level of nuclei assembled in mock depleted extracts in the presence of hNup153 (figure 19). This corroborated that the observed defect of the depletion in nuclear import was specific for Nup153. In addition, since the import rate of M9-containing substrates into these nuclei was normal, it appears very unlikely that the number of NPCs becomes limiting for nuclear import after depletion of Nup153.

3.1.8 The import defect observed in Nup153 depleted nuclei is due to an effect on translocation

The reduction of import of classical NLS containing substrates into Nup153 depleted nuclei could have at least three mechanistic explanations. First, the receptor/cargo complexes could be stalled at the NPC thereby blocking subsequent translocation events. In this case, one would expect a build-up of receptor/cargo complexes on the nuclear rim. Second, the recycling of either one or both components of the NLS receptor, importin α and β, could be impaired. In this scenario, it would be predicted that importin α and/or β would accumulate inside the nucleus or at the nuclear rim. Third, the translocation of receptor/cargo complexes through the NPC could be slowed down or made less efficient due to the depletion of Nup153. From this, it would be expected that not only the intranuclear concentration of the transported cargo should be decreased but also the concentration of the import receptors in the nuclei would be lower.
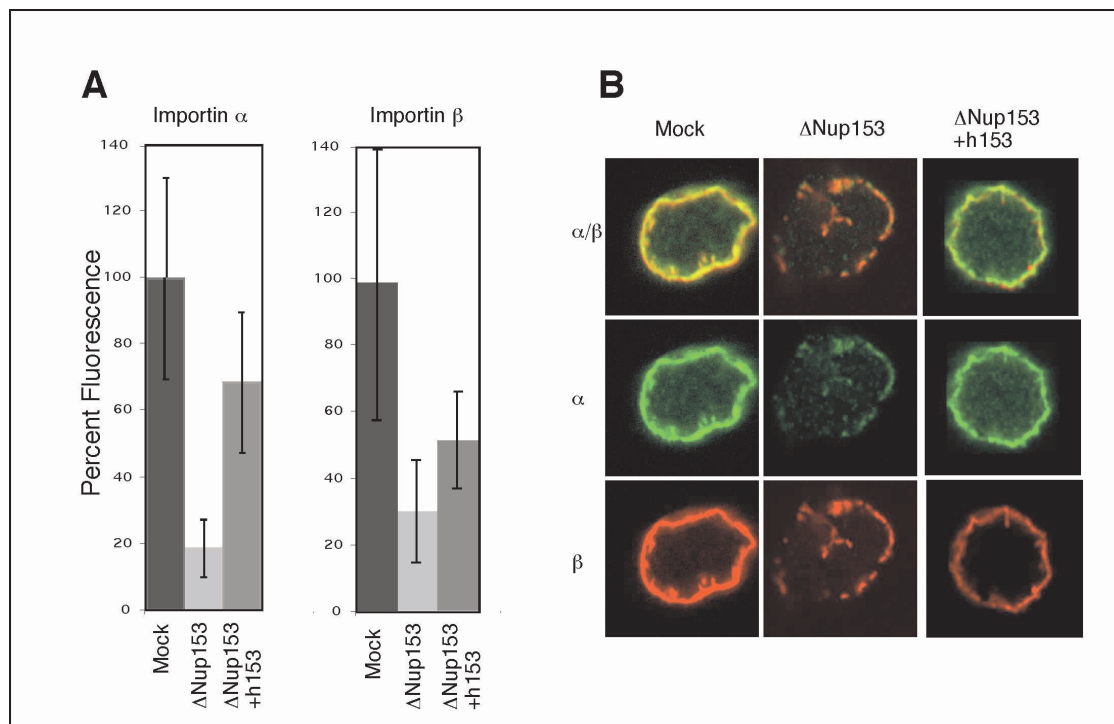
Figure 20: The import defect observed in Nup153 depleted nuclei is not due to a block in translocation or recycling. (**A**) Quantitation of nuclear importin α and β by immunofluorescene and direct fluorescence measurement of labelled protein in mock and Nup153 (ΔNup153) depleted nuclei in the presence (+hNup153) or absence of human recombinant Nup153. (**B**) Representative images of nuclei stained for impotin α (α) and importin β (β).

In order to discriminate between these possibilities, the localisation of importin β was investigated by immunfluorescence and importin α distribution was followed directly by addition of labelled protein to the reaction.

Firstly, the normal rim signal of importin α and β, indicating their binding to the NPC, was not increased, but very much reduced in Nup153 depleted nuclei (figure 20 B), indicating that there was no irreversible binding to or trapping of the receptors at the NPC that could block nuclear protein import. Secondly, the concentration of both receptors in the nuclei was not increased in nuclei that lacked Nup153 (figure 20) showing that they could be recycled to the cytoplasm. In contrary, the concentration of both transport receptors was greatly reduced in the nuclei that lack Nup153 and this argues for the third possibility, that the accumulation of cargo is directly affected by less efficient NPC translocation. The specificity of the depletion effect was again demonstrated by re-addition of recombinant hNup153 to the reconstitution reaction. The level of importin α at the nuclear rim and the nuclear interior was restored almost to the level of mock-depleted nuclei (figure 20). Figure 20 B shows that the localisation of importin β was also restored, albeit to a lesser extent. This was probably due to the binding of importin β to the recombinant hNup153 and the dominant negative fragments in the preparation (see above) and therefore also explains the imperfect restoration of import activity by re-addition of Nup153 to depleted extracts (Shah and Forbes, 1998).

Taken together, this data strongly suggest that the effect of Nup153 depletion on accumulation of substrates containing a classical basic NLS is due to a lower rate of their translocation through the NPC and not due to a defect in recycling of receptors or a blocking of NPCs for this import pathway.

3.2 Nucleoporins localised exclusively to the cytoplasmic side: Nup214/CAN and Nup358/RanBP2

The analysis of the exclusively nucleoplasmically localised nucleoporin Nup153 led to the conclusion that it, or another component of the nuclear basket, is required for at least one nuclear protein import pathway. This was somewhat unexpected since the nuclear basket topologically constitutes the final step of translocation and cargo complexes are actually already in the nucleus when they can bind to Nup153. Conversely, it has been frequently proposed in the literature that the nucleoporins localised exclusively to the cytoplasmic face and the filament structures of the NPC, have an important role in cargo complex docking to the NPC and subsequent translocation (see Discussion). This hypothesis has nonetheless not been directly investigated in a biochemically tractable system. Therefore, the function of two known nucleoporins that only localise to the cytoplasmic side of the NPC, Nup358/RanBP2 and Nup214/CAN, was analysed using electron microscopy and the nuclear reconstitution system derived from *Xenopus* egg extracts.

3.2.1 Localisation of Nup214/CAN and Nup358/RanBP2 within the NPC

Only three nucleoporins are known to be localised solely to the cytoplasmic side of the vertebrate NPC. Two of them, Nup214/CAN and Nup88, are known to be in a complex and the other one is the giant Nup358/RanBP2. Both Nup214/CAN and Nup358/RanBP2 have been reported to be part of the NPC cytoplasmic filaments (Kraemer et al., 1994; Pante et al., 1994; Wilken et al., 1995; Wu et al., 1995; Yokoyama et al., 1995). In order to be able to reinvestigate the localisation of these nucleoporins within the NPC by immunogold labelling and electron microscopy, an antibody against the N-terminal 213 amino acids of *Xenopus* Nup214/CAN was generated. For the localisation of Nup358/RanBP2, two different antibodies were obtained. Anti-Nup358F was raised against a C-terminal fragment comprising amino acids 2501 to 2900 of the human Nup358/RanBP2 and anti-Nup358V was directed against a sequence from amino acid

2285 to 2314 of the human protein of which amino acids 2290 to 2314 are identical to the predicted *Xenopus* protein. The antibodies were affinity purified using the corresponding antigens immobilized on sepharose beads and a band of the expected size in *Xenopus* egg extracts (see figure 21).
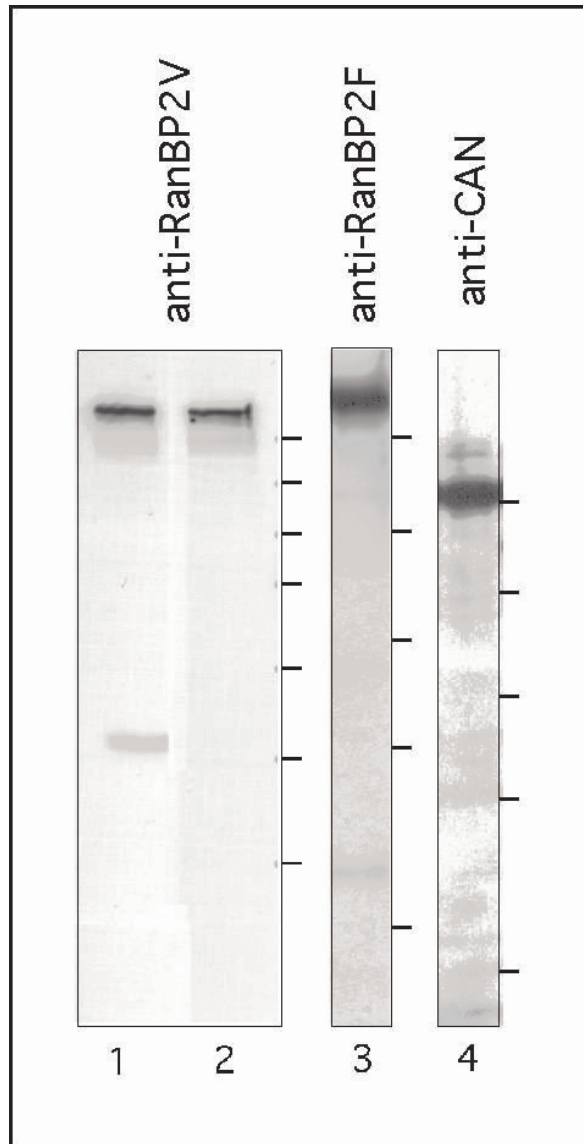
Figure 21: Specificity of antibodies against Nup214/CAN and Nup358/RanBP2**.** Proteins from 25 manually isolated *Xenopus* oocyte nuclei (lane 1) and from *Xenopus* egg extract from 4-5 cells, (lanes 2-4) were separated by SDS-PAGE and used for immunodetection of RanBP2/358V (lanes 1 and 2), RanBP2/358F (lane 3) and CAN (lane 4) by enhanced chemiluminiscence reaction. Note that independent of exposure time, RanPB2 is the only protein immunodetected in egg extracts. In the nuclear fraction, a minor cross-reaction with an unknown protein of ~ 40 kDa is seen only after prolonged exposure (lane 1). Positions of marker proteins of 250, 150, 100, 75, 50, 37 and 25 kD are given at the right margins.

In order to obtain high resolution for the localisation of the proteins within the NPC, a similar rationale as for the localisation of Nup153 was followed (see figures 8 and 9). For the high resolution in the plane of the nuclear envelope, FEISEM analyses of immunogold labelled samples was performed. Sectioning of the nuclei, subsequent labelling and image recording by TEM yielded images with a high resolution in the plane perpendicular to the nuclear envelope. In both cases, the samples consisted of manually dissected *Xenopus* oocyte nuclear envelopes that, after fixation, were first labelled with the antibodies against the nucleoporins Nup214/CAN or Nup358/RanBP2 and then with secondary antibodies conjugated to 10 nm colloidal gold. After recording a series of pictures, the distance of at least 100 gold particles from the centre of the NPC was measured on FEISEM micrographs and the position relative to the midplane of the nuclear envelope was determined on TEM images showing midsections of the NPC. Table 1 summarizes the results obtained for the three different primary antibodies against Nup358/RanBP2 and Nup214/CAN. The latter was localised centrally at a mean localisation of 11 nm from the middle of the NPC with a standard deviation of 0.9 nm in the data set (see Table 1). This corresponds to the inner side of the cytoplasmic coaxial ring or the cytoplasmic entrance of the translocation channel.

Table 1: Summary of the localisation of Nup214 and Nup358 using FEISEM and TEM.

Antibody	SEM				TEM			
	Sample size (n)	Mean distance of gold from centre of NPC (nm)	SD	SE	Sample size (n)	Mean distance of gold from midplane of NE (nm)	SD	SE
anti-Nup214	106	11	9.3	0.90	36	31	5.7	0.68
anti-Nup358F	229	39	10.3	0.68	50	57	10.9	1.54
anti-Nup358V	114	31	12.0	1.12	56	51	10.0	1.34

Representative images obtained by FEISEM that were used for the quantification are shown in figure 22.
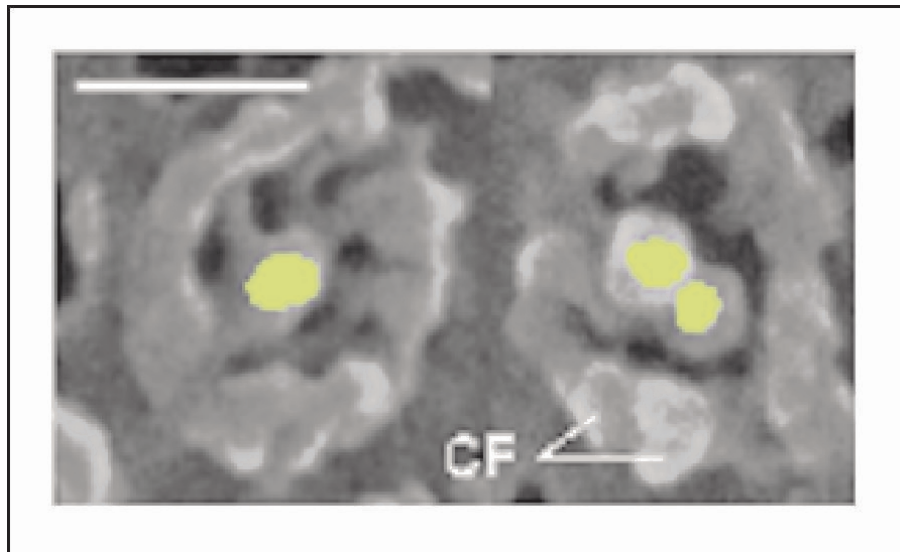
Figure 22: SEM localisation of Nup214/CAN on manually dissected *Xenopus* oocyte nuclear envelopes. Yellow dots indicate position of gold particles determined by overlay of backscatter images. CF; cytoplasmic filaments. Bar = 100 nm.

Also in TEM of 70 nm cross-sections through the nuclear envelope, Nup214/CAN was found in a position close to the core structures of the NPC (figure23).
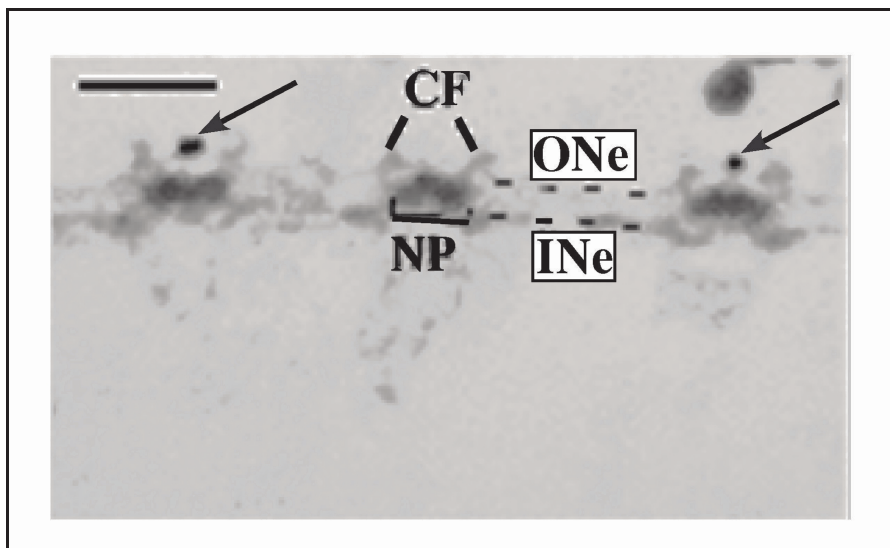
Figure 23: TEM localisation of Nup214/CAN on manually dissected *Xenopus* oocyte nuclear envelopes. The core of the NPC is seen as electron dense material between the two membranes. Gold particles are detected in a central position of the NPCs as black dots (indicated by black arrows). CF: cytoplasmic filaments; NP: NPC central core; ONe: outer nuclear envelope; INe: inner nuclear envelope. Bar = 100 nm.

The mean distance for the midplane of the nuclear envelope was determined as 31 nm (with a standard deviation of 0.68 nm within the n = 36 dataset). A representative image from this data set is shown in figure 23. In both techniques, FEISEM and TEM, no labelling of the nucleoplasmic side of the nuclear envelope was observed.

In contrast to the localisation of Nup214/CAN, which was determined to be part of the central framework of the NPC, Nup358/RanBP2 was located more peripherally.
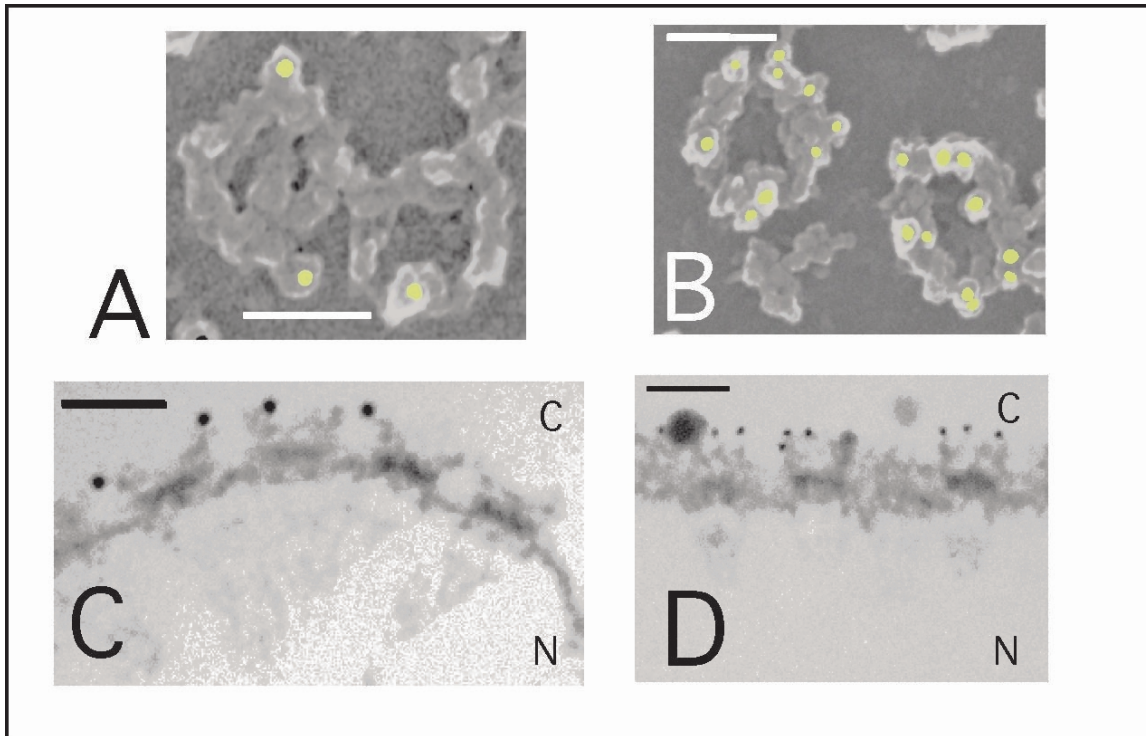
Figure 24: SEM and TEM localisation of Nup358/RanBP2 on manually dissected *Xenopus* oocyte nuclear envelopes using the anti-Nup358F and anti-Nup358V antibodies. Yellow dots indicate the position of 10 nm gold particles in SEM as determined by overlaying the backscatter image. Gold particles can directly be seen in TEM images as black dots. (**A**) SEM localisation of Nup358/RanBP2 on oocyte envelopes seen from the cytoplasmic side using anti-Nup358F. (**B**) SEM localisation as (A) using anti-Nup358V. (**C**) TEM localisation of Nup358/RanBP2 on *Xenopus* oocyte nuclear envelopes seen from the side using anti-Nup358F. (**D**) Localisation as in (C) using anti-Nup358V. C: cytoplasm; N: nucleus. Bar = 100 nm.

Figure 24 A shows a representative FEISEM image of an oocyte nuclear envelope immunolabelled with the anti-Nup358F antibody. The quantification and measurement showed that the epitope was localised 39 nm from the centre of the NPC with a standard deviation of 0.68 nm (see also Table 1). Similarly, the epitope of anti-Nup358V was

determined to be located 31 nm from the centre of the NPC with a standard deviation of 1.12 nm (see Table 1 and Figure 24 B). These two localisations correspond to the cytoplasmic filaments of the NPC. Accordingly, the result of the immunolabelling experiments with the two antibodies on cross-sections showed a distal localisation of the two epitopes in TEM pictures. Again no nucleoplasmic labelling was observed (data not shown).
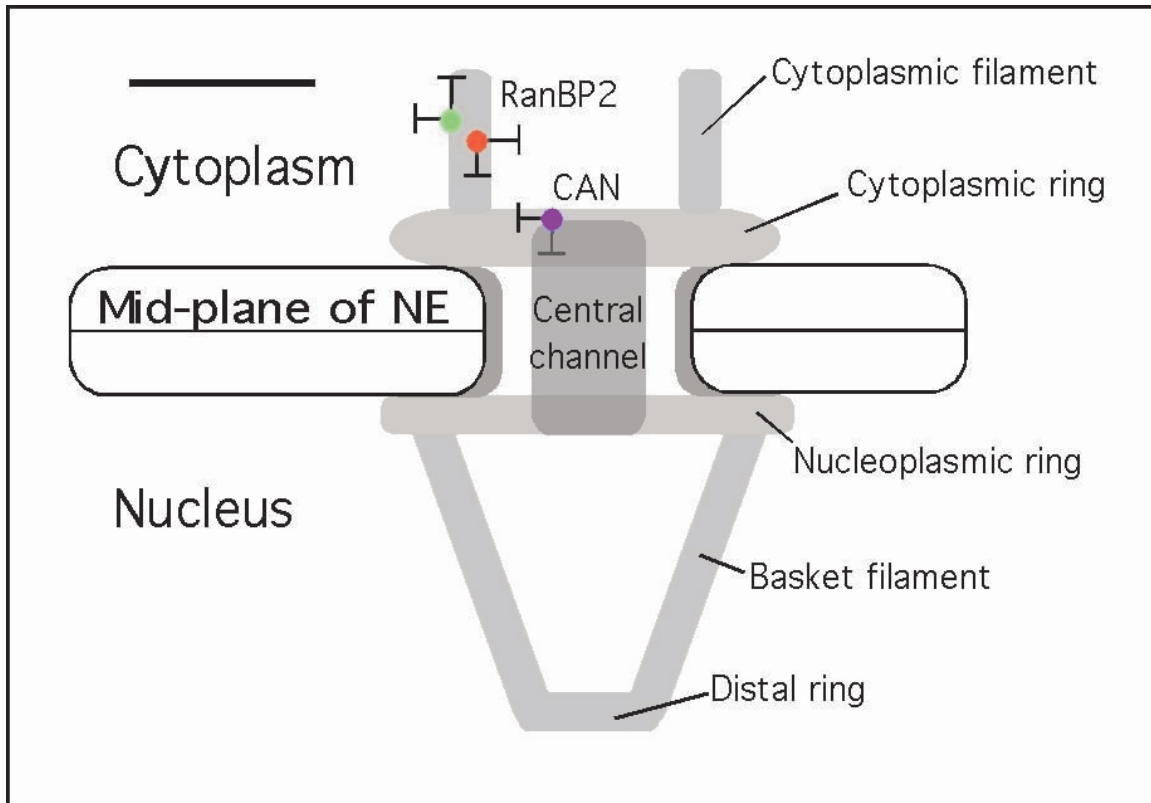
Figure 25: Model for the localisation of Nup214/CAN and Nup358/RanBP2 within the NPC. The position of gold particles in localisation experiments with anti-Nup358F is shown in green, anti-Nup358V in red and anti-Nup214 in blue. The substructures of the NPC are displayed in grey. Sizes were derived from (Akey and Goldfarb, 1989; Jarnik and Aebi, 1991; Akey and Radermacher, 1993; Goldberg and Allen, 1996) and own pictures. The standard deviation of the localisation mean is represented by error bars. Size bar = 50 nm.

Quantification demonstrated that the anti-Nup358V is located more proximal (51 nm from the midplane of the nuclear envelope with a standard deviation of 1.34 nm in a data set of n = 56) than the anti-Nup358F eptiope (57 nm from the nuclear envelope with 1.54 nm standard deviation in n = 50). This distance from the midplane of the nuclear

58

envelope also indicated that Nup358/RanBP2 was localised on the cytoplasmic filaments and this can be clearly seen on the TEM images shown in figure 24. Furthermore, the higher standard deviation for the datasets on Nup358/RanBP2 suggests that the epitopes localisation is more flexible than the localisation of Nup214/CAN. This is also consistent with Nup358/RanBP2 being part of the cytoplasmic filaments. From the relative localisation of the two epitopes of Nup358/RanBP2 one can further deduce that the N-terminus is located closer to the NPC core structure and that the C-terminus points out to the cytoplasm.

Taken together, the localisation experiments show that only Nup358/RanBP2, is part of the cytoplasmic filaments, whereas Nup214/CAN is likely to be part of the underlying cytoplasmic ring or the entrance of the translocation channel (see figure 25 for a summary). At this point however, it cannot be ruled out that Nup214/CAN is part of the base of the cytoplasmic filaments.

3.2.2 Antibodies against Nup358/RanBP2 decorate the cytoplasmic filaments but do not block NLS-mediated nuclear import when injected into *Xenopus* oocytes

To gain a first insight into the function of the cytoplasmic filaments in nuclear protein import, injection of high concentrations of antibodies against Nup358/RanBP2 into living *Xenopus* oocytes was performed. If the cytoplasmic filaments are required for nuclear protein import, a high concentration of antibody bound to Nup358/RanBP2 would sterically occlude them and thereby inhibit transport. The latter could be followed by a second injection of labelled cargo molecules in the cytoplasm at a later time point, subsequent dissection and analyses of the nuclear and cytoplasmic compartment. In order to calculate the amount of antibody that had to be injected, the number of Nup358/RanBP2 molecules was estimated on the basis of the following rationale. Given that stage VI oocytes contain an average of ca. 2.4×10^8 NPCs (of which 80% are in the annulate lamellae and 20% in nuclear envelope NPCs; Cordes et al., 1995) and assuming that maximally 16 copies of Nup358/RanBP2 (2 per rotational symmetry axis) are present per NPC, the maximal value of Nup358/RanBP2 molecules per cell, including a minor amount of soluble protein, is 4×10^9. Therefore 50 nl containing 4×10^{11} affinity purified

antibodies were microinjected per oocyte and this corresponded to a 100-fold molar excess over the epitope. In those experiments, no inhibition of the import of labelled BSA-NLS was observed (data not shown). It remained possible however, that a fraction of NPCs was not saturated by the antibody and that those mediated the observed protein import. To investigate this possibility, a more direct visualisation of protein import was employed. To this end, 10 nm colloidal gold was coated with BSA-NLS substrate. Together with the bound import receptors, this substrate has a diameter of up to 16 nm. After the first injection of anti-Nup358V into the cytoplasm, the oocytes were incubated for several hours to allow saturating binding of the antibody to the nucleoporin. Binding of the antibody to Nup358 was controlled by fixing a subset of the injected oocytes and immunogold labelling of the injected antibody and analysis by TEM. This showed that there was a cloud of gold particles around the NPCs in the nuclear envelope. Besides the staining of the annulate lamellae NPCs, there was no cytoplasmic staining detected and there was also no nucleoplasmic staining visible (data not shown). Then a second injection of the BSA-NLS coated gold particles in the cytoplasm was performed on the remaining oocytes (see figure 26 C for illustration). After further incubation to allow for import of the cargo, the oocytes were fixed and processed for TEM. Again, secondary antibody conjugated to 5 nm gold particles was used to detect the injected antibody in the fixed and sectioned samples. Figures 26 A show representative images where the peripheral cytoplasmic filaments of the NPC are densely decorated with 5 nm gold. Despite the strong labelling of the cytoplasmic filaments, the 10 nm gold particles carrying the import cargo could be detected both in to the central channel and the nuclear side of the NPC.
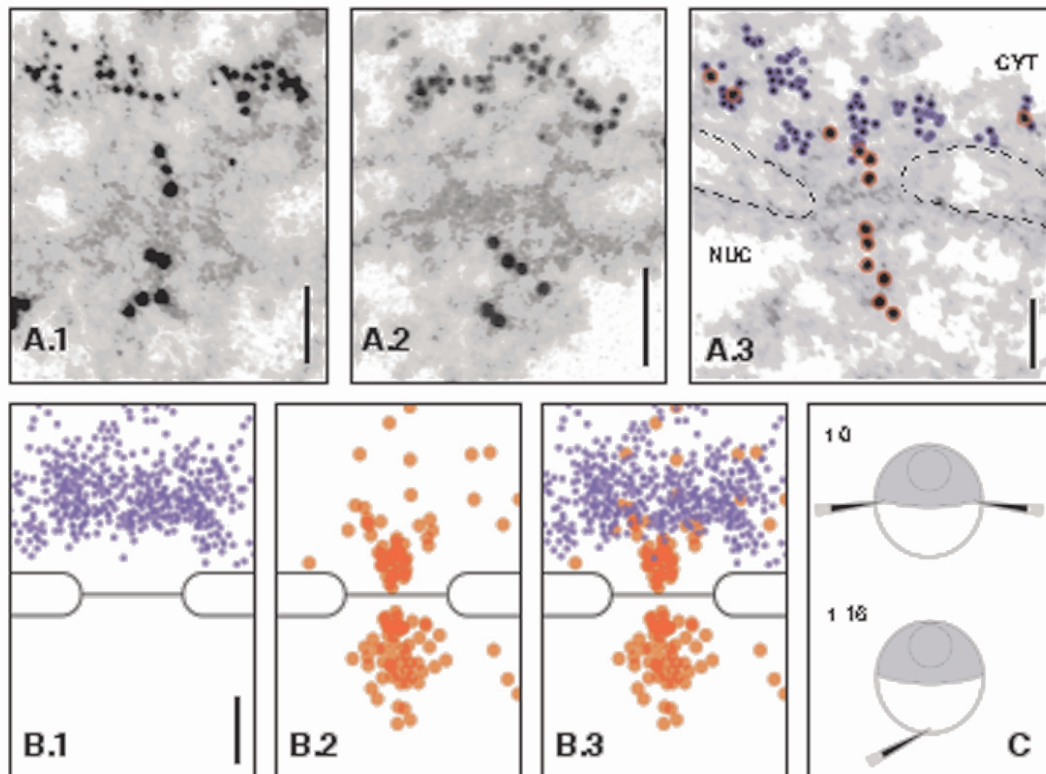
Figure 26: Antibodies against *Xenopus* Nup358/RanBP2 label NPC associated filaments *in vitro,* but do not prevent subsequent nuclear import of 10 nm golad particles coated with BSA-NLS. (**A**) TEM images of ultrathin sections through the NPCs of *Xenopus* oocytes following initial microinjection of 5 nm gold-coupled anti-Nup358V antibodies and subsequent injection of BSA-NLS coated 10 nm gold. (**B**) Overlay of several gold particles from several images relative to the nuclear membrane. 5 nm gold is shown in blue, 10 nm in red. (**C**) Schematic diagram of the performed injections.

In several experiments it was determined that the 10 nm gold particles were enriched at the nuclear periphery and throughout the nuclear interior independent of anti-Nup358V injection. The individual particles were traced on several pictures in different colours and the positions corresponding to the NPC were overlaid on a schematic summary figure (see figure 26 B). This shows that despite the blocking of the cytoplasmic filaments by antibody, the central translocation channel is still accessible and nuclear import, even of large cargoes, can still occur.

3.2.3   Depletion of Nup214/CAN and Nup358/RanBP2 from *Xenopus* egg extract

The cytosolic filaments and especially the Nup358/RanBP2 protein seemed to be dispensable for nuclear protein import. It remained possible, however, that the antibodies did not completely block the function of the protein. In order to more directly address the function of both Nup358/RanBP2 and also Nup214/CAN, the nuclear reconstitution system derived from *Xenopus* egg extracts was used. Analogous to the experiments performed to study the function of Nup153 (see figure 13), the aim was to deplete the two nucleoporins from the assembly reaction, assemble nuclei and study the effect on nuclear protein import in this clean loss-of-function situation.
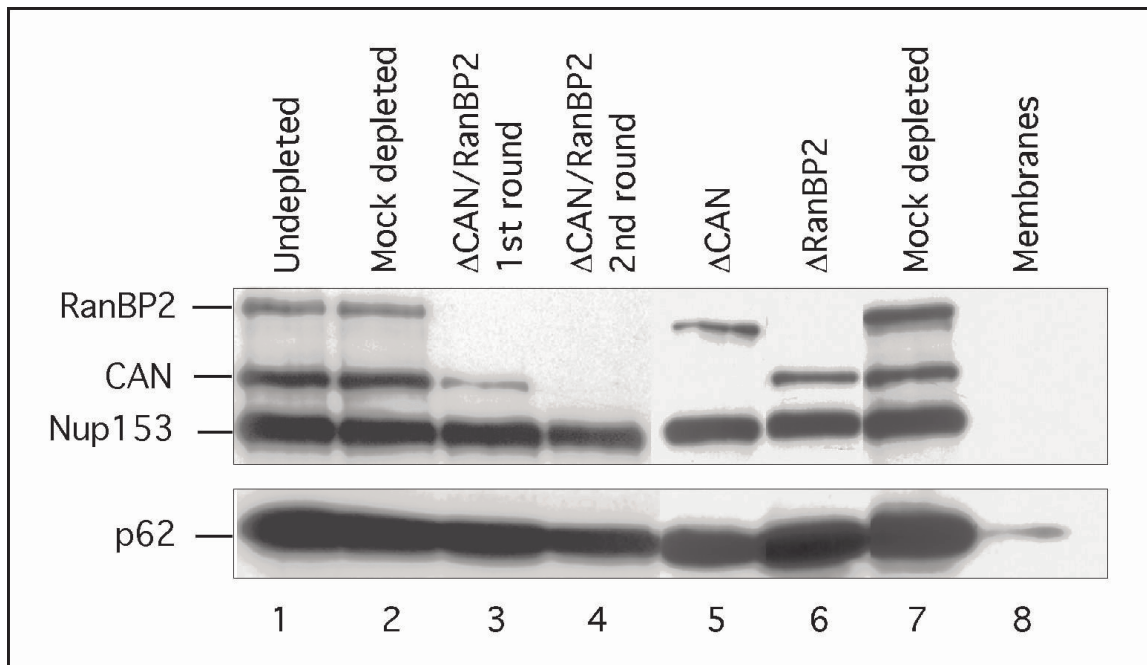
Figure 27: Immunodepletion of Nup214/CAN and Nup358/RanBP2 from *Xenopus* egg extracts. Western blot probed with the monoclonal mAb414 of undepleted (lane1) or immunodepleted (lane 2-7) extracts. Lane 8 shows the membrane fraction used for nuclear reconstitution. Positions of Nup358/RanBP2, Nup214/CAN, Nup153 and p62 are indicated on the left.

For the depletion, the anti-Nup358V and the anti-Nup214 antibodies were coupled to protein A-sepharose beads. In addition, columns were generated with a mixture of both antibodies. With these tools, Nup358/RanBP2, Nup214/CAN or both proteins were depleted from the soluble egg extract. Figure 27 shows a Western blot of the depleted

fractions probed with the monoclonal mAb414. For the complete removal of the proteins two rounds of depletion with equivalent volumes of saturated antibody resin and egg extract had to be performed. The Nup153 protein was not affected by the depletion and also the levels of the nucleoporin p62 remained constant, except for the depletions of Nup214/CAN for which a consistent co-depletion of a fraction of p62 was observed (figure 27). When a mock resin of protein A-sepharose cross-linked to non-immune rabbit IgGs was used in the same experiment, no reduction of any of the tested nucleoporins was observed. When the other components of the reconstitution system were analysed by Western blot, it was confirmed that the cytoplasmic soluble egg extract fraction was the only one that contained both Nup358/RanBP2 and Nup214/CAN (see also 3.1.3 above). Neither the membrane fraction (figure 27), nor the sperm chromatin preparation (see figure 13 above) contained any of the two proteins.

3.2.4 Nup214/CAN deficient nuclei retain cytoplasmic filaments and have a slight nuclear import defect

First, the effect of the absence of Nup214/CAN from the NPC was investigated. When the Nup214/CAN depleted extracts were combined with glycogen, an energy-regenerating system, a membrane fraction and chromatin prepared from sperm heads, nuclei were efficiently formed. In mock-depleted extracts, the anti-CAN antibody intensely stained the nuclear rim in immunofluorescence indicative of NPC staining. However, as expected, there was no Nup214/CAN detectable at the nuclear periphery of nuclei assembled from Nup214/CAN depleted extracts (figure 28 B.1).

When mAb414, which recognises mainly p62 under native conditions, was used there was a normal rim staining in both the mock and the Nup214/CAN depleted nuclei (figure28 B.2). When the nuclei were stained with the anti-Nup358V antibody the labelling intensity was the same for nuclei depleted from mock and Nup214/CAN depleted extracts (figure 28 C and D). Therefore, the incorporation of Nup358/RanBP2 is not dependent on Nup214/CAN.
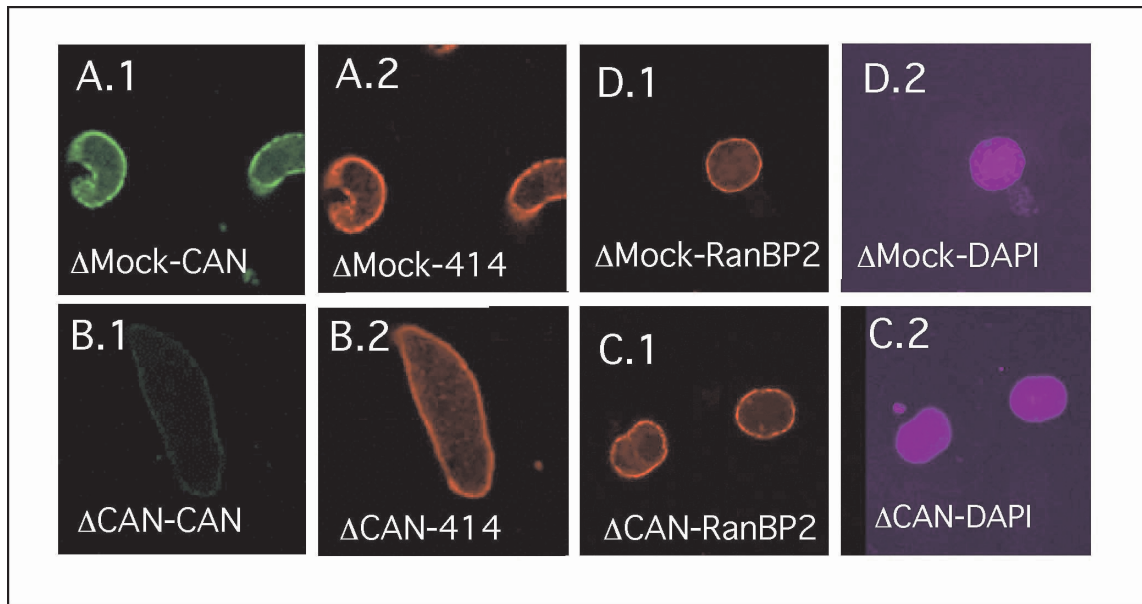
Figure 28: Nuclei assembled in Nup214/CAN depleted *Xenopus* egg extracts. Nuclei that lack Nup214/CAN retain Nup358/RanBP2 (**D.1** and **C.1**) The normal rim staining of with anti-CAN (**A.1**) however is completely abolished after depletion of Nup214/CAN (B.1). The chromatin appears normal in the nuclei depleted of Nup214/CAN (**C.2**) as compared to nuclei assembled from mock depleted extracts (**D.2**).

To analyse the effect of Nup214/CAN on the ultrastructure of the NPC, the cytosolic surface of the synthetic nuclei depleted of Nup214/CAN was imaged by FEISEM. For this purpose, nuclei were assembled *in vitro*, fixed, spun onto graphite chips, critical point dried and coated with chromium. Figure 29 shows a typical high resolution image of NPCs of Nup214/CAN depleted nuclei obtained in the FEISEM. The cytosolic filaments were clearly visible and appeared unaltered compared to the NPC filaments from nuclei assembled from mock depleted or undepleted nuclei (compare 29 with 32 A). This further supported the hypothesis that Nup214/CAN is not a part of the cytoplasmic filaments. The internal structures of the NPC were visible and sometimes the NPCs looked less dense than controls. However, this phenomenon was not reproducible and was not further analysed.
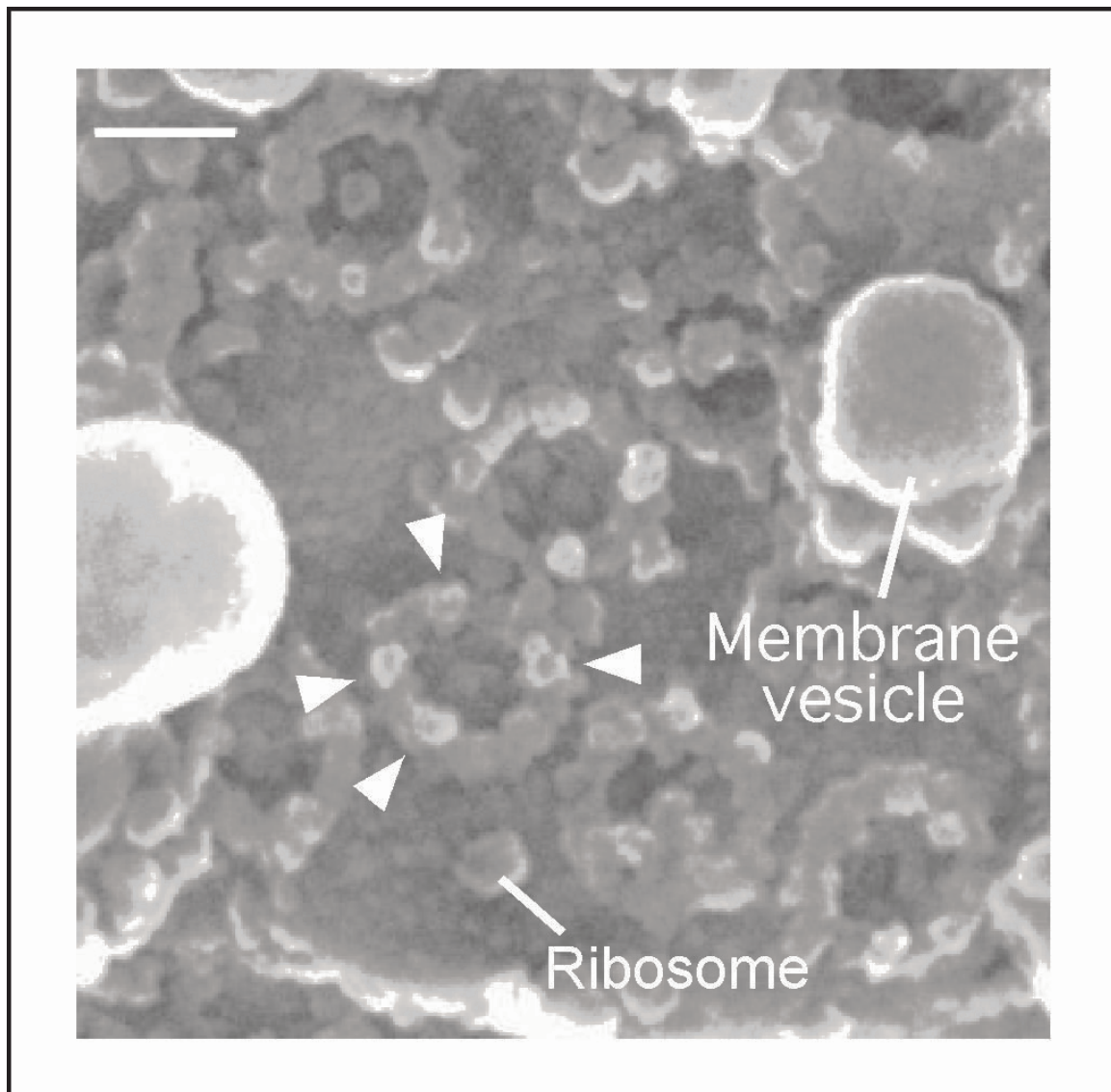
Figure 29: FEISEM image of a nucleus assembled in Nup214/CAN depleted extracts. The NPCs appear normal and retain their cytoplasmic filaments (indicated by arrowheads). Additionally, one of the ribosomes bound to the outer nuclear envelope and a membrane vesicle are indicated. Bar = 100 nm.

Previous genetic studies in mouse have demonstrated that knockout of Nup214/CAN is embryonic lethal. When the blastocysts of Nup214/CAN -/- embryos were studied pleiotropic effects were observed. The import of a substrate containing a classical basic NLSs into permeabilised cells derived from these blastocysts was reduced to 50% (van Deursen et al., 1996),

In synthetic nuclei deficient in Nup214/CAN, it is possible to address the function of Nup214/CAN in nuclear protein import more directly since labelled cargoes can be added

at defined time points and analysed after short periods in the complete absence of Nup214/CAN. This makes indirect effects less likely. To assess whether Nup214/CAN has a role in protein import into the nucleus, the model substrate described under 3.1.7. was used. BSA-NLS labelled with Alexa 488 was added to the assembled nuclei and after further incubation the nuclei were fixed. The imported cargo was visualised in these nuclei by confocal microscopy. After quantification, the import activity of Nup214/CAN nuclei was compared with the activity of mock nuclei and the efficiency was found to be reduced to ca. 75% of control levels (figure 30). This showed that the Nup214/CAN protein is not absolutely required for protein import into the nucleus.
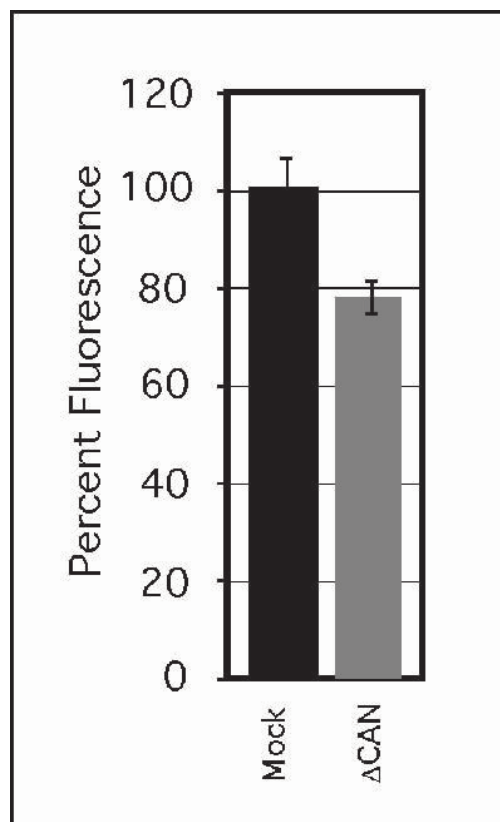
Figure 30: Nup214/CAN deficient nuclei show nuclear import of BSA-NLS reduced to 75%. *In vitro* assembed nuclei from mock or Nup214/CAN (ΔCAN) depleted extracts were incubated with FITC labelled BSA-NLS and TRITC labelled BSA-SLN. After 30 min the nuclei were fixed and the intranuclear signal was quantified on confocal microscopy images. Bars represent standard errors of mean values.

3.2.5   Nup358/RanBP2 deficient nuclei lack cytoplasmic filaments and import efficiently

Next, the effect of Nup358/RanBP2 depletion from the synthetic nuclei on NPC architecture and nuclear protein import was investigated. Similarly to extracts depleted of Nup214/CAN, Nup358/RanBP2 depleted extracts formed nuclei efficiently. Therefore, neither nucleoporin is required for the nuclear assembly process. In immunofluorescence experiments, no Nup358/RanBP2 could be detected at the nuclear rim of nuclei depleted of this nucleoporin. In contrast, a strong signal was observed in nuclei that were assembled in mock depleted extract (compare figure 31 A.1 with B.1).

Other nucleoporins were localised normally, as determined by immunofluorescence using mAb414 (figure 31 C). The exclusively cytoplasmically oriented Nup214/CAN was also present at the same level in nuclei assembled in mock and Nup358/RanBP2 depleted extracts (figure 31 E).

RanGAP, the GTPase activating protein for the RanGTPase required for nucleocytoplasmic transport (see Introduction 1.4.1.), is modified in the extract by the small ubiquitin like modifier SUMO. Sumoylation targets RanGAP to Nup358/RanBP2 (see Introduction 1.5.5. and Matunis et al., 1996; Mahajan et al., 1997; Matunis et al., 1998). Therefore, the localisation of RanGAP in the synthetic nuclei was examined by immunofluorescence. In contrast to the clear rim indicative of NPC staining detected in nuclei assembled from mock depleted extracts, there was no accumulation of RanGAP at the nuclear periphery of nuclei lacking Nup358/RanBP2 (figure 31 D).
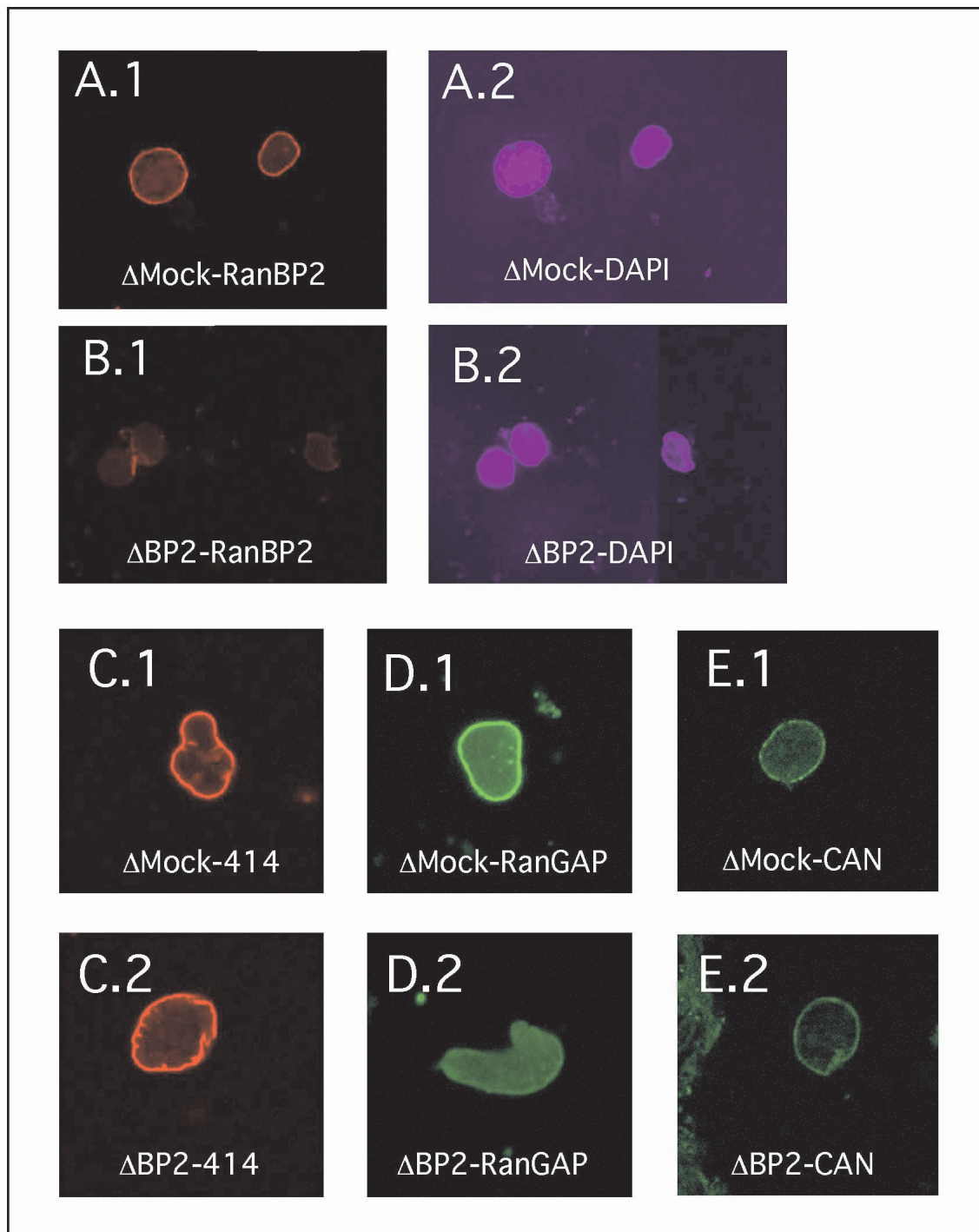
Figure 31: Nuclei assembled in Nup358/RanBP2 depleted *Xenopus* egg extracts. *In vitro* formed nuclei assembled either in mock (**A.1., A.2, C.1, D.1, E.1**) or Nup358/RanBP2 (**B.1, B.2, C.2, D.2, E.2**) depleted extracts were immunostained with anti-Nup358V (**A.1** and **B.1**), monoclonal mAb414 (**C.1** and **C.2**), anti-RanGAP (**D.1** and **D.2**) and anti-CAN (**E.1** and **E.2**) and stained with DAPI (**A.2** and **B.2**). Representative images are shown.

High resolution FEISEM was subsequently used to investigate the ultrastructure of the NPCs lacking Nup358/RanBP2, in particular of their cytoplasmic side. Representative images of NPCs without Nup358/RanBP2 are shown in figure 32 B and D.
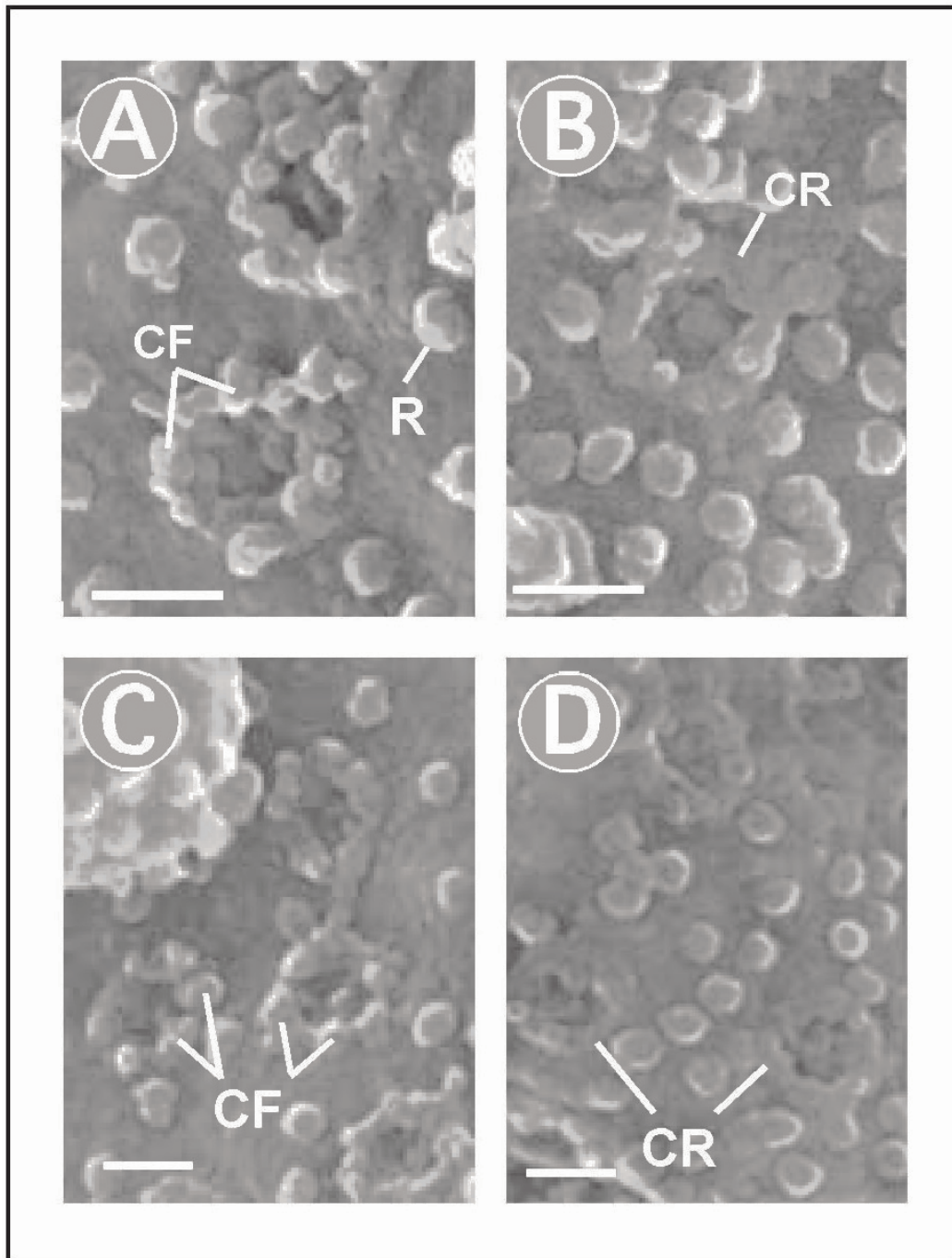
Figure 32: NPC lacking Nup358/RanBP2 show no cytoplasmic filaments. FEISEM images of the cytoplasmic surfaces of nuclei assembled in mock (**A** and **C**) or Nup358/RanBP2 depleted extracts (**B** and **D**). CF: cytoplasmic filaments; CR: cytoplasmic ring; R: ribosome. Bars = 100 nm.

In comparison to normal NPCs seen in nuclei assembled in mock-depleted extracts, these NPCs show an immature phenotype resembling intermediates in NPC assembly (Goldberg et al., 1992). More specifically, these NPCs lack the cytoplasmic filaments and the underlying cytoplasmic coaxial ring is exposed (compare figure 32 A and 32 B). This shows that the fibrillar structures on the cytoplasmic side of the NPC are dependent on the presence of Nup358/RanBP2 and, together with the localisation of the protein by electron microscopy (see 3.2.1), suggest that this nucleoporin is a major component of the filaments or is required for their attachment to the NPC.

Despite this apparent defect in NPC assembly and the lack of cytoplasmic filaments in Nup358/RanBP2 depleted nuclei, the import activity of the NPCs for classical NLS containing proteins remained unchanged (as determined by the accumulation of the import substrate BSA-NLS, see 3.1.7.). The quantification of the import reaction for nuclei from mock and Nup358/RanBP2 depleted extracts shown in figure 33 demonstrates that there is no significant difference in protein import activity.
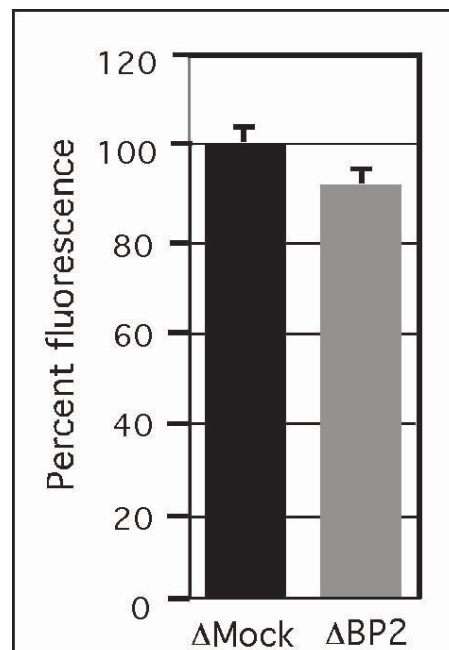
Figure 33: Nup358/RanBP2 deficient nuclei import BSA-NLS normally. *In vitro* assembled nuclei from mock (ΔMock) and Nup358/RanBP2 (ΔBP2) depleted egg extracts were assayed by addition of BSA-NLS and fixation after 30 min. Quantification of intranuclear fluorescence signal by confocal microscopy is shown. A small number of nuclei that did not exclude added BSA-SLN were excluded from the analysis.

3.2.6 Nup214/CAN and Nup358/RanBP2 deficient nuclei exhibit aberrant NPC morphology but show no further import defect

Although neither of the two cytoplasmically oriented nucleoporins, Nup358/RanBP2 and Nup214/CAN, was required for nuclear import, it was possible that the two proteins have a redundant function. In this case, a synthetic phenotype stronger than the defect observed in nuclei depleted of only one nucleoporin would be expected if both were removed.

To investigate this possibility, both Nup358/RanBP2 and Nup214/CAN were depleted from the *Xenopus* egg cytosolic fraction (figure 27). Nuclei formed efficiently in both mock and depleted extracts. These nuclei were analysed by immunofluorescence and figure 34 shows that, in contrast to nuclei assembled in mock-depleted extracts, the double depleted nuclei contain no Nup358/RanBP2 and Nup214/CAN at their nuclear rim. However, immunostaining with mAb414 demonstrated that NPCs were nevertheless present in the nuclear envelope of the depleted nuclei (figure 34 A.2 and C.2). The slight reduction in signal detected with this antibody on the depleted nuclei is probably due to the fact that mAb414 also recognises Nup358/RanBP2 and Nup214/CAN to a minor extent. To further characterise the nuclei assembled in Nup358/RanBP2 and Nup214/CAN double depleted extract, immunofluorescence with antibodies against several nucleoporins and nuclear proteins was carried out. No difference was detected in the nucleoporins Nup153, Nup98, and Tpr (see figure 34) that are all localised to the nucleoplasmic face of the NPC (Sukegawa and Blobel, 1993; Radu et al., 1995; Cordes et al., 1997b and 3.1.1). This indicated that the nuclear side of the NPCs was intact in the absence of Nup358/RanBP2 and Nup214/CAN.
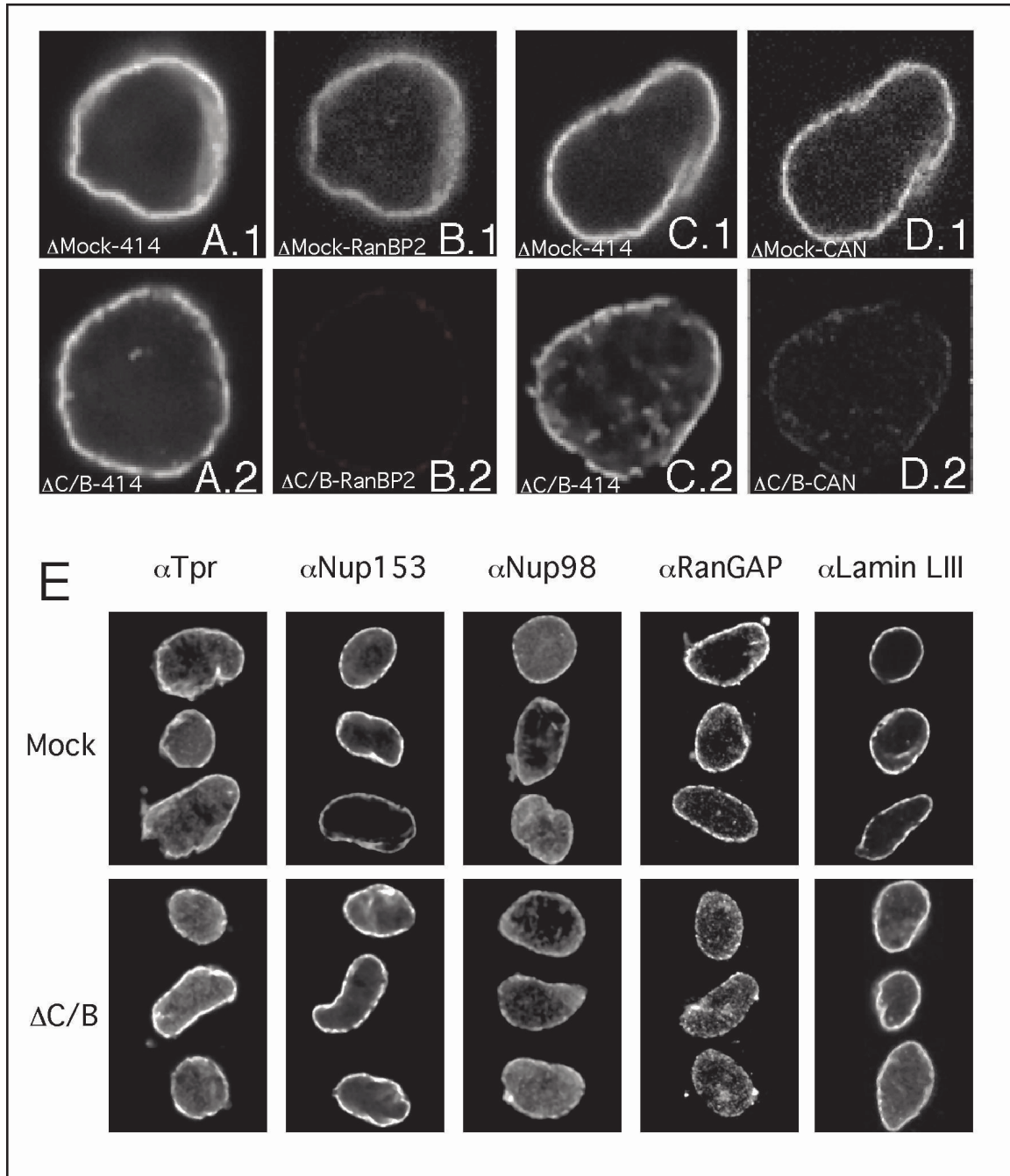
Figure 34: Nuclei depleted of Nup358/RanBP2 and Nup214/CAN. (**A-D**) Generation of nuclei that lack the nuceoporins Nup358/RanBP2 and Nup214/CAN. *In vitro* assembled nuclei in mock (Δmock, A.1, B.1, C.1, D.1) or double depleted (ΔC/B, A.2, B.2, C.2, D.2) *Xenopus* egg extracts were immunostained with the monoclonal antibody mAb414 (B.1, B.2, D.1, D.2) or the antibodies anti-Nup358V (B) or anti-CAN (D). Representative images are shown. (**E**) Nup214/CAN and Nup358/RanBP2-deficient nuclei retain nuclear NPC components and a nuclear lamina. Nuclei were assembled as above and immunostained with antibodies against Tpr, Nup153, Nup98, RanGAP and Lamin LIII as indicated.

The level of RanGAP staining was reduced to a similar level as in single Nup358/RanBP2 deficient nuclei (compare 34 E and 31 D.2). There was also no difference detected in the labelling with the monoclonal antibody S49 that is directed against the major form of lamins in *Xenopus* eggs, LIII (Lourim and Krohne, 1993; Lourim and Krohne, 1998), suggesting that the nuclear lamina is intact in the absence of Nup358/RanBP2 and Nup214/CAN (figure 34 E). Indeed, also nuclear growth, that is suggested to depend on a functional lamina (Meier et al., 1991; Spann et al., 1997; Yang et al., 1997b), appeared normal since the mean size of immunodepleted nuclei (diameter = 14.8 with a standard error of 0.5 µm) was similar to that of control nuclei (diameter = 15.6 with a standard error of 0.6 µm).
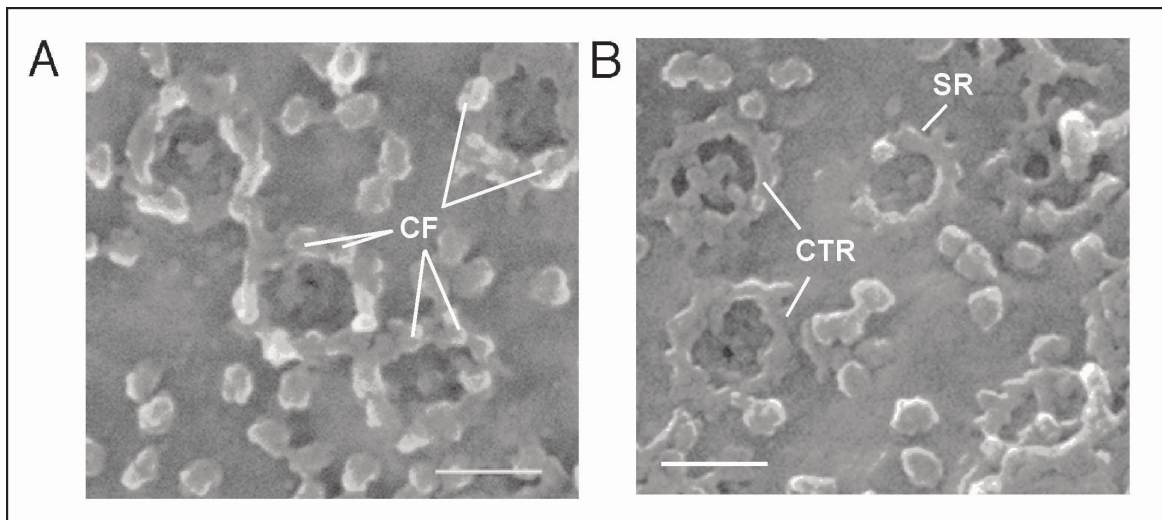
Figure 35: Nup358/RanBP2 and Nup214/CAN depleted nuclei lack cytoplasmic filaments and show an immature cytoplasmic coaxial ring. Nuclei assembled from Mock depleted (**A**) or double depleted (**B**) *Xenopus* egg extracts were imaged by FEISEM from the cytoplasmic side. CF: cytoplasmic filaments; CTR: cytoplasmic thin ring; SR: star ring. Bar = 100 nm.

When analysed by FEISEM, a striking phenotype of the cytoplasmic face of the NPCs became visible. None of the NPCs visualised on nuclei depleted of Nup358/RanBP2 and Nup214/CAN possessed any cytoplasmic filaments (compare figure 35 A and B). In most NPCs, not even the cytoplasmic coaxial ring could be detected (see figure 35 B). Instead, the underlying star rings with their ends buried in the nuclear envelope were often seen. These structures have earlier been described as intermediates during NPC assembly and

as functional subunits of NPC architecture (Goldberg et al., 1992; Goldberg and Allen, 1993).

The effect of these drastic alterations of NPC structure on nuclear protein import was assayed using the model substrates described in 3.1.7. Despite the complete absence of the cytoplasmic filaments, the import of labelled BSA-NLS was only mildly affected and reduced to 70% of the level of nuclei assembled from mock depleted extracts (see figure 36 A for quantification). This reduction is similar to the phenotype observed in nuclei deficient of Nup214/CAN alone (see above 3.2.4). Labelled BSA cross-linked to a peptide with the reverse sequence of the classical NLS was excluded from the depleted nuclei, indicating that the nuclei were intact and the accumulation of the substrate was signal dependent (figure 36 B).
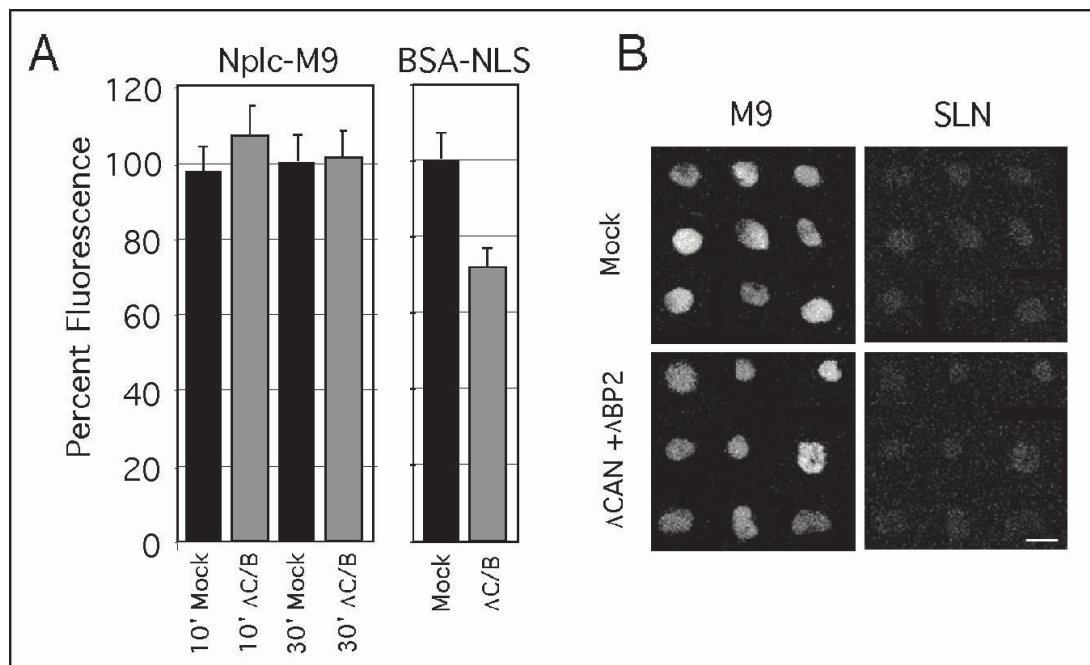
Figure 36: Nuclear import into Nup358/RanBP2 deficient nuclei. (A) Nuclei assembled in Nup358/RanBP2 and Nup214/CAN double depleted extracts (ΔC/B) show normal nuclear accumulation of M9-NPC (Nplc-M9) and slightly reduced accumulation of BSA-NLS, as compared to nuclei assembled in mock depleted extracts. The nuclei were fixed and imaged after 10 and 30 min for NPC-M9 or 40 min for BSA-NLS and the intranuclear signal was quantified. Bars indicate the standard error of the mean values of fluorescence intensity. (**B**) Nuclei that lack Nup358/RanBP2 and Nup214/CAN are not permeable to a 66 kDa protein. Random samples of (A) were analysed for their exclusion of BSA-SLN. No difference regarding nuclear exclusion of BSA-SLN was observed between nuclei reconstituted from mock or Nup358/RanBP2 and Nup214/CAN (ΔCAN+BP2) extracts. Bar =10 μm.

Another nuclear protein import pathway was tested by the addition of the labelled M9-NPC substrate. The level of nuclear import of this substrate was unaltered in nuclei formed in extracts depleted of Nup358/RanBP2 and Nup214/CAN both after a short time point and longer incubations (figure 36 A). To test for possible kinetic differences in nuclear import between control and Nup358/RanBP2 and Nup214/CAN deficient nuclei, M9 and GFP-NLS import was measured at 2 and 10 min, respectively, after the addition of substrate to the reaction. At the shorter time point, nuclear accumulation was still ongoing and therefore allowed a determination of the rate of import rather than the maximal level. As shown in figure 37 A, no differences in import rates were measured between nuclei formed in mock depleted and Nup388/RanBP2 and Nup214/CAN double depleted extracts. In addition, when GFP-NLS, which has one NLS per molecule, was used as a substrate, it accumulated even more efficiently in the depleted nuclei compared to the multivalent BSA-NLS, showing that the minor effect on import was not due to the presence of multiple input signals on each substrate.
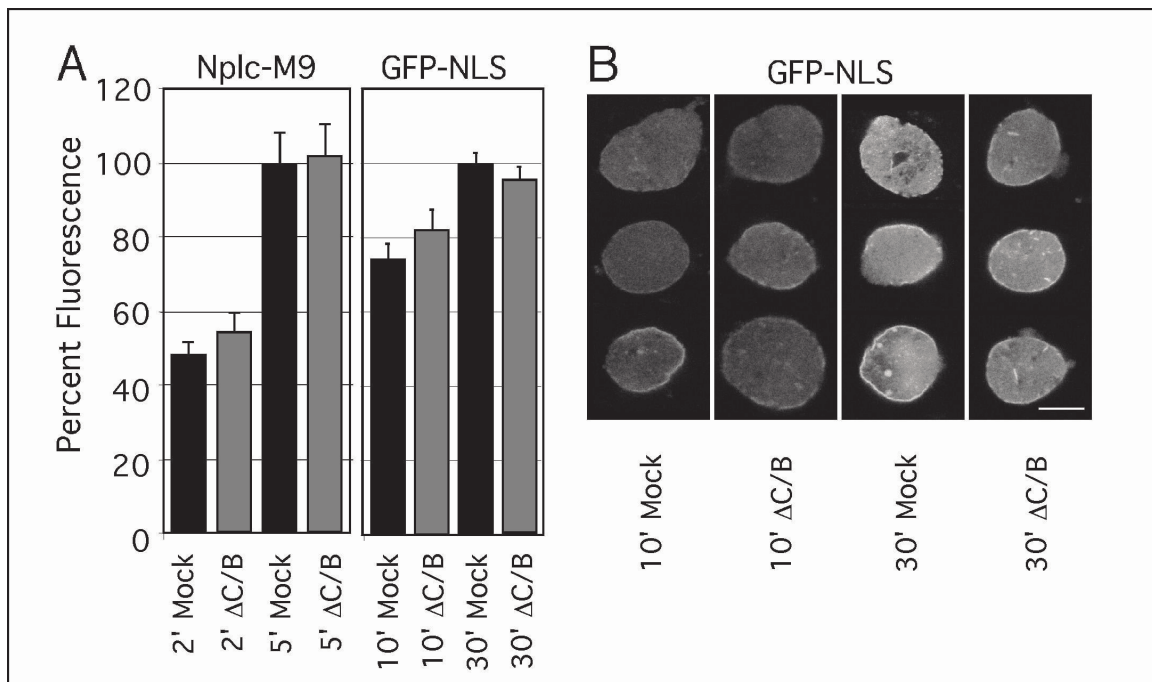
Figure 37: Initial importin β and transportin mediated protein import rates are unaltered in Nup358/RanBP2 and Nup214/CAN deficient nuclei. Nuclei assembled in mock or double depleted (ΔC/B) extracts were incubated with FITC labelled M9-NPC (Nplc-M9) or GFP-NLS. (**A**) After 2 and 5 min (NPC-M9) or 10 and 30 min the reactions were stopped by fixation and intranuclear signal was quantified by confocal microscopy. (**B**) Representative images of nuclei importing GFP-NLS are shown. Bar =10 μM

Synthetic nuclei are able to initiate a single round of semi-conservative DNA replication (Blow and Laskey, 1986), which is dependent on their ability to concentrate all the factors required for DNA replication in the nucleus (Walter et al., 1998). As a functional test for nuclear protein import of natural cargoes, DNA replication was assayed following the incorporation of the thymidine analogue 21-biotin-dUTP into the DNA of nuclei lacking both Nup358/RanBP2 and Nup214/CAN. As shown in figure 38, both double depleted and control nuclei showed a similar level of diffuse nuclear staining with numerous bright foci. The majority of this signal was absent when DNA polymerase alpha was inhibited by aphidicolin (figure 38), indicating that the signal resulted from DNA replication. Therefore one can conclude that in the absence of both Nup358/RanBP2 and Nup214/CAN, NPCs are capable of mediating the accumulation of replication factors inside the nucleus.
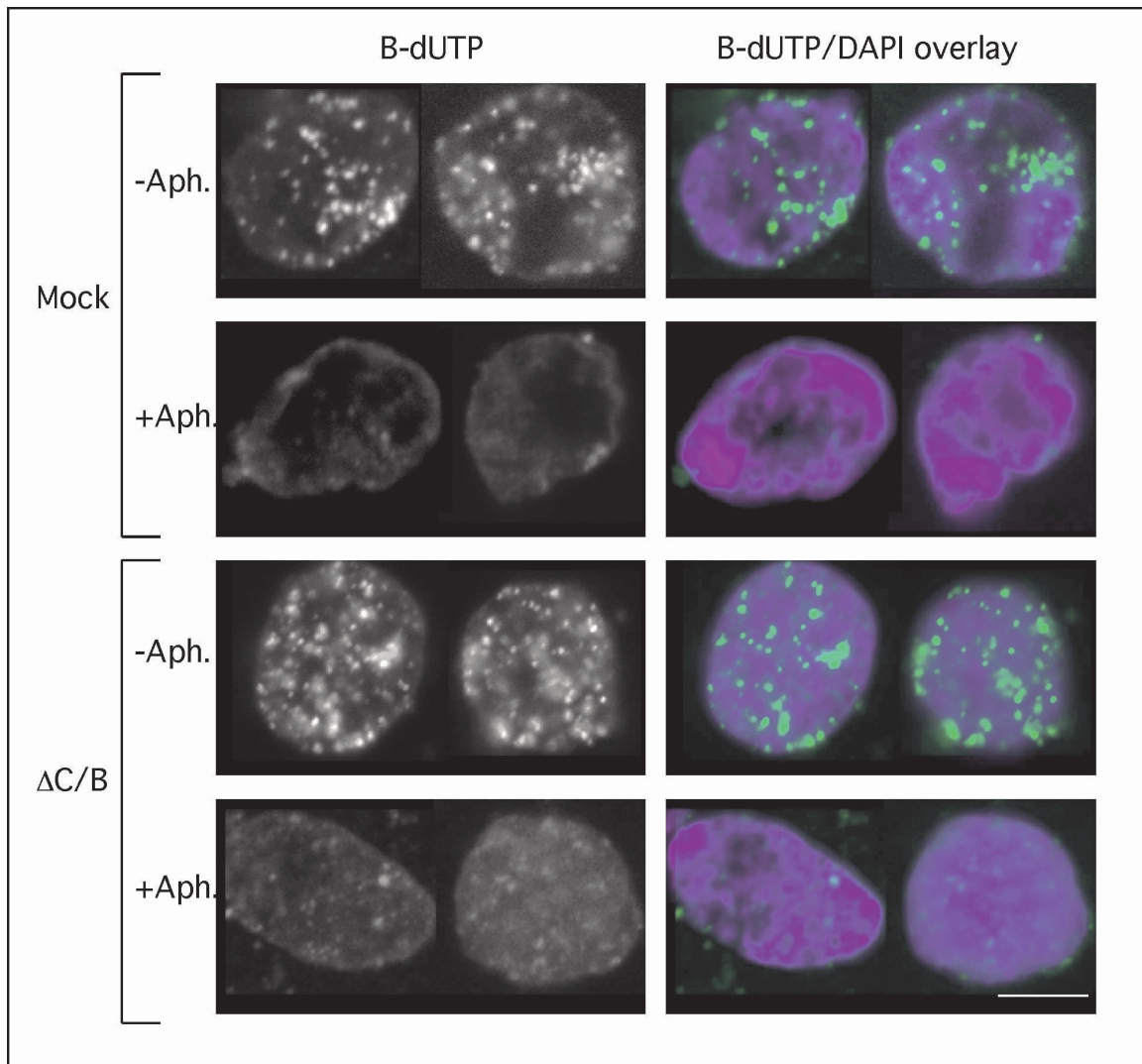
Figure 38: Nuclei deficient in Nup358/RanBP2 and Nup214/CAN are replication competent. Nuclei were assembled in mock or Nup358/RanBP2 and Nup214/CAN depleted (ΔC/B) extracts in the presence of 40μM 21-biotin-dUTP (B-dUTP) and in the presence (+Aph.) or absence of 14μM aphidicolin (-Aph.). Nuclei were fixed after 3 h and stained with streptavidin coupled to Alexa 488 (shown in the left panel and in green on the right) and DAPI. (blue in the right panel). Bar = 10 μm.

In summary, these data indicated that despite the drastic effect of the lack of Nup358/RanBP2 and Nup214/CAN on the morphology of the NPC, the translocation of proteins into the nucleus was not, or only mildly, affected.

4   <u>Discussion</u>

In this thesis, the localisation and function of several components of the NPC were investigated. The nucleoporins Nup153, Nup214/CAN and Nup358/RanBP2 that were known to be exclusively localised to one side or the other of the NPC were selected for analysis. Localisation of the proteins by immunogold labelling and electron microscopy confirmed this localisation and allowed the determination of their position within the NPC more precisely. Both Nup214/CAN and Nup153 were found to be located closer to the central core of the NPC than previously reported. The Nup358/RanBP2 protein was shown to likely be a major part of the cytoplasmic filaments.

To address the function of these asymmetric NPC structures in nuclear protein import, the nucleoporins Nup153, Nup214/CAN and Nup358/RanBP2 were depleted from a nuclear reconstitution system. The assembled nuclei lacked either the cytoplasmic filaments or the nuclear basket. Surprisingly, given previous publications on this topic, filaments were not required for nuclear protein import. In contrast, Nup153 deficient nuclei lacked the nuclear basket and did not accumulate a specific class of cargoes inside the nucleus. In addition, it could be shown that the nuclear basket is required for anchoring the NPC in the nuclear envelope.

4.1   <u>Synthetic nuclei assembled in *Xenopus* egg extracts: a system to study nucleoporin function</u>

Data on the function of nucleoporins has been obtained using genetic systems to create nucleoporin mutants. However, one problem with this approach is that these mutants often showed pleiotropic phenotypes and that deletion mutants are not viable. In addition, biochemical methods have been used to detect interactions between nucleoporins and transport factors (see Introduction 1.6). However, only nuclear reconstitution systems allow the removal of essential nuclear proteins and their characterisation in a loss-of-function situation independent from the constraint of viability of the organism.

In order to gain more insight into the function of nucleoporins, a system of nuclear assembly was developed following the pioneering work of Douglass Forbes and

colleagues (Finlay and Forbes, 1990; Finlay et al., 1991; Powers et al., 1995; Grandi et al., 1997). Compared to other systems of nuclear assembly, *Xenopus* egg extracts have several advantages. First, the starting material, the eggs, are readily available in relatively large quantities. This compares favourably to systems derived from cell culture, for example CHO cells (Burke and Gerace, 1986). In addition, the eggs and the extract prepared from them, are arrested in metaphase from which they can easily be released. *Xenopus* egg extracts can therefore recapitulate the cell cycle in a controlled manner and no synchronisation of cells is required to obtain an extract that assembles nuclear envelopes around chromatin. The major disadvantage of the system in the past was that the genome sequence of *Xenopus* is not known. This made cloning of genes of interest more laborious than in mammalian or yeast systems. However, in the recent years, an international EST project has provided considerable sequence information and thereby helped circumvent this problem (http://www.genome.wustl.edu/est/xenopus_esthmpg.html). Since *Xenopus* has been a model system for both cell biology and developmental biology for a long time, reagents, e.g. antibodies, are more frequently available than for comparable systems derived from starfish or other marine species (Collas and Poccia, 1998).

Together, these advantages allowed me not only to use the nuclear assembly assay described above for the characterisation of nucleoporin function, but also, in collaboration with members of the Mattaj laboratory, to characterise factors involved in nuclear envelope formation (Hetzer et al., 2000; Hetzer et al., 2001).

4.2   The nuclear basket: investigation of the Nup153 function

4.2.1   The localisation of Nup153 in *Xenopus* oocytes

To address the function of nucleoporins in transport and NPC architecture, it is very valuable to know their positions within the NPC to the highest possible resolution. This is especially important for those nucleoporins, which have been implicated in the mechanism of translocation by virtue of their binding to transport receptors or the phenotype resulting from their mutation. In order to obtain such structural information for

the FXFG repeat containing nucleoporin Nup153, a combination of electron microscopy techniques was used. Manually dissected *Xenopus* oocyte nuclear envelopes were chosen as samples because they are easily available, show a very high density of NPCs and therefore have been widely used for the characterisation of vertebrate NPC architecture (see for example Akey and Radermacher, 1993). Samples labelled with anti-Nup153 and a secondary antibody coupled to colloidal gold were imaged by FEISEM tomography to obtain a high resolution in the plane of the nuclear envelope with the relative position of the gold particles detected by their backscatter image. On the recorded images, the distance of Nup153 from the centre of the NPC could be measured. For best resolution in the perpendicular plane, thin sections were cut across the nuclear envelope and analysed by TEM. The images obtained were used to determine the position of the gold particles from the mid-plane of the nuclear envelope. It is important to obtain sections of only a fraction of the thickness of a NPC and to only use midsections in order to be able to use the images to measure the distance of the protein from the centre of the NPC. Since both methods, SEM and TEM, use the same buffer and fixation conditions up to the final stages of the preparation, the resulting data can be integrated into one model (see figure 11). That this is justified is also demonstrated by the observation that there is no significant difference in the position of the nucleoporins determined by the two methods. The localisation data suggests that Nup153 is most likely a component of the nuclear coaxial ring of the NPC or alternatively part of the base of the nuclear basket. However, since Nup153 remained on the NPC under conditions where the nuclear basket seems to be completely removed, the latter location is at least unlikely (see figure 10). These results are in agreement with the first localisation of Nup153 reported by Sukegawa and Blobel (1993). In this study, a polyclonal antibody against a N-terminal and a C-terminal portion of Nup153 was used to show that the protein is exclusively localised to the nuclear side of the NPC (Sukegawa and Blobel, 1993). A second study also reports a localisation similar to the one obtained here. When a monoclonal antibody against the human Nup153 was used, the protein was found to be located 50-55 nm away from the nuclear envelope midplane. However, gold particles were also found at larger distances from the nuclear envelope (200-300nm) (Cordes et al., 1993). This was interpreted to be in agreement with a third report that localised Nup153 to the terminal ring of the nuclear

basket (Pante et al., 1994). In this publication, which has been frequently quoted in the subsequent literature, an antibody was used that was directed against a 10 amino acid peptide derived from a C-terminal sequence of the human Nup153. However, later cloning and sequencing of *Xenopus* Nup153 showed that only 2 residues are conserved in this peptide between the two species (Shah et al., 1998). Since the peptide also contained an FXFG sequence, cross-reactivity with other nucleoporins seems very likely and can explain the apparent discrepancy between the data shown here and the localisation obtained with this antibody.

4.2.2 <u>The role of Nup153 in anchoring NPCs</u>

To understand the role of Nup153 in the architecture and assembly of the NPC, the composition of NPCs in Nup153 depleted nuclei was analysed by immunofluorescence. At least two additional components of the nuclear basket, Nup93 and Nup98 are missing in those nuclei (see figure 17). In addition, the Tpr protein, which is also localised to the nuclear side of the NPC and which is thought to form a filamentous network protruding into the nucleus, was not incorporated into NPCs lacking Nup153. Recently, experiments using RNA interference and immunolocalisation have suggested that Tpr might be the main constituent of the nuclear basket (Cordes et al., 1993; Cordes et al., 1997b; V. Cordes, personal communication). Importantly, none of these three nucleoporins was co-depleted with Nup153 as determined by Western blot. In addition, the reversal of the observed phenotypes by the addition of recombinant hNup153 demonstrates that the failure to localise these nucleoporins can be specifically attributed to the lack of Nup153. The effect on nucleoporin incorporation was not a general NPC defect since there was no difference observed in the incorporation of nucleoporins located further away form Nup153. The cytoplasmically oriented Nup358/RanBP2 and Nup214/CAN were present as was the major antigen recognised by mAb414, p62.

In contrast to NPCs in normal nuclei in either living vertebrate cells or assembled in extracts, the NPCs that lack Nup153, Nup93, Nup98 and Tpr became mobile within the nuclear envelope (Daigle et al., 2001; figure 18). This suggests that at least one of the components that is missing from the NPCs in nuclei assembled from Nup153 depleted extracts, forms a link to a stable nuclear structure, for example to chromatin, the

intranuclear filamentous network or the nuclear lamina. A good candidate for the protein providing a link between the NPC and chromatin or an intranuclear filament network is Tpr (Cordes et al., 1993; Galy et al., 2000; Zimowska et al., 1997). It is possible, albeit controversial, that Tpr forms an intranuclear network and it has been demonstrated that Nup98 interacts with Tpr (Fontoura et al., 2001). In the yeast *S.cerevisiae*, one of the two homologues of Tpr, Mlp2p, also interacts with the homologue of Nup93, Nic96p (Kosova et al., 2000; Strambio-de-Castillia et al., 1999). However, the anchoring of NPCs is not conserved across evolution since yeast NPCs are mobile within the nuclear envelope even though the interactions between the nucleoporins Tpr, Nup93 and Nup98 are also found in this organism. The loss of one of these interactions could rationalise the absence of these nucleoporins after the depletion of Nup153 and suggests that at least one of them directly requires Nup153 for its incorporation into the nuclear basket.

Alternatively, the nuclear lamina could anchor the NPC. Previously, several studies have implicated the lamina in maintenance of a normal NPC distribution. The P-element insertional mutation of lamin, Dm0, leads to a misdistribution of NPCs in the *Drosophila* nuclear envelope (Lenz-Böhme et al., 1997). In another invertebrate, the nematode *C.elegans*, the inhibition of the expression of the only identifiable lamin gene by RNA interference leads to a clustering of NPCs similar to the observation in Nup153 deoleted nuclei (Liu et al., 2000). A negative argument for a function of the nuclear lamina in NPC anchoring comes from yeast that does not have a clear lamin gene homologue and has NPCs that are mobile within the nuclear envelope.

Together, these arguments allow the formulation of three hypotheses for the explanation of the observed phenotype of NPC clustering in nuclei deficient of Nup153 that are not mutually exclusive. First, an interaction between Nup153 and the nuclear lamina could provide an anchoring link for the NPCs. In the absence of Nup153 the NPCs become mobile, stick together unspecifically, and this then leads to the observed clustering. A second possibility is that the Tpr protein links NPCs to the chromatin or an intranuclear filament network. Although this possibility is not supported by evolutionary arguments, at this point it can not be ruled out that Tpr mediates or contributes to the anchoring of

NPCs by a stable nuclear structure within the nuclear envelope. Third, Nup153 could be required for the assembly of the nuclear basket of the NPC and any of its components could make contact with the nuclear lamina or chromatin. In the absence of Nup153, the nuclear basket would not form and the NPCs would lose their attachment. Again, this could lead to NPC clustering due to unspecific protein-protein interactions between nucleoporins in a hydrophobic lipid environment.

4.2.3 The role of Nup153 in protein import

Since Nup153 interacts biochemically with several factors required for nucleocytoplasmic transport, including importin β, importin α, RanGDP and transportin, it was proposed that this nucleoporin has an important function in this process (Moroianu et al., 1997; Shah and Forbes, 1998; Shah et al., 1998). The interaction of Nup153 with importin β is very stable and can be readily detected in *Xenopus* egg extracts (Shah et al., 1998). Together with the localisation of the protein to the nuclear face of the NPC, this has led to the suggestion that Nup153 mediates the last step of the import reaction and/or the first step of the recycling of the transport receptor back to the cytoplasm. Consistent with such a model, it could be shown here that the depletion of Nup153 leads to a drastic reduction of the efficiency of nuclear import of cargoes with a "classical" basic NLS. However, Nup153 was not the only nucleoporin that was missing from the NPC after the depletion and the mislocalisation of some other component could also be responsible for the observed phenotype on nuclear protein import.

Two nucleoporins, Nup98 and Nup93, which also localise to the nuclear face of the NPC, were shown not to be incorporated in nuclei assembled from extracts depleted of Nup153 (see figure 17). However, genetic and biochemical depletion of the two nucleoporins that were found to be missing from the NPC do not support a role of these proteins in importin α/β mediated protein import into the nucleus.

When the murine Nup98 gene was disrupted by gene targeting, homozygous null mutant offspring were not viable. However, an embryonic fibroblast cell line could be cultivated from the inner cell mass. These cells showed a reduction in both M9 and classical NLS mediated protein import,which could be rescued by transfection of a Nup98 cDNA. However, in the CAN deficient fibrobasts other FG-repeat containing nucleoporins like

Nup214/CAN, Nup358/RanBP2 and p62 were not targeted correctly to the NPC (Wu et al., 2001). Therefore, a likely explanation of the observed defects in nucleocytoplasmic transport is that it is an indirect consequence of the inactivation of the Nup98 gene. In accordance with this hypothesis, biochemical depletion of Nup98 from an *in vitro* nuclear reconstitution system derived from *Xenpus* eggs does not lead to a reduction of importin α/β mediated protein import into assembled nuclei (Powers et al., 1995).

Independently, it has been shown tha immundepletion of a complex containing Nup93 from a nuclear assembly assay did not lead to a decrease of the import activity of the synthetic nuclei (Grandi et al., 1997).

A contribution of the mislocalisation of Tpr to the observed defect in nuclear protein uptake also seems unlikely. Initially, Tpr was found to localise to the NPC and protrude into in the nuclear interior as filamentous structure (Cordes et al., 1993; Zimowska et al., 1997). Subsequently it was widely believed that Tpr forms an intranuclear filament network that could serve as a nuclear matrix (see for example Fontoura et al., 2001; Zimowska et al., 1997). Recent experiments with anti-Tpr antibody injection into cells, electron microscopy localisation and RNAi knock down of Tpr expression suggest that Tpr is the main constituent of the nuclear basket and does not form a network in the nucleus of somatic cells (Frosst et al., 2002; V. Cordes pers. communication). Injection of anti-Tpr antibodies into mitotic cells led to a failure in protein incorporation into the NPC and subsequent degradation of Tpr. In those cells, Tpr was not detectable by immunofluorescence, but Nup153 was still present in normal levels. Protein export was impaired but importantly the import of cargoes carrying a classical NLS was unaffected. Thus, the defect in importin α/β mediated protein import into Nup153 deficient nuclei is not due to the concomitant loss of Tpr from these nuclei.

In summary, these observation suggest that the observed drastic reduction in classical NLS mediated nuclear import in the depleted nuclei is either due to Nup153 directly or due to the loss of another, as yet unidentified, nucleoporin from the NPC.

The fact that the import of M9 containing substrates into the nuclei reconstituted in Nup153 depleted extracts was not reduced shows that the NPC number does not become limiting for transport under the conditions applied. This also supports the hypothesis that

the interaction between Nup153 and transportin is not required for the M9 import pathway but rather for the nuclear import of Nup153 (Nakielny et al., 1999).

The very stable, RanGTP-sensitive, interaction between Nup153 and importin β, together with the fact that mutants of importin β that cannot bind to Ran bind the NPC strongly and block nuclear import in a dominant negative fashion, suggested that Nup153 might be the site of a terminal release step of the importin β cargo at the end of protein translocation (Kutay et al., 1997; Shah et al., 1998). If this were the case, one would have predicted an accumulation of importin α and β in Nup153 deficient nuclei due to inefficient recycling of the receptors to the cytoplasm. This was clearly not the case.

Another hypothesis for the function of the stable interaction of Nup153 with importin β is that this strong binding is required to remove receptor/cargo complexes from weaker binding sites within the NPC (Melchior and Gerace, 1998; Rout et al., 2000). In the Nup153 deficient nuclei, the lack of this strong binding site would lead to a build-up of trapped complexes inside the NPC, which would result in a strong increase of the rim signal of cargo and receptors. This was also not observed. In addition, one could predict a general block of all pathways through the NPC, which was also not the case. The defect of importin α/β mediated nuclear import is therefore most likely due to a reduction in the actual translocation and accumulation efficiency of import complexes (see also 4.5).

The requirement of Nup153 for the efficient transport by the importin β pathway, but not transportin mediated import supports a model in which different import pathways require different interactions between transport receptors and nucleoporins for their translocation through the NPC. Nehrbass and colleagues originally proposed this hypothesis on the basis of a mutation in the yeast nucleoporin Nsp1 (Nehrbass et al., 1993).

The reduction of import that was observed could also cause the failure to incorporate Nup98, Nup93 into the NPC and explain the lack of nuclear Tpr in the absence of Nup153, if any of these proteins is imported into the nucleus by a pathway that requires Nup153. One can speculate that this could be used for a hierarchical mechanism of NPC biogenesis in which the function of an import receptor mediating the import of one nucleoporin into the nucleus is dependent on the presence of another one. This would be an attractive mechanism to ensure the presence of the binding partner at the NPC, thereby

reducing the amount of free nucleoporins in the nucleoplasm and might be used for a cascade of interactions to assemble the nuclear parts of the NPC in an ordered way.

4.3 The cytoplasmic filaments: characterisation of Nup214/CAN and Nup358/RanBP2

Having established a role of the nuclear basket in nuclear protein import, the next question in the course of this thesis was to address the function of the asymmetric cytoplasmic structures of the NPC.

The cytoplasmic filaments have previously been implicated in nuclear protein import on the basis of several observations. First, the filaments have been colocalised with colloidal gold particles that were coated with BSA coupled to NLS peptides (Newmeyer and Forbes, 1988; Pante and Aebi, 1996a; Richardson et al., 1988; Rutherford et al., 1997). Secondly, they have been found to associate with a variety of factors involved in transport, namely, RanGTP, RanGAP, importin β and other transport receptors (Melchior et al., 1995; Yaseen and Blobel, 1999a; Yaseen and Blobel, 1999b). Thirdly, it was described that antibodies to Nup358/RanBP2, which was thought to be a component of the cytoplasmic filaments, can inhibit nuclear protein import when injected into cells (Yokoyama et al., 1995). In addition, it has also been suggested recently that the cytoplasmic NPC filaments contribute to the exclusion of non-imported proteins by Brownian motion, which would make the central channel non-accessible to proteins that are not able to bind to the filaments (Rout et al., 2000).

In contrast to the expectation from the indirect evidence in the literature, it was foundin this study that the cytoplasmic filaments are not required for at least two different nuclear protein import pathways.

4.3.1 <u>The composition of the cytoplasmic filaments</u>

Based on electron microscopical observations, two nucleoporins are commonly referred to as a part of the cytoplasmic filaments: Nup214/CAN and Nup358/RanBP2 (see for example Ohno et al., 1998; Stoffler et al., 1999a; Allen et al., 2000).

Two previous studies localised Nup214/CAN within the NPC by electron microscopy and concluded that this protein is part of the cytoplasmic filaments of the NPC. The images presented in the study of Kraemer et al. (1994) using an antibody directed against the central part of Nup214/CAN, are consistent with the data obtained in this thesis with an antibody recognising the N-terminus. When the mean distance from the mid-plane of the NPC of the 11 gold particles shown in Kraemer et al. (1994), is measured, one obtains 27 nm with a standard deviation of 7 nm. The localisation from the centre of the NPC, obtained in the same way, is 10 nm with a standard deviation of 7 nm. This localisation is not only within the spread of the data presented in this thesis, but also within the error. The second report in the literature by Pante et al. (1994), however, shows a clear and convincing labelling of the cytoplasmic filaments by their antibody against Nup214/CAN in immunogold labelling/electron microscopy. This antibody was raised against the purified native full length rat protein and was used to localise Nup214/CAN on *Xenopus* oocyte nuclear envelopes. The C-terminal domain of CAN/Nup214 is highly repetitive and contains numerous FG repeats and it remains to be shown to what extent cross-reaction of the latter antiserum with *Xenopus* proteins is specific for CAN/Nup214.

The data obtained in this thesis, however, show that Nup214/CAN is localised not on the cytoplasmic filaments, but close to the entrance of the central channel of the NPC. At least three lines of evidence contributed to this conclusion. First, high resolution tomography, in combination with immunogold labelling and detection gold on backscatter images, placed Nup214/CAN in a central position of the NPC as seen from the cytoplasmic side. Secondly, this localisation was confirmed by immunogold localisation by TEM on thin sections of nuclear envelopes, which also shows Nup214/CAN at a position close to the centre of the NPC rather than at the cytoplasmic filaments. Thirdly, the reconstitution of nuclei from extracts that were depleted of another nucleoporin, Nup358/RanBP2, yielded NPCs that did not possess any cytoplasmic filaments, but showed a normal labelling of Nup214/CAN by immunofluorescence. In

comparison to these nuclei, NPCs that are devoid of both Nup358/RanBP2 and Nup214/CAN not only lack the cytoplasmic filaments but also the underlying cytoplasmic coaxial ring. This suggests that Nup214/CAN might be part of this ring structure rather than the cytoplasmic filaments.

How can the localisation of Nup214/CAN reported in this thesis be connected to protein interactions of Nup214/CAN with other nucleoporins? Biochemical studies have demonstrated that Nup214/CAN interacts with the nucleoporin p62 (Finlay et al., 1991; Matsuoka et al., 1999). This interaction is easier to reconcile with a position of Nup214/CAN close to the entrance of the NPC channel than on the filaments, since p62 has been localised to this position as well as to the entrance of the channel on the nuclear side by pre-embedding and post-embedding immunogold labelling and TEM (Cordes et al., 1995; Grote et al., 1995).

The proposed localisation of Nup214/CAN at the cytoplasmic side close to the entrance of the translocation channel is also very similar to the localisation of Nup159/Rat7p, the closest homologue in the yeast *S.cerevisiae*, and suggests that there is a greater degree of evolutionary conservation between the two proteins than assumed so far (Kraemer et al., 1995; Rout et al., 2000).

Furthermore, the position of Nup214/CAN close to the entrance of the translocation channel would allow its FG repeats to be incorporated into the recently proposed meshwork of hydrophobic interactions required for the maintenance of the permeability barrier of the NPC (Ribbeck and Görlich, 2001).

In contrast to Nup214/CAN, the other asymmetrically localised nucleoporin Nup358/RanBP2 was clearly localised to the cytoplasmic filaments by two different antibodies, consistent with earlier reports in the literature (Wilken et al., 1995; Wu et al., 1995; Yokoyama et al., 1995).

Two more lines of evidence support the hypothesis that Nup358/RanBP2 is part of the cytoplasmic filaments and may be their major component. First, electron microscopy after negative staining of purified Nup358/RanBP2 shows particles of filamentous shape that are roughly 35 nm long (Delphin et al., 1997). This is in the range predicted for an extended molecule of 3224 amino acids and would also be consistent with the length of

the cytoplasmic NPC filaments. Secondly, the depletion of Nup358/RanBP2 from a nuclear reconstitution resulted in nuclei whose NPCs lacked their cytosolic filaments (see 3.2.5) and shows that the formation of the fibrillar structures is dependent on the presence of Nup358/RanBP2. This can be most easily explained by the hypothesis that Nup358/RanBP2 is the main component of the cytoplasmic filaments, even though other models cannot be ruled out at this point.

The localisation was performed using two different antibodies against Nup358/RanBP2. The anti-Nup358V antibody is directed against amino acids 2290-2314 of the human protein and anti-Nup358F recognises a sequence closer to the C-terminus of the protein corresponding to amino acids 2501-2900. On Western blots, both of these antibodies recognised only a single band of the expected size in *Xenopus* egg extracts. The use of these two different antibodies recognising different parts of the proteins allows to propose an orientation of Nup358/RanBP2. Since the anti-Nup358F antibody gave a more distal localisation than the anti-Nup358V antibody, one can suggest that the C-terminus of Nup3258/RanBP2 points out towards the cytoplasm. Consequently in this scenario, the N-terminus, which contains the leucine rich sequence and the leucine zipper, might be used to make contacts to other nucleoporins, anchoring the protein at the core structures of the NPC.

Nup358/RanBP2 is conserved throughout the evolution of metazoans but the yeast *S.cerevisiae* does not have a discernible homologue of this protein. Therefore, it remains to be determined, whether NPCs of this organism have functionally equivalent cytoplasmic filaments and if so, what their composition is.

In summary, the data in the literature and presented in this thesis strongly suggest that Nup358/RanBP2 is a component of the cytoplasmic filaments, whereas Nup214/CAN is not. Instead, Nup214/CAN is more likely part of the cytoplasmic coaxial ring. Furthermore, since NPCs deficient of Nup214/CAN had normal cytoplasmic filaments, it is not required for their anchoring at the NPC.

4.3.2 The role of the cytoplasmic filaments in nuclear protein import

One aim of this thesis was to investigate the role of nucleoporins which are localised on only one side of the NPC in nuclear protein import. Nup214/CAN and Nup358/RanBP2 have been selected for this analysis because both have been suggested earlier to have an important role in this process.

When Nup214/CAN was removed from the NPC, only a minor reduction of NLS mediated import by ~25% was observed. In an earlier report, the Nup214/CAN gene was inactivated by gene targeting in mouse. The resulting depletion of maternal gene product lead to Nup214/CAN being completely absent from blastocyst NPCs. At this stage, besides other effects, a reduction of the import of a classical NLS cargo to 50 % was observed (van Deursen et al., 1996). Even though the observations by van Deursen et al. (1996) and the data presented above result from two different model systems and differ quantitatively, in both cases import mediated by importin α/β was not completely blocked. This result is also in agreement with data from experiments in *S.cerevisiae*, where mutations in the closest homologue of Nup214/CAN, the Nup159/Rat7 gene, led to only limited and modest effects on protein import into the nucleus (Del Priore et al., 1997; Belgareh et al., 1998; Hurwitz et al., 1998).

However, the most surprising finding was, that there was no reduction in nuclear import mediated by either the M9 signal or a classical NLS in the absence of the cytoplasmic NPC filaments after depletion of Nup358/RanBP2. In contrast to previous suggestions, this demonstrates that the cytoplasmic NPC filaments do not serve as essential docking sites for cargo/receptor complexes (Newmeyer and Forbes, 1988; Richardson et al., 1988; Akey and Goldfarb, 1989; Moore and Blobel, 1992; Melchior et al., 1995; Pante and Aebi, 1996a; Mahajan et al., 1997).

How can the presented data be reconciled with previous observations that suggested an important role for Nup358/RanBP2 in an early step of nuclear protein import?

An early indication that Nup358/RanBP2 is involved in nuclear protein import came from an experiment where a polyclonal antibody directed against a GST-fusion to a fragment of Nup358/RanBP2 containing two Ran binding domains, several Zinc fingers and several FG repeats was injected into cells. This inhibited the import of cargoes containing a classical NLS (Yokoyama et al., 1995). The specific inhibition of the nuclear import

pathway mediated by importin α/β by some antisera cannot be excluded at this point, but the antibody used by Yokoyama et al. (1995) additionally labelled the nuclear face of the NPC when used in electron microscopic localisation experiments. This suggests that at least some of the antibodies of the polyclonal serum cross-reacts with other nucleoporins, like the Zinc-finger containing Nup153 or the FG repeat containing p62.

Additional evidence supporting a function of the cytoplasmic NPC filaments in nuclear protein uptake was obtained in electron microscopy studies that found "classical" basic NLS containing cargoes associated with them (Newmeyer and Forbes, 1988; Richardson et al., 1988; Akey and Goldfarb, 1989). This observation suggested a temporal arrest of the complexes before the actual translocation step. However, these studies did not address the necessity of such interactions for NPC translocation and therefore it is possible that they have another function unrelated to nuclear protein import.

A second line of evidence for a role of the cytoplasmic filaments in nuclear protein uptake came from reports showing accumulation of NLS cargoes at the nuclear envelope and, more specifically, at the cytoplasmic filaments under conditions of energy depletion, lack of the GTPase Ran, chilling to 4 °C or after the addition of the lectin WGA that binds a subset of nucleoporins and blocks nuclear transport (for example Dabauvalle et al., 1988; Featherstone et al., 1988; Richardson et al., 1988; Moore and Blobel, 1992; Chi et al., 1996; Rutherford et al., 1997). However, all these observations can also be explained without invoking a function of the cytoplasmic NPC filaments in nuclear protein import. Following the argumentation presented by Englmeier et al. (1999), the perinuclear accumulation of classical NLS containing substrates after energy depletion or lack of Ran can be explained by the failure in these situations to produce nuclear RanGTP (Newmeyer et al., 1986; Richardson et al., 1988; Moore and Blobel, 1992; Melchior et al., 1995). This however, is required for the terminal release of receptor/cargo complexes from the nuclear side of the NPC (Rexach and Blobel, 1995; Görlich et al., 1996). If this dissociation cannot occur, the central channel of the NPC might be blocked for subsequent rounds of import (Kutay et al., 1997) and receptor/cargo complexes would build-up at the cytoplasmic face and the filaments of the NPC. The "docking" that is observed under these conditions might therefore reflect association of

the import complexes with sites at the NPC that they would normally not bind to during translocation. It is noteworthy in this connection that Nup358/RanBP2 has only sparsely distributed FG repeats (which are believed to be interaction sites with transport receptors) and also has only a low affinity for importin β (Wu et al., 1995; Yokoyama et al., 1995; Ben-Efraim and Gerace, 2001).

Similarly, chilling of the import reactions to 4 °C could stabilise interactions between the receptors and FG repeat containing nucleoporins stalling the translocation complexes at the NPC and blocking further import. The block of nuclear protein import that is observed upon the binding of the lectin WGA to glucosamine O-linked to nucleoporins can readily be explained by the obstruction of sites that are normally required for translocation through the NPC. This would also lead to a build-up of complexes at the NPC, which might result in the apparent "docking" to the cytoplasmic NPC filaments Moreover, the association of Ran with the cytoplasmic filaments after the addition of non-hydrolysable GTP analogous can also be easily explained by the binding of RanGTP to the Ran-binding domains of Nup358/RanBP2 and does not necessarily reflect an early intermediate of the transport process (Melchior et al., 1995).

One model for the function of the cytoplasmic NPC filaments is that their induced bending towards the NPC translocation channel after the binding of receptor/cargo complexes "feeds" those into the NPC. This model was derived from TEM observations of colloidal gold particles coated with NLS substrates crossing the NPC (Pante and Aebi, 1996a; Rutherford et al., 1997). In these studies, the cargo possessed multiple NLS sequences, so it can be envisioned that the bound importin β molecules made contact to both the cytoplasmic filaments and FG repeat containing nucleoporins of the more central structures of the NPC and therefore led to a cross-link of these structures, which resulted in the observed occasional bending.

An alternative hypothesis for the function of the cytoplasmic filaments and Nup358/RanBP2 assumes that they serve to increase the concentration of the receptor /cargo complexes in the vicinity of the translocation channel and thereby to facilitate the translocation and to increase import efficiency (Rout et al., 2000; Ben-Efraim and

Gerace, 2001). In contrast to the prediction form such a model however, there was not even a minor reduction of import activity detected in the absence of Nup358/RanBP2, whereas the depletion of Nup214/CAN lead to a modest reduction. This shows that the system employed allows detection of minor changes and such changes were not measurable for nuclei deficient in Nup358/RanBP2 and Nup214/CAN.

In conclusion, the data presented here argue strongly against an essential role of the cytoplasmic filaments in nuclear protein import and therefore, by default, support models for the translocation mechanism that do not involve them (see below 4.5). All the indirect data present in the literature hinting to a function of the cytoplasmic filaments in transport can also be explained by alternative possibilities.

Of course, it is still possible that import of other cargoes, which are imported by pathways not dependent on the classical NLS or the M9 signal, require the cytoplasmic filaments for their nuclear import. However, nuclei that lack both Nup214/CAN and Nup358/RanBP2 support DNA replication showing that most major import pathways are intact, because this process is dependent on the accumulation of multiple nuclear replication factors (Walter et al., 1998). There also remains the possibility that very large cargoes require the filaments of the NPC for their efficient import. However, decoration of the filaments with antibodies injected into oocytes did not inhibit the import of colloidal gold particles that have a diameter of 10-16 nm (together with the protein coated onto them).

What then is the function of the cytoplasmic filaments? In this context it is interesting to note that the cyclophilin domain of Nup358/RanBP2 has been reported to interact with the 19S regulatory subunit of the proteasome (Ferreira et al., 1998). This subunit of the 26S proteasome has been shown to possess an unfolding and chaperone activity towards proteins. Such an activity is unlikely to be required for the nuclear import of proteins but could have another function.

Recently, it has been demonstrated that Nup358/RanBP2 also has E3 ligase activity for the sumoylation reaction (Pichler et al., 2002). The E3 enzymes direct the specificity of the final step of the protein modification by the SUMO moiety. All known substrates for

this reaction, except Nup358/RanBP2 and NPC targeted RanGAP, are nuclear proteins (Müller et al., 2001). This raises the interesting possibility that an interaction with Nup358/RanBP2 may be required for some cargoes so that they can be modified before being translocated through the NPC into the nucleus.

Another, not mutually exclusive possibility for the function of the cytoplasmic filaments is that they might be used to connect the nucleus to other structures in the cell. This would be important for processes of the cell cycle, like nuclear envelope breakdown, but also interphase processes, like nuclear migration. Recently, it has been shown that the microtubule network facilitates nuclear envelope breakdown at prometaphase by peeling the nuclear envelope off chromatin (Beaudouin et al., 2002; Salina et al., 2002). Since the only known structures that distinguish the outer nuclear envelope from the ER are the NPCs, it is possible that they mediate this process by binding to motor proteins or adaptors, which in turn connect to the cytoskeleton. The same rationale also applies for processes of nuclear migration, which are also dependent on the microtubule network (Reinsch and Karsenti, 1997; Reinsch and Gönczy, 1998). In this context, it is interesting to speculate that one of those functions could be mediated by the kinesin motors KIF5B and KIF5C that interact with Nup358/RanBP2 (Cai et al., 2001b).

That the NPC might be used to connect the nucleus to the cytoskeleton is also suggested by the localisation of the intermediate filament protein vimentin close to and possibly protruding from the NPC (Cai et al., 1997).

4.4 <u>Implication of the analysis of peripheral nucleoporins for NPC assembly</u>

One of the reasons to choose the nucleoporins that are more peripherally located within the NPC was that their removal was assumed to be less likely to result in a drastic change of the overall NPC architecture. Such a change would have made any result on the effect of the removal of the nucleoporin very hard to interpret. However, since there is hardly any data available on the assembly mechanism of the NPC, this proposition was speculative. Since the cytoplasmic filaments and the nuclear basket could be removed from the nuclear reconstitution system without affecting NPC formation, these structures are not required for the assembly. How can this be related to the published data on NPC biogenesis? NPC assembly in yeast occurs during the whole cell cycle, throughout which the nuclear envelope never breaks down (Winey et al., 1997). In contrast, in higher Eucaryotes two potentially different phases of NPC assembly can be distinguished. During S phase of the cell cycle the number of pore complexes roughly doubles (Maul et al., 1971; Maul et al., 1972). As the nuclear envelope remains intact during this phase, the new assembly of NPCs requires a fusion between the outer and inner nuclear envelope membrane. Since this two membranes face the ER lumen, they can topologically be considered outside surfaces of the cell. A fusion between inner and outer nucelar envelope therefore topologically resembles vesicle fission from the ER (Burke, 2001). However, the sheet character of both nuclear envelope membranes (as opposed to ER tubules) makes a similar fission mechanism unlikely. Similarly to the situation in S-phase, the number of NPCs increases after stimulation of quiescent cells by mitogenic agents (Maul et al., 1972). A second type of insertion occurs at the time of postmitotic nuclear envelope reassembly. In this process, the chromatin is first wrapped into an ER-like network. NPCs could be inserted into the holes that remain after membrane expansion and this process would not require any fusion of the nuclear envelope membranes.

One of the models for how NPC insertion occurs has been derived form the observation of ordered recruitment of nucleoporins to the nuclear envelope after mitosis. Nup153 and Nup358/RanBP2 are targeted to the chromatin early during the reformation of the nuclear

envelope, as compared to p62 or gp210 (Bodoor et al., 1999; Haraguchi et al., 2000). The hypothesis based on this observation is that the NPC is built sequentially, most likely starting from the nuclear side with Nup153 being recruited and subsequent targeting of the other nucleoporins. This hypothesis was indirectly supported by the isolation of Nup153 as homopolymeric complexes from extracts that could be a seed for NPC formation (Pante et al., 1994). A structure that could correspond to such a seed was directly observed in surface imaging of chromatin during early steps of nuclear envelope assembly in the *Xenopus* nuclear reconstitution system (Sheehan et al., 1988; Goldberg et al., 1992). The data presented in this thesis clearly show that Nup153 is not required for the formation of the central framework of the NPC. In addition, since the NPCs that still formed in the absence of Nup153 are likely to lack the entire basket structure, this peripheral structure as a whole seems not to be involved in NPC assembly. Instead, it is likely that Nup153 is recruited to the forming NPC via its interactions with a recently described subcomplex containing Nup96, Nup107, Nup133 and Nup160 (Vasu et al., 2001). This complex has been shown to be recruited to the chromatin even earlier than Nup153 (Belgareh et al., 2001). Nup153 in turn could then mediate the ordered assembly of the missing nuclear nucleoporins for whose import into the nucleus it is required.

Since the removal of the cytoplasmic filaments by depletion of Nup214/CAN and Nup358/RanBP2 did not abolish the formation of NPC, it can be concluded that only the central components are required for the assembly of the NPC. The function of the early recruitment of Nup358/RanBP2 and Nup153 to the chromatin after mitosis remains to be elucidated in the future (Boodor et al., 2000; Haraguchi et al., 2000). The data obtained in this thesis therefore indirectly support a model in which the NPC assembly starts with a fusion event between the inner and outer nuclear envelope, rather than with targeting of of nucleoporins to chromatin to first build-up the nuclear basket. This fusion between the outer and inner nuclear envelope membrane might also be connected to the fusion leading to a closed nuclear envelope (Kiseleva et al., 2001).

4.5   The role of peripheral nucleoporins in nucleocytoplasmic transport

Another main goal of this thesis was to gain a better understanding of the potential role of the peripheral asymmetric nucleoporins in the mechanism of protein translocation through the NPC. Especially the stable interaction of Nup153 with importin β and the observation of "docking" of NLS cargoes to the cytoplasmic filaments suggested a role of these nucleoporins in nuclear protein uptake. The generation of nuclei with NPCs that do not contain either the nucleoplasmic or the cytoplasmic asymmetric structures, namely the cytoplasmic filaments and the nuclear basket allowed several models for the mechanism of nuclear transport to be tested and ruled out. It also allows the formulation of a more precise hypothesis.

One of the models, proposed by Pante and Aebi is that the cytoplasmic filaments bind to the transport cargos in the cytoplasm and then feed them into the central translocation channel (Pante and Aebi, 1996a; and 4.3.2). With the demonstration that the actual translocation through the NPC can be reversed by inverting the gradient of RanGTP across the NPC it became very unlikely that such induced filament bending represents a necessary step during protein import (Nachury and Weis, 1999). The data presented in this thesis, that the removal of the cytoplasmic filaments does not result in even a modest decrease of nuclear import efficiency for at least two major protein import pathways, further shows that this model cannot accurately describe protein translocation into the nucleus.

In the "Brownian gated diffusion" model, the cytoplasmic filaments have also been suggested to play a major role in protein translocation. In this scenario, the random Brownian movement of the cytoplasmic filaments would beat away all proteins that cannot bind to them and thereby prevent their entry into the central NPC channel. Receptor/cargo complexes that could bind to the filaments would not be excluded from the entrance area but, in contrary, would be concentrated by the docking step. Subsequently, the receptor cargo complexes would diffuse along the FG repeat containing nucleoporins of the central translocation channel into the nucleus, where they

would be disassembled by RanGTP (Rout et al., 2000). The data of the Nup214/CAN and Nup358/RanBP2 depletions argue against such a mechanism. First, the removal of the cytoplasmic filaments would be predicted to result in an increase of the passive permeability of the NPC, which was not observed when labelled BSA coupled to a peptide with the reverse NLS sequence was used. Second, in the absence of the filaments, there is no docking-mediated concentration of receptor/cargo complexes in the vicinity of the NPC entrance. If this were important for nuclear protein uptake, as suggested by this model, this should result in at least a reduction of import efficiency. However, no such decrease was observed.

A third model that has recently been proposed on the basis of kinetic experiments is that the FG repeats of nucleoporins form a hydrophobic meshwork within the central NPC channel and that most proteins get excluded from this due to their hydrophilic surfaces. Transport receptors can incorporate into this meshwork and thereby quite freely diffuse through the NPC channel. The RanGTP gradient would allow their disassembly only on the nuclear side and thereby provide directionality (Ribbeck and Görlich, 2001). This model has been backed up by data showing that import receptors bind to hydrophobic interaction resins like phenyl-sepharose and that the permeability barrier can be compromised by the addition of hexandiole, which is thought to weaken or break-up the meshwork (Ribbeck and Görlich, 2002). Whereas this hypothesis can quite convincingly explain the nature of the diffusion barrier through the central channel of the NPC, it fails to explain the role of some nucleoporins for specific transport pathways. Such specificity has been demonstrated for several yeast nucleoporin mutants and in this thesis for the vertebrate Nup153. If the only role of the Nup153 FG-repeats was to contribute to a hydrophobic meshwork, then it cannot be explained that their removal would selectively affect one import pathway. Furthermore, Nup153 is located at the nuclear side of the NPC where translocation is thought to have reached completion and its removal would therefore not affect the acces to the NPC channel from the cytoplasmic side.

Another model that has been put forward is that increasing affinities between nucleoporins and transport receptors along the distance of the NPC determine the direction of translocation. Due to the observed stable interaction between importin β and Nup153 this nucleoporin has been proposed to be the terminal and highest affinity binding site of such a chain (Ben-Efraim and Gerace, 2001). However, several considerations and experimental datasets indicate that this "affinity gradient" model cannot explain the mechanism of translocation into the nucleus. Thermodynamics states that only the last and strongest interaction between the receptor/cargo complex and a nucleoporin would contribute with its free binding energy ΔG to the directionality of transport. All other binding reactions have to be reversed during transport. Since the rate constant for association is predicted to be the same for all the interactions, the increasing affinity would be achieved by decreasing dissociation rates. This would lead to a less effective, rather than a more rapid translocation as compared to diffusion. Only the terminal interaction could provide binding energy since it would not be directly reversed, but compensated by the binding of RanGTP to the receptor and therefore indirectly by the unequal gradient of RanGTP versus RanGDP across the nuclear envelope. Two lines of evidence argue that this cannot be a general mechanism for transport. The actual translocation does not need any nucleotide hydrolysis and the directionality of transport is only indirectly driven by the energy stored in the RanGTP gradient across the nuclear envelope (Schwoebel et al., 1998; Englmeier et al., 1999). Together with the observation that directionality can be reversed by the reversal of the RanGTP gradient across the nuclear envelope, this indicates that the ΔG of the nucleoporin/receptor interactions are not a necessary prerequisite to obtain directionality of transport (Nachury and Weis, 1999). Instead, this again demonstrates that the RanGTP gradient alone is sufficient to drive directionality of translocation.

Another argument against the "affinity gradient" model is provided by the fact that the lack of Nup153 from the NPC does not result in a reduction of import of M9-containing cargoes. Whereas the decreased efficiency of import of cargoes with a classical NLS would argue that the binding of receptor/cargo complexes could facilitate nuclear import, this demonstrates that it is not an absolute requirement. It is not even a requirement for all transport pathways mediated by importin β since the large U snRNPs can be imported

into the nucleus in a Ran independent manner, specifically when bound to importin β via the IBB of the canonical adaptor Snurportin 1, but not when bound via the IBB of importin α (Huber et al., 2002). If the free binding energy ΔG of importin β and Nup153 would contribute to the directionality of this transport, then a build-up of cargo complexes at the NPC in the absence of RanGTP, which is required to release the complexes, would be expected. However, this was clearly not observed in the experiments by Huber and colleagues (2002).

An explanation for the role of the stable interaction between transport receptors and transport cargo is provided by the "tethered diffusion" model (Fornerod, M., personal communication). In this model, some nucleoporins, which are anchored on one side of the NPC, would reach through the central NPC channel with their unstructured FG-repeat domains. Nup153 for example would then bind to importin α/β cargo complexes in the cytoplasm. The domain would then swing through the channel and the bound complex could be disassembled in the nucleoplasm by RanGTP. In this scenario, the binding to the nucleoporin in the cytoplasm would be made more favourable by the release of ΔG in the cytoplasm The dissociation of import complexes from the NPC in the nucleoplasm could energetically be compensated by the very stable binding of RanGTP to importin β. This model would rationalise that Nup153 seems to be accessible for antibodies from the cytoplasmic side (Nakielny et al., 1999). However, some of the restrictions that apply to the "affinity gradient" model may also be valid here: There seems to be no general requirement for a stable interaction since some very large cargoes can be translocated even in the absence of RanGTP.

A synoptic model that tries to incorporate published data, results obtained in this thesis and theoretical considerations, is based on the concept of two-dimensional diffusion (figure 39).
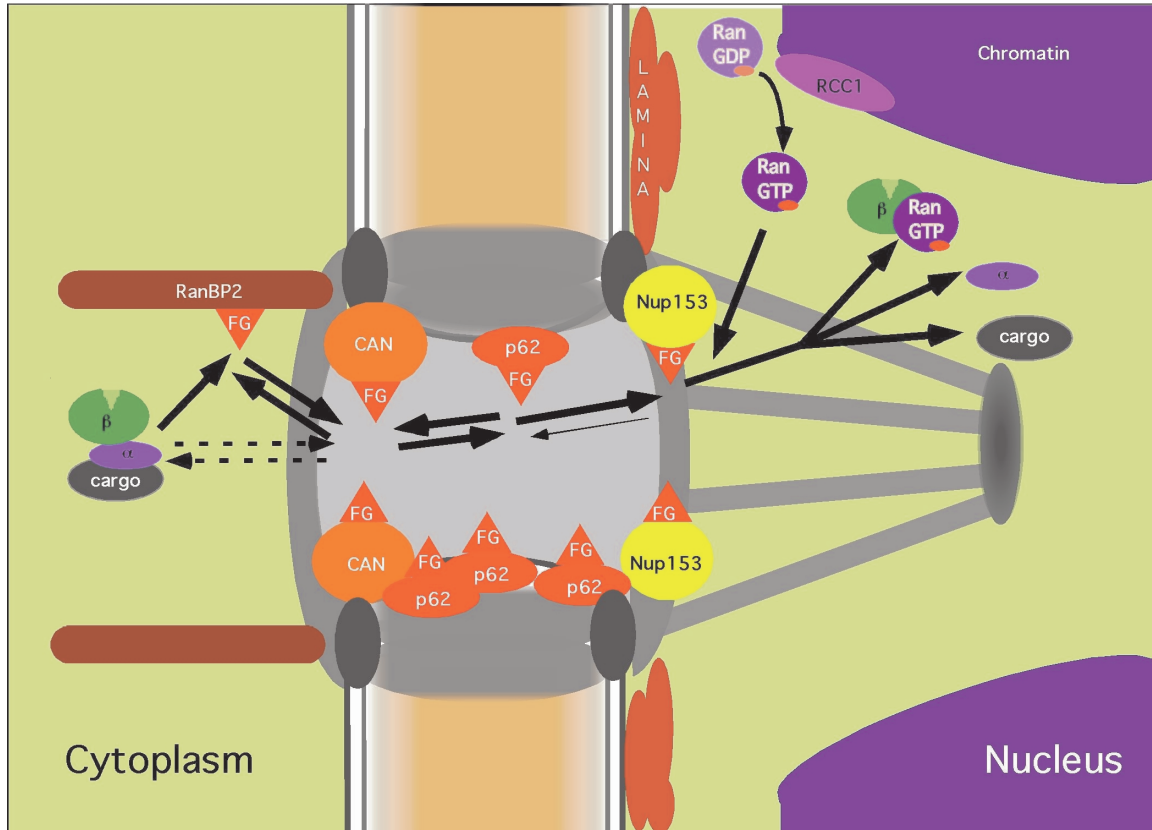
Figure 39: Model for the mechanism of nuclear transport. The black arrows represent association or dissociation rates between import complexes and nucleoporins. The thin line from Nup153 represents the low dissociation rate. The dashed line shows the pathway in the absence of the cytoplasmic filaments. Detailed explanation in the text.

It is necessary for an accurate description of nuclear import to make a distinction between the actual translocation and the processes that allow accumulation of cargoes in the nucleus. For the actual translocation the FG repeats that line the central channel could provide a track-like "gliding" surface along the central channel of the NPC. Similar, low association rates and the low affinities of the nucleoporins to transport receptors predict high dissociation rates, which would allow rapid movement back and forth in the channel.

In this model, accumulation of cargo complexes and the directionality of import are provided by the Ran system, which allows disassembly of transport complexes in the nucleoplasm. Additionally, the stable binding of import complexes to Nup153 would facilitate accumulation of nuclear proteins. These interactions lead to an increase in resident time of the import complexes at the nuclear side of the NPC by a lowered dissociation rate from Nup153. This would lead to a higher probability to meet nuclear RanGTP and thereby assist the import reaction. The defect in nuclear accumulation observed in nuclei whose NPCs lack Nup153 can therefore be explained not by a block in translocation, but a reduced efficiency of accumulation. In the absence of Nup153 "reverse" translocation back out of the NPC into the cytoplasm would be more likely. Again, binding to stable nucleoporins would not be an absolute requirement for import, but a facilitator. A similar role of facilitating import by shifting the equilibrium distribution of import complexes between cytoplasm and nucleoplasm may be provided be release of binding energy upon binding to nuclear sites away from the NPC, like chromatin or nuclear bodies. This would also lead to an increased rate of dissasembly of import complexes in the nucleus by RanGTP. The diffusion barrier for proteins above a certain size limit could be provided by repulsion of the surfaces of soluble proteins from the hydrophobic NPC channel or by a meshwork of FG interactions.

From such a model, as well as from the "tethered diffusion" model, one could predict that the removal of Nup214/CAN, which has a stable binding site for the export receptor CRM1, from the NPC would lead to a decreased efficiency of nuclear protein export (Fornerod et al., 1997b). This possibility and others will have to be investigated in the future to further clarify the translocation mechanism through the NPC.

5 Materials and Methods

5.1 Materials

5.1.1 Chemicals

2-Mercaptoethanol	Sigma-Aldrich (Steinheim, Germany)
A23187	
(1-(4,5-dimethoxy-2-nitrophenyl)ethyl ester)	Molecular Probes (Göttingen, Germany)
Acetic acid	Merck (Darmstadt, Germany)
Acrylamide/Bisacrylamide, 37.5:1 (30% w/v)	
(Protogel®)	National Diagnostics (Hull, UK)
Alexa Fluor® 546 C5 maleimide	Molecular Probes (Göttingen, Germany)
Ampicillin, Binotal®	Grünenthal (Aachen, Germany)
APS (ammonium peroxodisulfate)	Sigma (St. Louis, USA)
ATP (adenosine 5´-triphosphate)	Sigma-Aldrich (Steinheim, Germany)
Bacto agar	Gibco BRL (Eggenstein, Germany)
Bacto tryptone	Gibco BRL (Eggenstein, Germany)
Bacto yeast extract	Gibco BRL (Eggenstein, Germany)
BH_3O_3 (boric acid)	Merck (Darmstadt, Germany)
Bio-Rad protein assay	Bio-Rad (München, Germany)
Bromophenol blue (3',3'',5',5''-tetrabromo-	
phenolsulfonephthalein)	Sigma (St. Louis, USA)
$CaCl_2$	Merck (Darmstadt, Germany)
Complete EDTA-free Protease Inhibitor	Roche (Mannheim, Germany)
Coomassie brilliant blue G-250	Sigma-Aldrich (Steinheim, Germany)
Creatine phosphate	Roche (Mannheim, Germany)
Cycloheximid (3-[2-(3,5-dimethyl-2-	
oxocyclohexyl)-2-hyroxyethyl]glutarimide)	Sigma-Aldrich (Steinheim, Germany)
Cysteine	Sigma-Aldrich (Steinheim, Germany)
Cytochalasin B	Sigma-Aldrich (Steinheim, Germany)
DAPI (4',6-diamidino-2-phenyindole)	Sigma-Aldrich (Steinheim, Germany)
$DiOC_{18}$	
(3,3'-dioctadecyloxacarbocyanine perchlorate)	Molecular Probes (Göttingen, Germany)
DMSO (dimethyl sulfoxid)	Merck (Darmstadt, Germany)
DTT (1,4-dithio-L-threitol)	Merck (Darmstadt, Germany)
EDTA (1-(4-aminobenzyl)ethylenediamine-	
N,N,N',N'-tetraacetic acid)	Sigma-Aldrich (Steinheim, Germany)
EGTA (ethylene glycol-bis(2-aminoethyl)-	
N,N,N',N'-tetraacetic acid)	Sigma-Aldrich (Steinheim, Germany)
GDP (guanosine 5´-diphosphate)	Sigma-Aldrich (Steinheim, Germany)
Glutaraldehyde (50% aqueous solution)	Sigma-Aldrich (Steinheim, Germany)
Glycerol (87% aqueous solution)	Merck (Darmstadt, Germany)
Glycine	Merck (Darmstadt, Germany)

Glycogen (source: oyster)	Amersham (Freiburg, Germany)
GTP (guanosine 5´-triphosphate)	Merck (Darmstadt, Germany)
GTPγS (guanosine 5'-[γ-thio]triphosphate)	Sigma-Aldrich (Steinheim, Germany)
HCl (hydrochloric acid, 37%)	Merck (Darmstadt, Germany)
HEPES (4-(2-hydroxyethyl-)piperazine-1-ethansulfonic acid)	Sigma-Aldrich (Steinheim, Germany)
Imidazole (1,3-diaza-2,4-cyclopentadiene)	Sigma-Aldrich (Steinheim, Germany)
Immersion oil	Leica (Bensheim, Germany)
IPTG (isopropyl β-D-thiogalactopyranoside)	Sigma-Aldrich (Steinheim, Germany)
K_2HPO_4	Merck (Darmstadt, Germany)
Kanamycin	Serva (Heidelberg, Germany)
KCl	Merck (Darmstadt, Germany)
KAc (potassium acetate)	Merck (Darmstadt, Germany)
$MgCl_2$	Merck (Darmstadt, Germany)
MgAc (magnesium acetate)	Merck (Darmstadt, Germany)
$Na_2B_4O_7 \cdot 10\ H_2O$ (sodium borate, borax)	Merck (Darmstadt, Germany)
NaCl	Merck (Darmstadt, Germany)
NLS-peptide (CGGGPKKKRKVED)	Sigma GenoSys (London, UK)
Paraformaldehyde	Sigma-Aldrich (Steinheim, Germany)
PIPES (piperazine-1,4-bis(2-ethanesulfonic acid))	Sigma-Aldrich (Steinheim, Germany)
PMSF (phenylmethylsulfonyl fluoride)	Sigma-Aldrich (Steinheim, Germany)
Poly-L-Lysine solution	Sigma (St. Louis, USA)
SDS (sodium dodecylsulfate)	Serva (Heidelberg, Germany)
Sephadex G-50	Amersham (Freiburg, Germany)
Sucrose	Merck (Darmstadt, Germany)
Sulfo-SMCC (sulfosuccinimidyl 4-(N-maleimidomethyl) cyclohexane-1-carboxylate)	Pierce (Rockford, USA)
TALON™ resin	Clontech (Palo Alto, USA)
TEMED (N,N,N',N'-tetramethyl-ethylendiamine)	Sigma-Aldrich (Steinheim, Germany)
Tris (tris-(hydroxymethyl)-aminoethane)	Merck (Darmstadt, Germany)
Triton X-100 (t-octylphenoxypolyethoxyethanol)	Sigma-Aldrich (Steinheim, Germany)
Vectashield® mounting medium H-1000	Vector Laboratories (Burlingame, USA

5.1.2 Commonly used buffers, solutions and media

All solutions were prepared with double de-ionised water. Solutions were sterile filtered and, unless otherwise indicated (in brackets), stored at room temperature.

30% Sucrose (-20 °C)	30% (w/v) Sucrose in PBS
AB (acetate buffer)	150 mM Sucrose 100 mM KAc 3 mM MgAc 5 mM EGTA 1 mM DTT 20 mM HEPES, pH 7.4
Ab-TS (antibody buffer)	0.1% (v/v) Triton X-100 0.02% (w/v) SDS 10 mg/ml BSA dissolved in PBS
Ab-TS 410	Ab-TS supplied with 410 mM NaCl
Blotting buffer	25 mM Tris base 192mM Glycine
Borate buffer pH 7.6	300 mM NaCl 50 mM $Na_2B_4O_7 \cdot 10\ H_2O$ adjusted to pH 7.6 with boric acid
Borate buffer pH 8.5	300 mM NaCl 100 mM $Na_2B_4O_7 \cdot 10\ H_2O$ adjusted to pH 8.5 with boric acid
Dejellying solution	2% Cysteine (w/v) in 0.25x MMR adjusted to pH 7.8 with 5N NaOH
Energy mix (-20 °C)	100 mM Creatine phosphate 5 mM GTP 5 mM ATP 0.5 mg/ml Creatin kinase
Fix (-20 °C)	4% (w/v) Paraformaldehyde in PBS
EM Fix (-20 °C)	80mM Pipes, pH 6.8; 1mM $MgCl_2$; 150mM sucrose; 2% paraformaldehyde; 0.5% glutaraldehyde
Glycogen buffer	50 mM $MgCl_2$ 50 mM KCl 10 mM Tris, pH 7.5

Laemmli buffer (6x, -20 °C)	0.6% (w/v) Bromophenol blue 12% (w/v) SDS 60% (v/v) glycerol 300 mM Tris, pH 6.8
LB agar (autoclaved)	1.5% (w/v) Bacto agar in LB medium
LB medium (autoclaved)	1% (w/v) Bacto tryptone 0.5% (w/v) Bacto yeast extract 170 mM NaCl adjusted to pH 7.6 with 5N NaOH
MMR (20 °C)	100 mM NaCl 10 mM $MgCl_2$ 20 mM $CaCl_2$ 1 mM EDTA 50 mM HEPES, pH 8.0
PBS (phosphate buffered saline)	130 mM NaCl 100 mM Na_2HPO_4, pH 7.0
PCR buffer	20 mM TrisCl, pH 8.8 10 mM KCl 10 mM $(NH_4)SO_4$ 2mM MgSO4 1 % (v/v) Triton X-100 1 mg/ml BSA
Phosphate buffer pH 6.0	100 mM Na_2HPO_4, pH 6.0
Resolving gel (12 %) solution (4 °C) modified accordingly for other percentages	375 mM Tris, pH 8.8 12% (w/v) Acrylamide/Bisacrylamide 0.1% (w/v) SDS
Running buffer (5x)	303 g Tris base 1.44 kg Glycine 50 g SDS H_2O added to 10 l final volume
S250 / S500 (sucrose buffer)	250 mM / 500 mM Sucrose 50 mM KCl_2 10 mM HEPES, pH 7.5
S250 + / S500 +	S250 / S500 supplemented with 1 mM DTT 44 µg/ml Cycloheximid 10 mg/ml Cytochalasin B 1x Complete™ protease inhibitors

Stacking gel (3%) solution (4 °C)	125 mM Tris, pH 6.8 3% (w/v) Acrylamide/Bisacrylamide 0.1% (w/v) SDS
Staining solution	0.2% (w/v) Coomassie brilliant blue G-250 in methanol : acetic acid : water (5:1:4)
WB (wash buffer)	200 mM NaCl 2 mM $MgCl_2$ 8 mM imidazole 10 µM GTP / GDP 10% (v/v) glycerol 50 mM Tris, pH 7.5

5.1.3 Commonly used material

0.2 ml reaction tubes (Thermo Tube™)	PEQLAB (Erlangen, Germany)
0.5 ml micro tubes	Sarstedt (Nümbrecht, Germany)
1.5 ml reaction tubes	Eppendorf (Hamburg, Germany)
5 ml columns	MoBiTech (Göttingen)
Aluminium foil	Conresco (Minden, Germany)
Bottle top filters, 0.22 µm pore size	Millipore (Molsheim, France)
Costar® Transfer Pipettes	Corning Costar Corporation (Cambridge, USA)
Coverslips (11 mm diameter)	Menzel-Gläser (Braunschweig, Germany)
Filter paper	Whatman (Maidstone, UK)
General glass ware	Schott (Nürtingen, Germany)
General plastic ware	Greiner (Nürtingen, Germany)
Microcon® YM –10 centrifugal filter units	Amicon Millipore (Eschborn, Germany)
Microlance™ sterile needles	Becton Dickinson (Temse, Belgium)
Microscope slides	Menzel-Gläser (Braunschweig, Germany)
Millex®-GV 0.22 µm filter units	Millipore (Molsheim, France)
Multitest slides 10-well	ICN Biomedicals (Aurora, USA)
Nail polish	Manhattan (Stuttgart, Germany)
Plastic cuvettes	Ratiolab (Dreieich, Germany)
Spectra/Por® Membrane, MWCO 3.5 kDa	Spectrum Laboratories (Broadwick, USA)
Syringes	Becton Dickinson (Temse, Belgium)
Ultracentrifuge tubes	Beckman (Palo Alto, USA)

5.1.4   <u>Instrumental equipment</u>

Homogeniser (EmulsiFlex-C5)	Avestin (Toronto, Canada)
Incubator Model G-25	New Brunswick (Edison, USA)
Leica TCS SP2 (confocal microscope)	Leica Microsystems (Bensheim, Germany)
Topcon DS130F FEISEM	Topcon Corporation (Tokyo, Japan)
JEOL 1220 TEM	JEOL (Seoul, Korea)
Zeiss LSM 510	Carl Zeiss Mikroskopsysteme (Jena, Germany)
PHM 82 Standard pH Meter	Radiometer Copenhagen (Willich-Schiefbahn, Germany)
SDS-PAGE equipment Bio-Rad Power Pac 300	Provided by the mechanical workshop of EMBL (except for power supply) Bio-Rad (München, Germany)
FPLC	LKB/Pharmacia (Uppsala, Sweden)
Spectrometer (ULTROSPEC II)	LKB/Pharmacia (Uppsala, Sweden)
Test-tube-rotator Model 34528	Snijders Scientific (Tilburg, Holland)
Thermomix® BU waterbath	B. Braun Melsungen AG (Melsungen, Germany)
UV light box (UVT-28 MP)	Herolab (Wiesloch, Germany)

<u>Centrifuges:</u>

Biofuge A	Heraeus (Hanau, Germany)
Megafuge 1.0 R	Heraeus (Hanau, Germany)
RC-5B Centrifuge Rotor GSA Model SLA-1500	Sorvall (Clearwater, USA)
L8-70M Ultracentrifuge Rotor SW40 TI Rotor SW55 TI	Beckmann (Palo Alto, USA)

5.1.5   Plasmids

pGFP-NLS: Kind gift of Dr. Maarten Fornerod (Netherlands Cancer Institute, Amsterdam).

pGST-hNup153H: The complete open reading frame of human Nup153 was amplified by Pfu PCR from the plasmid pcDNA-153HA vector (kind gift of Dr. Brian Burke, University of Calgary, Canada) using the oligonucleotides h153-N5 (5'-CAT GCC ATG GCC TCA GGA GCC GGA GG-3') and h153-CB (5'-GGA GAT CTT TTC CTG CGT CTA ACA GCA-3'). After restriction with *BglII* and *NcoI*, the open reading frame was inserted in a modified form of pGEX2T (Pharmacia) containing an additional C-terminal HIS-tag (pGEX-pluscHIS, generated by Dr. Sam Gunderson, Mattaj laboratory, EMBL). The sequence of the resulting vector was confirmed by DNA sequencing at SeqLab (Konstanz, Germany).

pQE-NPC-M9: Generated by Dr. Ludwig Englmeier, described in (Englmeier et al., 1999). The *Xenopus* nucleoplasmin core sequence was cloned before the M9 sequence derived from hnRNPA1 (Pollard et al., 1996)

pQE70-imp α: Generated and provided by Christoph Schatz (Mattaj laboratory, EMBL). The sequence of *Xenopus* importin α was amplified by PCR and cloned into the SphI and BamHI restriction sites of pQE70 (Qiagen).

px153-N: Generated by Dr. Jerome Cavaille (Mattaj laboratory, EMBL). A cDNA fragment corresponding to aminoacids 1-149 of the known *Xenopus* Nup153 sequence (Shah et al., 1998) was generated by RT-PCR on RNA from *Xenopus* oocytes and cloned into the *SacI* and *SalI* restriction sites of pQE30 (Quiagen).

pxCAN-N: Generated by Dr. Maarten Fornerod (Mattaj laboratory, EMBL). An N-terminal fragment spanning amino acids 1-213 of the published *Xenopus* Nup214/CAN sequence (Askjaer et al., 1999) was cloned directly after the HIS-tag of pQE31 (Qiagen).

5.1.6   Proteins

5.1.6.1   *Expression and purification of xNup153-N*

The expression conditions for xNup153-N were optimised and routinely the following protocol was followed: The px153-N vector was transformed into the *E.coli* strain BL21[Rep4] (QIAgen) and grown on LB-Agar plates containing 1μg/ml ampicillin and kanamycin overnight. A single colony was used to inoculate 1l of LB medium containing 1μg/ml ampicillin. This culture was grown to an optical density of 0.7 at 600nm and then induced with 1 mM IPTG for 2h at 37 °C. After this incubation period, the cells were harvested by centrifugation.
For purification, the pellet was resuspended in 10 ml PBS containing 8mM imidazol and lysed with an EmulsiFlex-C5. The lysate was cleared by centrifugation at 20 000g in an

Ultracentrifuge for 20 min and the supernatant was incubated with 200 μl Ni-NTA resin (QIAgen) for at least 1h. Subsequently, the resin was washed at least 3 times with large volumes of PBS containing 20mM imidazol. The resin was then poured into a column and eluted by gravity flow with PBS containing 500 mM imidazol. The protein was dialysed against PBS containing 15% (v/v) glycerol, snap frozen and stored at -80 °C. Alternatively, for the generation of affinity-resin to purify antibody from serum, the protein was further purified by FPLC on a MonoQ column (Pharmacia) and eluted with a linear gradient of NaCl from 150mM to 1M NaCl. The peak fractions were dialysed as above and snap frozen for storage.

5.1.6.2 *Expression and purification of xCAN-N*

For the expression of xCAN-N the pxCAN-N vector was transformed into the *E.coli* strain BL21 [Rep4] (QIAgen). An overnight culture inoculated from a single colony was grown in the presence of 1μg/ml ampicillin and on the following day diluted 1/200 into 6 l LB medium. When the culture had grown to an optical density of 0.7 at 600 nm, IPTG was added to a final concentration of 0.5 mM. After 4h of further incubation at 28 °C, the cells were harvested by centrifugation. The bacteria were lysed in an EmulsiFlex-C5, the lysate was cleared by centrifugation at 10 000g for 20 min. The protein was then purified on Ni-NTA (QIAgen) under denaturing conditions using 8M urea following exactly the protocol supplied by the manufacturer.
The eluted protein containing fractions were dialysed against PBS containing 30% glycerol and snap frozen for storage at -80 °C.

5.1.6.3 *Expression and purification of importin α*

For expression of *Xenopus* importin α, pQE70-impα was transformed into the *E.coli* strain BL21[pRep4] (QIAgen). An overnight culture inoculated from a single colony was grown in the presence of 1μg/ml ampicillin and kanamycin and on the following day diluted 1/200 into LB medium. When the culture had grown to an optical density of 0.7 at 600 nm, IPTG was added to a final concentration of 0.3 mM. The bacteria were lysed in an EmulsiFlex-C5 using PBS containing 8.7 % (v/v) glycerol and 5 mM β-mercaptoethanol, the lysate was clarified by centrifugation at 10 000g for 20 min. To 40 ml lysate, 1ml TALON® (Clontech) resin was added and incubated on a rotating wheel for at least 1h. The resin was washed in batch with large volumes of the lysis buffer, poured into a column and subsequently eluted in 1 ml fractions with PBS containing 8.7 % (v/v) glycerol, l,5 mM β-mercaptoethanol and 300mM imidazol. Peak fractions were determined by BIOrad protein assay. The protein was dialysed against PBS with 8.7 % (v/v) glycerol, snap frozen and stored at -80°C.

5.1.6.4 *Expression and purification of GFP-NLS*

The pGFP-NLS vector was transformed into the *E.coli* strain BL21[Rep4] (QIAgen) and grown on a plate containing 1μg/ml ampicillin and kanamycin. An overnight culture inoculated from a single colony was grown in the presence of 1μg/ml ampicillin and on the following day diluted 1/200 into 6 l LB medium. When the culture had grown to an optical density of 0.7 at 600 nm IPTG was added to a final concentration of 0.5 mM. The bacteria were then incubated another 4 h at 37 °C and subsequently spun down at 10000g.

For purification, the pellet was resuspended in 40 ml PBS containing 8mM imidazol, lysed with an EmulsiFlex-C5. The lysate was cleared by centrifugation at 20 000g in an Ultracentrifuge for 20 min and the supernatant was incubated with 4 ml Ni-NTA resin (QIAgen) for at least 1h. After this, the resin was washed at least 3 times with large volumes of PBS containing 20mM imidazol. The protein was then poured into a column, eluted by gravity flow with PBS containing 500 mM Imidazol. Peak fractions were determined by BIOrad protein assay, pooled and dialysed against PBS containing 15% (v/v) glycerol, snap frozen and stored at -80 °C.

5.1.6.5   *Expression and purification of NPC-M9*

The nucleopolasmin core domain fused to the M9 transport signal of hnRNP A1 was expressed and purified exactly as described in Englmeier et al., (1999).

5.1.6.6   *Expression and purification of Recombinant human Nup153*

For expression of hNup153, the pGST-hNup153H plasmid was transformed into *E.coli* strain BL21 [DE3] Codonplus. Cultures of BL21 [DE3; pGST-hNup153H] Codonplus were grown from a single colony to an OD of 0.7 at 600 nm and induced with 1 mM IPTG for 4 h at room temperature. GST-Nup153 was purified on Glutathione Sepharose (Pharmacia) following the manufacturers instructions. The fractions obtained were analysed by immunoblot and the peak fractions were dialysed against S250, snap frozen and stored at -80°C.

5.1.6.7   *Preparation of fluorescently labelled BSA-NLS*

To follow importin β mediated nuclear protein import, BSA was labelled with a fluorophore, usually FITC, and then cross-linked to NLS peptide following the protocol descibed in Palacios et al. (1996). All incubations were done in the dark to avoid bleaching of the fluorophore.

For the labelling of BSA, 100 μl of 10 mg/ml bovine serum albumin (BSA) in borate buffer pH 8.5 was slowly mixed with an equimolar amount of FITC-succinimidyl ester in dimethyl sulfoxid (DMSO) in a 1.5 ml reaction tube. Labelling was carried out for 1 h at room temperature under continuous mild mixing (rotation). The addition of 10 μl of 1M TrisCl pH 7.6 terminated the reaction by quenching non-reacted dye molecules. Sephadex G-50 resin (Amersham) was equilibrated in borate buffer pH 7.6 and prepared for gel filtration (5 ml bed volume in a 10 ml column). Only the peak fraction of labelled protein were collected. Labelled protein separated well from unincorporated label and could be readily identified due to slight differences in colour. The protein fraction was concentrated to 150 μl by centrifugation in Microcon® YM –10 filter units (Amicon Millipore).

To cross-link the protein to NLS peptide, 150 μl of labelled BSA was mixed with an equal volume of 20 mg/ml sulfosuccinimidyl 4-(N-maleimidomethyl) cyclohexane-1-carboxylate (Sulfo-SMCC) in borate buffer pH 7.6 and incubated for 1 h at room temperature with continuous mild mixing. The protein was recovered by gel filtration over a 5 ml Sephadex G-50 column equilibrated in phosphate buffer pH 6.0 and concentrated in Microcon® YM –10 filter units as described above. NLS-peptide was dissolved at 10 mg/ml in phosphate buffer pH 6.0 and 90 μl were added to the concentrated and labelled BSA. After incubating for 1 h at room temperature with continuous mild mixing, the

reaction was terminated by addition of TrisCl pH 7.6 and 2-mercaptoethanol, each to a final concentration of 30 mM. The product was isolated by chromatography over a 5 ml G-50 column equilibrated in S250 and was concentrated in Microcon® YM –10 filter units as described above. An aliquot (1 to 5 µl) was analysed on a 12% SDS-polyacrylamide gel and labelled protein was visualized on a UV light box. The modified protein migrated as a smear with an average molecular weight that indicated that on average 10-15 NLS peptides cross-linked to each BSA molecule. The labelled peptide-protein conjugate was further concentrated to a final concentration of roughly 10 mg/ml and was stored in 20 µl aliquots at –80 °C.

5.1.6.8 *Preparation of colloidal gold-coupled proteins*

Coupling of BSA-NLS to 5 nm colloidal gold, as well as to 10 nm colloidal gold was performed essentially as described (Cordes et al., 1997a). To avoid overloads of protein, which may result in subsequent leaching of bound material, Igs or BSA-NLS were added to the gold particles at amounts just sufficient to maintain colloidal stability upon addition of NaCl (Slot and Geuze, 1984). Remaining binding sites were blocked by incubating the gold suspension with 0.1% BSA for 15 min before dilution in 20 volumes of injection buffer (88 mM NaCl, 1 mM KCl, 20 mM HEPES, pH 7.4). To remove the excess of unbound protein, the suspension was centrifuged at 10 000g for 1 or 2 h, depending on particle size. The supernatant and an occasionally observed minor solid pellet consisting of coagulated gold were discarded, whereas the fluffy and loose major part of the sediment, containing the gold conjugates in colloidal form, was resuspended in injection buffer and washed again. Following a final centrifugation, the loose sediment was collected as a concentrated, black suspension and used either directly for injection or stored at 4 °C.

5.1.6.9 *Preparation of fluorescently labelled proteins:*

Alternatively to immunofluorescence, the localisation of proteins was followed by direct observation of proteins labelled by conjugation to a fluorophore with a fluorescence microscope. For this, FITC or rhodamine-succinimidyl ester in dimethyl sulfoxid (DMSO) was slowly mixed with an equimolar amount of the protein of interest, which was exchanged to borate buffer pH 8.5 by dialysis prior to this. Labelling was carried out for 1 h at room temperature under continuous mild mixing (rotation). The addition of 10 µl of 1M Tris HCl pH 7.6 terminated the reaction by quenching non-reacted dye molecules. Sephadex G-50 resin (Amersham) was equilibrated in borate buffer pH 7.6 and prepared for gel filtration (5 ml bed volume in a 10 ml column). Only the peak fractions of labelled protein were collected. Labelled protein separated well from unincorporated label and could be readily identified due to slight differences in color. The protein fraction was concentrated to 150 µl by centrifugation in Microcon® YM –10 filter units (Amicon Millipore).

5.1.7 <u>Antibodies</u>

anti-Nup153	xNup153-N was mixed with Ribi®(Coaxia) adjuvant and injected into rabbits. After several boosts in four weeks intervals with the same procedure, blood was taken, serum obtained by agglutination for 30 min at 37 °C and centrifugation. The antibodies were affinity purified as described below.
anti-CAN	Generated by Dr. Maarten Fornerod. xCAN-N was mixed with Ribi®(Coaxia) adjuvant and injected into rabbits. After several boosts in four weeks intervals with the same procedure, blood was taken, serum obtained by agglutination for 30 min at 37 °C and centrifugation. The antibodies were affinity purified as described below.
anti-Nup358F (Pichler et al., 2002)	Kind gift of Dr. Frauke Melchior, MPI for Biochemistry, Martinsried.
anti-Nup358V	Kind gift of Dr. Dr. Volker Cordes, Karolinska Inst., Denmark. Raised in guinea pig against a peptide corresponding to amino acids 2285-2314 of human RanBP2 (of which aa 2290-2314 are identical to a partial sequence of RanBP2 from *Xenopus laevis* (accession number BG233383). The peptide was coupled via an N-terminal cystein residue to maleimide-activated keyhole limpet hemocyanin and used for immunisation as described (Cordes et al., 1997b).
anti-Nup93 (Grandi et al., 1997)	Kind gift of Dr. Ed Hurt, University of Heidelberg.
anti-Nup98 (Kasper et al., 1999)	Kind gift of Dr. Jan van Deusern, Mayo Clinic, Rochester, USA
anti-TPR (Cordes et al., 1997b)	Kind gift of Dr. Volker Cordes, Karolinska Inst.
anti-importin β	Generated by Alexandra Segref (Mattaj laboratory, EMBL

anti-RanGAP (Pu and Dasso, 1997)	Kind gift of Dr. Marry Dasso, NIH, USA.
mAb414 (monoclonal mouse antibody raised against the nuclear pore-lamina complex of rat liver nuclei; (Davis and Blobel, 1987))	BabCO (Richmond, USA).
S49H2 (monoclonal mouse antibody that recognizes B type lamin L_{III} of *Xenopus*; (Lourim and Krohne, 1993; Lourim and Krohne, 1998))	Kind gift of Dr. Georg Krohne, University of Würzburg.

5.1.7.1 *Affinity purification of antibodies:*

For affinity purification of antibodies from serum, an antigen column was prepared first. To this end, any amino reactive buffer components were dialysed away by two successive rounds of dialysis against large volumes (1000 times of the protein solution) PBS. Saturating amounts of antigen, at least 2 mg protein/1 ml resin, were added to Affigel (Biorad) -10 or - 15 (according to the pI of the protein and following the manufacturers specifications), which was washed once with ice cold water. The mixture was rotated for one hour at room temperature and the efficiency of the binding was compared by analysis of input and flow-through of the column by SDS-PAGE.

Antibodies were affinity purified on this resin according to the following protocol: a ten-fold excess of serum (v/v) was incubated with the resin. After incubation for one hour, the resin was collected by quick centrifugation and washed extensively with PBS. The antibodies were then eluted in one column volume fractions with 100 mM glycine pH 2.0. The fractions were instantly neutralised by the addition of 1/10 vol. 1.5 M TrisCl pH 8.8.

After several repetitions of this purification, the IgG containing fractions were pooled and IgGs were precipitated overnight with 60% of the saturating concentration of ammonium sulfate.

After spinning (20 min, 20 000g) the pellet was resuspended in PBS and dialysed against PBS containing 30% glycerol. Small fractions were snap frozen and stored at -80 °C.

5.1.7.2 *Secondary antibodies for immunofluorescence and immunogold labelling:*

Alexa Fluor® 546 goat anti-mouse IgG	Molecular Probes (Göttingen, Germany)
Alexa Fluor® 546 goat anti-rabbit IgG	Molecular Probes (Göttingen, Germany)
Alexa Fluor® 488 goat anti-mouse IgG	Molecular Probes (Göttingen, Germany)
Alexa Fluor® 488 goat anti-rabbit IgG	Molecular Probes (Göttingen, Germany)
FITC conjugated rabbit anti-guinea pig IgG	Sigma-Aldrich (Steinheim, Germany)

Colloidal gold coupled goat anti-rabbit IgG	Amersham (Freiburg, Germany)

5.1.7.3   *Secondary antibodies for immunobloting*

Horse radish peroxidase (HRP) coupled goat anti-mouse IgG	Pharmacia (Freiburg, Germany)
Horse radish peroxidase (HRP) coupled goat anti-rabbit IgG	Pharmacia (Freiburg, Germany)

5.2 Methods

5.2.1 Microbiological methods and cloning

All methods were conducted as described in (Sambrook et al., 1989), unless otherwise stated.

5.2.1.1 *Bacteria strains:*

The following *Escherichia coli* (*E. coli*) strains were used in this thesis

XL1Blue: genotype: F'::Tn10 proA+B+ lacIq Δ(lacZ)m15/recA1 endA1 gyrA96(NaIr)thi hsdR17 (rk- mk+) supE44 relA1 lac; (Stratagene), used for cloning.

BL21(DE3): genotype: F- ompT gal[dcm][lon] hsdSb (rB-mB-) with DE3, a lamda prophage carrying the T7 RNA polymerase gene, used for protein expression.

BL21(DE3)[pREP4]; genotype see above; (Qiagen), used for protein expression.

BL21 (DE3) Codonplus: genotype of BL21(DE3) plus plasmids expressing rare tRNAs (Stratagen), used for protein expression.

5.2.1.2 *Transformation of* **E. coli**

Preparation of transformation-competent *E.coli* cells was typically done from 200 ml culture in LB medium inoculated 1/200 from an overnight culture. When the cells reached an optical density of 0.7 (at 600nm wavelength) the cells were cooled, down spun for 10 min at 4 °C at 10 000rpm in a Sorvall RC-5B centrifuge. The pellet was resuspended in 100 ml 50 mM $CaCL_2$ and put on ice for 20 min. After this incubation, the cells were spun down as before and resuspended in 16 ml 50 mM $CaCl_2$/15% (v/v) glycerol. After spinning, the resulting pellet was again resuspended in approximately 4 ml 50 mM $CaCl_2$/15% (v/v) glycerol, aliquoted in 200 µl and snap frozen. The aliquots were stored at -80 °C.

Transformation of *E.coli* $CaCl_2$ competent cells was done by gently mixing 50 µl of cells with 0.5 µl of 2 M 2-mercaptoethanol and 5-10 ng plasmid DNA. After incubation for 30 min on ice, bacteria were heat-shocked for 45 sec at 42 °C, cooled for 3 min on ice and 300 µl of LB medium was added. Bacteria were incubated for 0.5 h at 37 °C to allow expression of antibiotic resistance and were plated out on LB agar plates containing 200 µg/ml ampicillin (amp) and/or 50 µg/ml kanamycin (kan). The plates were incubated overnight at 37 °C.

5.2.1.3 *Preparation of DNA from E.coli*

DNA from *E.coli* was prepared using QIAPrep® (Qiagen) kits according to the manufacturers instructions.

5.2.1.4 *Subcloning of DNA*

Standard methods like precipitation, restriction and electrophoresis of DNA were done following exactly the protocols described in (Sambrook et al., 1989).

5.2.1.5 *PCR reactions*

PCR reactions were used to generate fragments of DNA for subcloning. A typical reaction contained 10 ng of template DNA, the two oligonucleotides in a final concentration of 1 μM, dNTPs (Pharmacia, final concentration of 200 μM each) in PCR buffer, as well as 1 u of Pfu DNA-Polymerase (Stratagene). A typical PCR thermocycle protocol was as follows: initial 2 min denaturing at 94 °C; 1 min annealing at 65 °C, 1 min per kilobase template for amplification at 74 °C. This was repeated with shorter denaturing times (typically 1 min) for 25 times, followed by a final extension of 10 min at 74 °C in a Robocycler[®] (Stratagene).

5.2.2 Molecular biology and standard methods

5.2.2.1 *SDS polyacrylamide gel electrophoresis*

Analytical sodium dodecylsulfate polyacrylamide gel electrophoresis (SDS PAGE) was carried out under conditions that ensure dissociation of protein complexes into their individual subunits. To this end, samples were heated with the detergent SDS and reducing agent (2-mercaptoethanol). In a discontinuous buffer system the sample passes a stacking gel of high porosity before it concentrates in a very thin zone (or stack) on the surface of the resolving gel.

In this thesis, acrylamide gels were prepared using an electrophoresis system provided by the mechanical workshop of EMBL, Heidelberg. 3% stacking and 6-15% resolving gels (depending on the size of the resolved proteins) were polymerised by mixing the respective solutions with 0.04% ammonium peroxodisulfate (APS) and 0.0625% N,N,N',N'-tetramethyl-ethylendiamine (TEMED, resolving gel) or with 0.1% APS and 0.05% TEMED (stacking gel). Protein samples were mixed with 6x Laemmli buffer and heated for 5 min at 95 °C prior to loading an aliquot of 15-20 μl per lane. Electrophoresis was carried out in 1x running buffer at constant current of 170 mA until the bromophenol dye reached the bottom. After electrophoresis, gels were placed in staining solution and shaken for 1-10 h at room temperature. Gels were then transferred to destaining solution and shaken for 4-12 h with several changes of the solution.

5.2.2.2 *Determination of protein concentration*

Protein concentrations were determined with the BioRad protein assay kit, according to the manufacturers instructions. The concentrations were confirmed by comparing the intensity of stained bands after SDS-PAGE to BSA standards run on the same gel.

5.2.2.3 *Immunological detection of resolved proteins (Western Blot)*

Proteins bigger than 150 kDa are difficult to transfer by semidry Western blotting. The blots of nucleoporins shown in this thesis were therefore generated by running the protein samples on 7% SDS polyacrylamide gels. Onto the gel, an activated (by a short incubation in Methanol) PVDF membrane was placed and together with the gel sandwiched between two thick Whatmann 3MM papers that have been equilibrated in blotting buffer. This sandwich was then mounted into a BIOrad wetblot chamber and current (usually 400 mA for a 10 x 10cm gel) was applied for 4 hours,

The blot was then blocked in PBST (PBS containing 0.05% Tween) with 5% dry fat free milk for at least 30 min. Next, the blot was incubated in the same buffer containing the primary antibodies for 1h to 12 h. The blot was washed five times with PBST, incubated with secondary, horseradish peroxidase coupled antibody in PBST containing 3% milk for 1h. After this incubation, the blot was washed again at least 5 times for at least 30 min with PBST. The secondary antibody was then detected using the RENAISSANCE® (NEN) chemiluminescence kit.

5.2.3 **Biochemical methods**

5.2.3.1 *Xenopus egg extract preparation and immunodepletion*

5.2.3.1.1 *Xenopus* **egg extract preparation:**

Xenopus eggs are arrested in the second meiotic metaphase, which is very similar to a mitotic state. To obtain extracts that promote nuclear assembly, the egg cytoplasm is converted into an interphase state by addition of the Ca^{2+} ionophore 1-(4,5-dimethoxy-2-nitrophenyl)ethyl ester (A23187). Following this treatment, the eggs are crushed by centrifugation. The supernatant is fractionated at high speed into soluble and lipid components (figure 40; (Lohka, 1988). The clear cytosolic fraction supplied with membranes is competent for forming an ER network (Dreier and Rapoport, 2000) and an NE around exogenously added sperm chromatin (Lohka and Masui, 1983). Although unfractionated extract is active in nuclear assembly, the separation of membranes from the cytosolic phase is carried out for two reasons. First, crude extracts cannot be frozen reliably, whereas the separate components can be stored under liquid nitrogen for several months. Secondly, this separation allows the independent examination of either membranes or soluble fraction without affecting the other component of the nuclear assembly reaction.
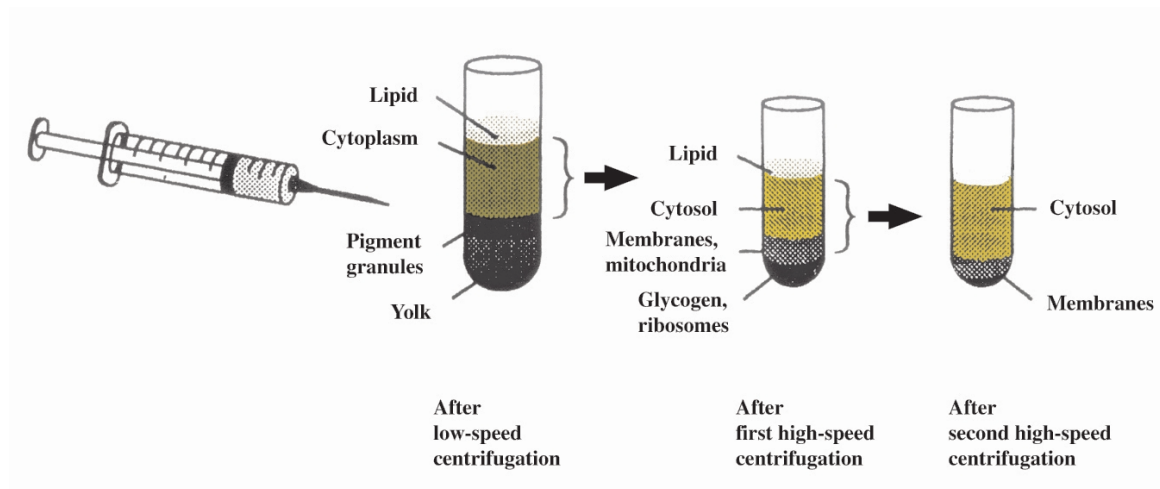
Figure 40: Preparation of *Xenopus laevis* interphase egg extract. (modified from (Newmeyer and Wilson, 1991).

Extracts were prepared as described in the literature with slight modifications (Hetzer et al., 2000; Newmeyer and Wilson, 1991). Owing to their fragility, eggs were generally handled with extreme caution. All washing steps were carried out gently and exposure to air was strictly avoided. While MMR buffer had a temperature of 20 °C, the buffers used after dejellying the eggs were precooled to 4 °C.

Frogs were primed by injection of PMSG and 4-14 days later, egg laying was induced by injection of chorionic gonadotropin (CG, 0.5 ml of 2 000 U per ml H_2O). The frogs were transferred into plastic boxes containing MMR and put into the dark for 16 h at 16 °C. Each batch of eggs was decanted into a separate beaker. Batches that contained eggs of bad quality (big, white, blotchy or furrowed) were discarded and the remaining eggs were pooled. Extensive washing with MMR removed debris. Eggs were then treated with freshly prepared dejellying solution for up to ten minutes with gentle swirling every 30 sec. As soon as eggs became closely packed they were extensively rinsed with MMR. Eggs were allowed to settle and excess of MMR was removed to a remaining volume of 250 ml. For activation, 20 µl of 2 mg/ml A23187 in DMSO were added. The completion of this process could be judged by the contraction of the animal cap that usually occurred after 7 min. The exposure to the ionophore was kept to a minimum as this reagent caused some eggs to disintegrate. Eggs were washed well with MMR and incubated at room temperature up to 25 min. During this time, necrotic eggs were removed with a pasteur pipette.

Eggs were transferred to clear ultracentrifuge tubes (13x51 mm) and centrifuged for 20 sec at 800 rpm and 2 sec at 1 600 rpm at 4 °C (Megafuge 1.0 R). After removal of excess buffer, they were spun for 20 min at 15 000 rpm at 4 °C (L8-70M Ultracentrifuge, Rotor SW 55 TI). The supernatant was supplied with 1 mM 1,4-dithio-L-threitol (DTT), 44 µg/ml cycloheximide, 4 µg/ml cytochalasin B and 1x Complete™ EDTA-free Protease Inhibitor (Roche). Cycloheximide inhibited protein synthesis and thereby blocked progression into mitosis, while cytochalasin B prevented actin polymerisation that would have lead to "gelling" of the extract.

This "low speed extract" was centrifuged for 35 min at 45 000 rpm at 4 °C (L8-70M Ultracentrifuge, Rotor SW 55 TI) to separate soluble and lipid components (Figure 40). The cytosolic phase (orange) was collected by side puncture of the centrifuge tube, diluted roughly 0.3 fold with S250+ and spun again for 35 min at 45 000 rpm at 4 °C (L8-70M Ultracentrifuge, Rotor SW 55 TI). The obtained "high speed extract" was supplied with glycerol to a final concentration of 3% (v/v), snap frozen and stored as 50 µl aliquots (0.2 ml reaction tubes) under liquid nitrogen.

The membranes were diluted in roughly 20-fold their volume and spun through a 800 µl S500+ cushion for 15 min at 12 000 rpm at 4 °C (L8-70M Ultracentrifuge, Rotor SW 40 TI). The obtained pellets were resuspended in 1/10 of the cytosolic volume, snap frozen as 12 µl aliquots (0.2 ml reaction tubes) and stored under liquid nitrogen.

5.2.3.1.2 **Immunodepletion of "high speed extracts"**

For the immunodepletion of proteins from "high speed" *Xenopus* egg extracts, an antibody column was generated first.

To this end, at least 2mg antigen protein fragment was added per 1 ml Protein A Sepharose (Pharmacia) in PBS. The resin was incubated with the protein at room temperature for 1 h. The beads were then washed two times with borate buffer (0.2 M Sodium borate, pH 9.0). The beads were always collected by quick centrifugation at 500g. After the wash, the beads were resuspended in 10 mM Dimethylpimelimidate (DMP, Sigma) in borate buffer. After 30 min rotation at room temperature, the beads were collected and resuspended again in fresh 10 mM DMP in borate buffer. After an additional half hour, the beads were collected and the cross-linker was blocked with 0.2 M ethanolamine for 2h. The beads were washed again with PBS and stored at 4 °C.

Before use, the beads were once eluted with 100 mM Glycine pH 2.0 to remove non-cross-linked antibodies. The beads were then divided in two aliquots and transferred to small Mobicol (Mobitech) columns and blocked for 1h with S250 containing 2 mg/ml BSA. Afterwards, the columns were washed extensively with S250. Then one of the two aliquots was incubated with an equal volume of freshly prepared "high speed" cytosolic egg extract. After half an hour the flowthrough of this first depletion column was collected and applied to a second round in the same way. The depleted extracts were aliquoted in 30 µl, snap frozen and stored under liquid nitrogen.

5.2.3.2 *Xenopus sperm head preparation*

Sperm was recovered from *Xenopus* testis in HSP (15 mM HEPES pH 7.5, 250 mM sucrose; 0.5 mM spermidine tetrachloride; 0.2 mM spermine) and chromatin was prepared to a final concentration of $1x10^3$ sperm/µl as described (Gurdon, 1976).

In brief, the dissected testis from one male frog were homogenised carefully in HSP. The sperm was pelleted by centrifugation at room temperature at 2 000g for 10 minutes. The resulting pellet was washed twice by resuspending it in HSP and centrifugation. The pellet resuspended in 1 ml HSP and 50 µl 10 mg/ml Lysolecithin (Sigma) was added to permeabilise the plasma membrane. After 5 min incubation at room temperature, 10 ml of HSP including 3 % (w/v) BSA were added to quench. After centrifugation, the pellet was resuspended in 3 ml HSP containing 0.3 % (w/v) BSA, centrifuged again and resuspended in HSP containing 30 % glycerol and 0.3 % (w/v) BSA. In order to ensure

permebealisation and to determine the density of the sperm heads, the number of typically screw-shaped particles that did not exclude 0.4 % Trypan blue was counted using a Neugebauer counting chamber. The sperm chromatin was diluted to a final concentration of 5000/µl, snap frozen and stored at -80 °C.

5.2.3.3 *In vitro nuclear assembly*

Cytosol and membranes were rapidly thawed and kept on ice. A typical nuclear assembly reaction consisted of 13 µl cytosol, 1 µl energy mix (ATP-regenerating system), 1 µl glycogen (20 mg/ml in glycogen buffer), 1 µl sperm chromatin (at 1,000 sperm/µl) and 1.5 µl membranes. In general, sperm chromatin was allowed to decondense for 10 min by incubation at 20 °C prior to the addition of membranes. The assembly reactions were normally incubated for 2 h at 20 °C.

For fixation, the assembly reaction was diluted with 400 µl of Fix solution supplied with 0.5 µl of 2 mg/ml 4',6-diamidino-2-phenyindole (DAPI). The mixture was held in the dark and on ice for 30-60 min and was then layered over 0.8 ml 30% (w/v) sucrose in phosphate buffered saline (PBS) in a tube containing a polylysine coated coverslip. After centrifugation for 10 min at 3 000 rpm at 4 °C (Megafuge 1.0 R), liquid was removed and the coverslip was recovered using a pair of forceps. The coverslip was dipped in PBS, mounted on top of a drop of Vectashield® mounting medium (Vector Laboratories, Burlingame, USA) and sealed on the slide with nail polish applied to the perimeter.

5.2.3.4 *Nuclear import into synthetic nuclei*

Nuclear protein import could easily be followed by the addition of fluorescently labelled substrates to the synthetic nuclei after 2 h of nuclear assembly. After further incubation for 2-40 min depending on the experiment and substrate, the nuclei were either directly viewed by confocal microscopy or fixed by the addition of 400 µl of Fix solution supplied with 0.5 µl of 2 mg/ml 4',6-diamidino-2-phenyindole (DAPI) and processed as described under 5.2.3.3.

5.2.3.5 *Immunofluorescence of synthetic nuclei*

Nuclei were assembled, fixed and spun onto a coverslip as described in 5.2.3.3. Nuclei were permeabilised by incubating the coverslips for 30 min with antibody buffer TS (Ab-TS), and subsequently incubated for 30 min in Ab-TS containing the first antibody. Polyclonal antibodies were used in 1:250 dilution, the monoclonal antibodies (mAb414, S49H) in 1:1000 dilution. The coverslip was washed with Ab-TS 3 x 10 min and incubated for 30 min with fluorescently labelled secondary antibody diluted 1:500 in Ab-TS. Then, the coverslip was washed with antibody buffer TS 410 (Ab-TS 410) 3 x 10 min, with PBS containing 0.1 mg/ml DAPI and with PBS. After draining of excess buffer, the coverslip was mounted using a drop of Vectashield® as medium.

5.2.3.6 *Membrane labelling with DiOC$_{18}$*

To visualise membranes in the nuclear assembly reaction, the membrane fraction obtained during the preparation was pre-stained with a lipophilic dye.

All steps were carried out gently to avoid foaming and on ice. The buffers used were freshly prepared and cooled to 4 °C. 3,3'-dioctadecyloxacarbocyanine perchlorate (DiOC$_{18}$) was dissolved just before use.

500 µl freshly prepared membrane fraction was thoroughly mixed with 25 µl 0.5 mg/ml DiOC$_{18}$ in DMSO. After 20 min incubation on ice, this mixture was diluted with 20 ml S250+ and spun through a 500 µl S500+ cushion for 15 min at 11 000 rpm at 4 °C (L8-70M Ultracentrifuge, Rotor SW 40 TI). The membrane pellet was resuspended in an appropriate volume of S500+ to obtain a 10x stock. 10 µl aliquots were snap frozen and stored under liquid nitrogen.

5.2.3.7 *Replication in synthetic nuclei*

Replication of DNA was assayed by addition of 40 µM 21-Biotin-dUTP (Clontech) to the nuclear assembly reactions in the presence or absence of 14µM of aphidicolin (Sigma). Samples were treated as for immunofluorescence and incorporated biotin was detected with Alexa Fluor® 488 -linked streptavidin (Molecular Probes).

5.2.3.8 *Size measurement in synthetic nuclei*

To determine the size of synthetic nuclei, midsection images of nuclei of either immunofluorescence reactions or of nuclei with labelled membranes were taken on an Zeiss LSM510 confocal microscope. The diameter of the nuclei in pixels was measured with NIH image or ImageJ (NIH, Bethesda, USA) and converted to µm using the physical size of a pixel as calculated by the microscope software.

5.2.4 **Light Microscopy**

5.2.4.1 *Fluorescence microscopy*

Routinely, a Zeiss Axiophot 200 or a Zeiss LSM 510 confocal microscope were used together with the software provided by Zeiss. Alternatively, a Leica SP2 confocal microscope was used with the respective software. For confocal microscopy, the laser lines at 356, 488 and 546 nm were used.

For all experiments, the settings of the different channels were chosen so that there was no cross-talk between them. Images were processed using the NIH Image and ImageJ software (NIH, Bethesda, USA). This software was also used to quantify intranuclear signals for import reactions.

5.2.4.2 *Deconvolution and 3-D reconstruction from fluorescence microscopy images*

For 3D-reconstructions, image stacks were recorded at the Zeiss LSM 510 confocal microscope with a 3-fold oversampling in the Z direction. These images were then deconvoluted on a Silicon graphics workstation with the Huygens software (Bitplane) using a calculated point spread function. Projections from the deconvoluted images were generated using the Imaris software (Bitplane).

5.2.4.3   *Fluorescence recovery after photobleaching (FRAP) on synthetic nuclei*

Nuclei were assembled as described above. After assembly, 4 µl of 1 mg/ml Oregon Orange – WGA (Molecular Probes) were added and the reaction was further incubated for 10 min at 20 °C. The samples were diluted in 300 µl S250 and spun through a 0.8 ml cushion of 30% w/v sucrose onto a L-polylysine coverslips. The coverslip was mounted in chambers containing AB for *in situ* imaging. Photobleaching was performed using the LSM 510 microscope and the accompanying software. Quantitative analysis was performed after background subtraction with NIH image software (NIH, Bethesda, USA). Average intensities were corrected for fluorescence loss during the bleach.

5.2.5   **Electronmicroscopical techniques**

5.2.5.1   *Microinjection and electron microscopy of injected oocytes*

Microinjections into the cytoplasm of non-defolliculated *Xenopus* stage VI oocytes were performed at room temperature essentially as described (Cordes et al., 1997a). Four to six oocytes were injected for each experiment. Injections of gold-coupled antibodies were done at two sites opposite to each other at the equatorial borderline between animal and vegetal hemisphere. Injections of gold-coupled BSA-NLS, or of gold-coupled BSA without NLS as control, were performed at a single site near the pole of the vegetal hemisphere. Oocytes were then incubated in modified Barth's medium at either 4 °C in the cold-room or in a 19 °C incubator for 3, 5, 8, 16, 22, or 30 h. For experiments in which antibody injections preceeded the injection of gold-coupled BSA-SV40NLS, oocytes injected with 5nm-gold anti-RanBP2V, or mock-injected with buffer alone, were first incubated at 4 °C for 16 h. Following subsequent injection of 10nm-gold BSA-NLS, oocytes were further incubated at 19 °C for 6 h. Oocytes were then fixed in glutaraldehyde and processed for electron microscopy exactly as described (Cordes et al., 1997a).

5.2.5.2   *Isolating Nuclear Envelopes from Xenopus laevis*

Oocytes were obtained by partial laparotomy of mature *Xenopus laevis* females, and stored in amphibian Ringers solution (111.2mM NaCl; 1.88mM KCl; 1.08mM MgCl$_2$; 0.4% NaHCO$_3$) at 4°C. To isolate the nuclei, the oocytes were washed in 5:1 buffer (83mM KCl, 17mM NaCl, 10mM HEPES, pH 7.4) and pierced with a fine needle to extract the nucleus. Nuclei were transferred to either silicon chips for SEM analysis, or plastic petri dishes for TEM analysis, and manually sheared using a fine glass needle. Envelopes were initially fixed in EM Fix for 30 minutes at room temperature, or overnight at 4°C. Envelopes to be immunolabelled were fixed in EM Fix without the glutaraldehyde.

5.2.5.3   *Immunolocalisation and EM*

Samples were removed from EM Fix, washed briefly in PBS and transferred to 100mM glycine in PBS for 10 minutes. Samples were blocked in 1% fish scale gelatine in PBS for 1 hour. Primary antibodies were diluted in PBS and incubated with the samples at room temperature for 1 hour or 4°C overnight. Samples were washed 6 times for 5 minutes in PBS, and incubated with 10 nm colloidal gold-conjugated secondary

antibodies (Amersham) diluted 1:20 in PBS at room temperature for 1 hour or 4°C overnight. Samples were washed 6 times for 5 minutes in PBS and those for FEISEM analysis fixed in EM Fix for 30 minutes at room temperature, or 4°C overnight. To strip nuclear baskets, nuclear envelopes were first incubated in 10mM HEPES pH 7.4, 1 mM EDTA for 30 min and subsequently in the same buffer containing 500 mM KCl. For TEM analysis, samples were postfixed in Tannic acid fix (100mM HEPES, pH 7.4; 0.2% tannic acid; 2% glutaraldehyde) for 30 minutes at room temperature, or 4°C overnight. Controls for non-specific labelling of the secondary antibody were conducted by incubating samples in secondary antibodies only.

5.2.5.3.1 Post-fixation Preparation for EM Analysis

Samples were removed from the EM Fix and washed in 0.2M cacodylate, pH 7.4, then postfixed in 1% (w/v) OsO_4 in 0.2M cacodylate, pH 7.4. Samples were washed twice in double-distilled water and incubated in 1% (w/v) aqueous uranyl acetate for 10 minutes. Samples were dehydrated through an ethanol series (30%; 50%; 70%; 95%; 100%), and processed for either SEM or TEM analysis.

5.2.5.3.2 Preparation for FEISEM Analysis

After ethanol dehydration the silicon chips were incubated in Arklone (ICI, Runcorn, UK) for 1 minute and critical point dried from high purity CO_2. Samples were sputter coated with 4 nm chromium in an Edwards Auto 306 cryopump sputter coater (Edwards High Vacuum International, Crawley, UK) and viewed using a Topcon DS130F FEISEM (Topcon Corporation) at 30 kV accelerating voltage. Colloidal gold particles were imaged by a solid state backscatter electron detector (KE developments).

5.2.5.3.3 Preparation for TEM Analysis

After ethanol dehydration samples were embedded in Epoxy Resin 100. Initially, samples were incubated for 4 hours in 20% resin diluted in ethanol, then transferred to 50% resin in ethanol for 4 hours, before an overnight incubation in 100% resin. The resin was exchanged and the samples placed at 60°C for 24 hours for the resin to polymerise. 70 nm thin sections were cut and visualised in a JEOL 1220 TEM.

5.2.5.3.4 Analysis of Antibody Localisation

The localisation of gold-conjugated antibodies in relation to NPC structures was measured using Analysis (SIS) software.

For FEISEM images, NPCs were visualised at 100kx to 300kx magnification, and secondary and backscatter images were taken and realigned using Photoshop®, 6.0 (Adobe Systems). The primary antibodies exclusively labelled the nucleoplasmic face of the NPCs and together with their specificity on Western blots were assumed to be specific. A negative control for non-specific labelling of the secondary antibody was performed.

The position of the gold particles, corresponding to the gold and the antibody, in relation to the centre of the NPC were measured using Analysis (SIS) software. Circles of best fit were placed over each NPC and each gold-labelled particle, and the distance between the centre of each circle was measured (figure 41).
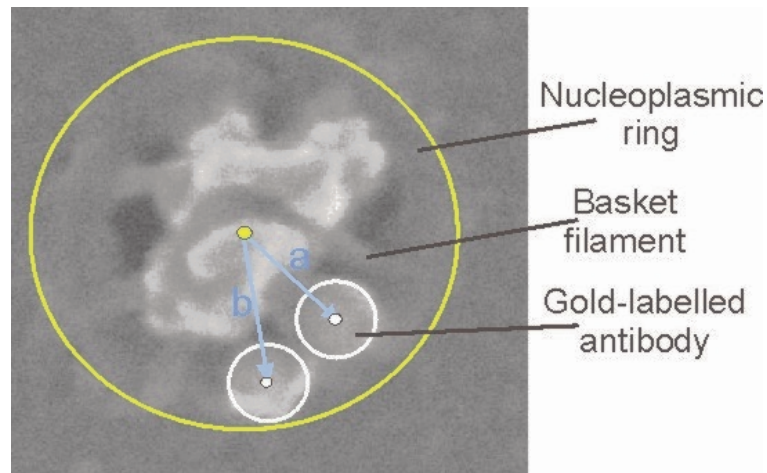
Figure 41: Method for quantifying the localisation of gold-labelled particles using FEISEM. Circles of best fit were overlayed onto NPCs (yellow circle) and gold-labelled particles (white circles). The distance between the centre of these circles representing the NPC and the gold-labelled particles was measured, e.g. distance a and distance b.

The data was recorded for 100 gold particles and plotted on a histogram to show the data spread.

The diameter of the gold particles was also measured and found to be an average 27.9 nm, which corresponds to the 10 nm gold, the primary and the secondary antibodies (estimated to be ~3 nm each, C.Feldherr unpublished observations) and the 4 nm chromium coating that could increase the diameter up to 8 nm.

For quantification of TEM images, sections were cut and images portraying cross-sections through the NE were used for quantification.

The distance of the gold particles from the midplane of the NE were measured using Analysis (SIS) software (figure 42). The midplane was estimated by overlaying rectangles between the ONM and INM and finding the midpoint between the two.
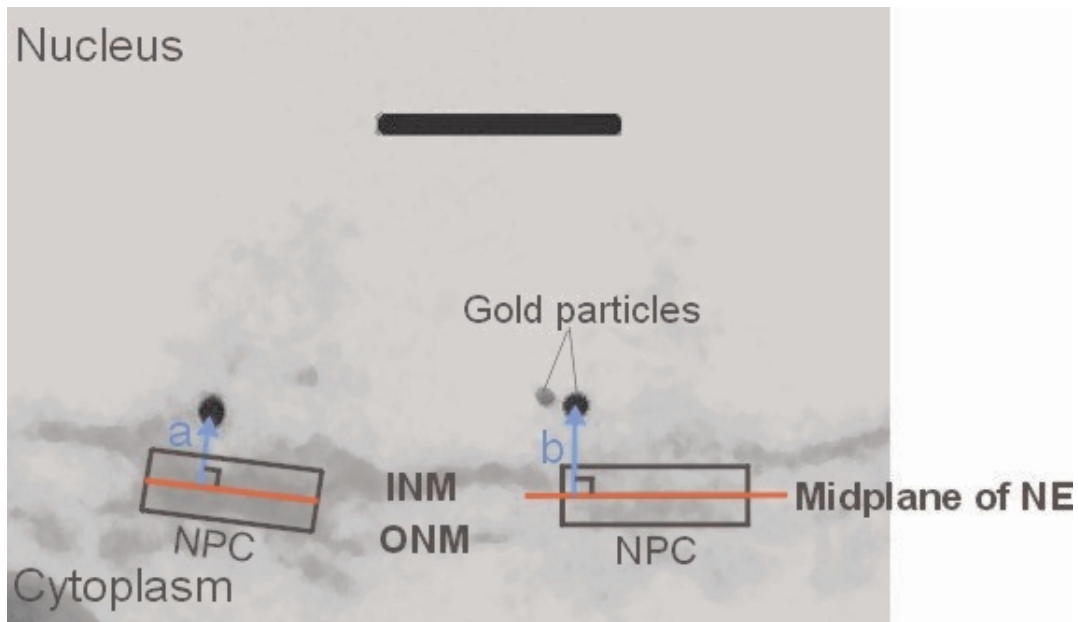
Figure 42: Method for quantifying the localisation of gold-labelled antibodies along the z axis using TEM. Squares of best fit were overlayed onto each NPC in line with the INM and ONM, to identify the midplane of the NE, represented by the red lines. The distance from the midplane of the NE to the centre of the gold was measured at right angles to the midplane, e.g. distance a and distance b. Bar = 100nm.

The two techniques of FEISEM and TEM involve different methods of preparation, which may alter the structure of the NPC and therefore could potentially be incomparable with respect to localisation. To compare the two methods and to show that they can be used in parallel, the gold-labelled anti-Nup153 was localised along the xy axis from selected TEM images portraying cross-sections through the centre of the NPC for comparison with the FEISEM data (figure 43). The TEM images used for quantification were selected to ensure an accurate xy-localisation could be measured. This is because the plane of the section through the NPC can affect the apparent localisation of the gold.
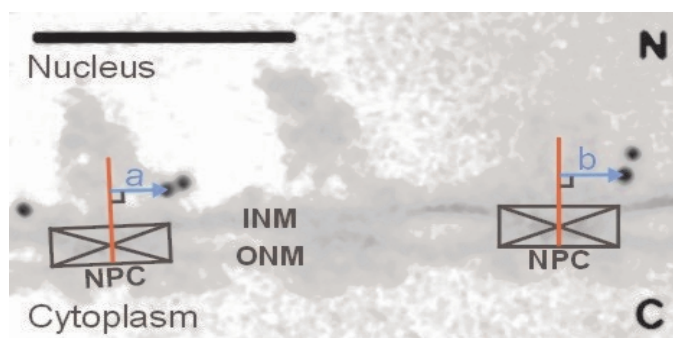

Figure 43: Method for quantifying the localisation of gold-labelled antibodies along the xy axis using TEM. Squares of best fit were placed onto each NPC to identify the centre, which is represented by the red lines. The distance from the centre of the NPC to the centre of the gold was measured parallel to the NE, e.g. distance a and b. Bar = 200nm.

The mean distance of gold-labelled Nup153 from the centre of the NPC measured using FEISEM was 47nm, and using TEM was 48.1nm. The two data sets were compared using statistical analysis. Attempts to normalise the data from TEM images using logarithms was unsuccessful, therefore, a non-parametric test was used to compare the difference between the two samples. The Mann Whitney U test compares the medians of two samples to determine if they are significantly different i.e. come from two different populations. The Mann Whitney-U test revealed no significant difference between FEISEM and TEM, for the localisation of Nup153, P = 0.4149.

6 <u>Literature</u>

Adam, E.J., and S.A. Adam. 1994. Identification of cytosolic factors required for nuclear location sequence-mediated binding to the nuclear envelope. *J. Cell Biol.,* 125:547-55.

Adam, S.A., and L. Gerace. 1991. Cytosolic proteins that specifically bind nuclear location signals are receptors for nuclear import. *Cell,* 66:837-47.

Adam, S.A., R. Sterne-Marr, and L. Gerace. 1992. Nuclear protein import using digitonin-permeabilized cells. *Methods Enzymol.,* 219:97-110.

Aitchison, J.D., and M.P. Rout. 2000. The road to ribosomes. Filling potholes in the export pathway. *J. Cell Biol.,* 151:F23-6.

Akey, C. 1989. Interactions and structure of the nuclear pore complex revealed by cryo-electron microscopy. *J. Cell Biol.,* 109:955-70.

Akey, C.W., and D.S. Goldfarb. 1989. Protein import through the nuclear pore complex is a multistep process. *J. Cell Biol.,* 109:971-82.

Akey, C.W., and M. Radermacher. 1993. Architecture of the *Xenopus* nuclear pore complex revealed by three-dimensional cryo-electron microscopy. *J. Cell Biol.,* 122:1-19.

Alberts, B., Bray, D., Lewis, J., Raff, M., Roberts, K. and J. Watson. 1994. Molecular Biology of the Cell. Garland Publishing, New York.

Allen, T.D., J.M. Cronshaw, S. Bagley, E. Kiseleva, and M.W. Goldberg. 2000. The nuclear pore complex: mediator of translocation between nucleus and cytoplasm. *J. Cell Sci.,*113:1651-9.

Arts, G.J., M. Fornerod, and I.W. Mattaj. 1998a. Identification of a nuclear export receptor for tRNA. *Curr. Biol.,* 8:305-14.

Arts, G.J., S. Kuersten, P. Romby, B. Ehresmann, and I.W. Mattaj. 1998b. The role of exportin-t in selective nuclear export of mature tRNAs. *EMBO J.*, 17:7430-41.

Askjaer, P., A. Bachi, M. Wilm, F.R. Bischoff, D.L. Weeks, V. Ogniewski, M. Ohno, C. Niehrs, J. Kjems, I.W. Mattaj, and M. Fornerod. 1999. RanGTP-regulated interactions of CRM1 with nucleoporins and a shuttling DEAD-box helicase. *Mol. Cell Biol.*,19:6276-85.

Bachi, A., I.C. Braun, J.P. Rodrigues, N. Pante, K. Ribbeck, C. von Kobbe, U. Kutay, M. Wilm, D. Görlich, M. Carmo-Fonseca, and E. Izaurralde. 2000. The C-terminal domain of TAP interacts with the nuclear pore complex and promotes export of specific CTE-bearing RNA substrates. *RNA,* 6:136-58.

Bailer, S.M., C. Balduf, J. Katahira, A. Podtelejnikov, C. Rollenhagen, M. Mann, N. Pante, and E. Hurt. 2000. Nup116p associates with the Nup82p-Nsp1p-Nup159p nucleoporin complex. *J. Biol. Chem.,* 275:23540-8.

Bastos, R., A. Lin, M. Enarson, and B. Burke. 1996. Targeting and function in mRNA export of nuclear pore complex protein Nup153. *J. Cell Biol.,* 134:1141-56.

Bastos, R., L. Ribas de Pouplana, M. Enarson, K. Bodoor, and B. Burke. 1997. Nup84, a novel nucleoporin that is associated with CAN/Nup214 on the cytoplasmic face of the nuclear pore complex. *J. Cell Biol.,* 137:989-1000.

Beaudouin, J., D. Gerlich, N. Daigle, R. Eils, and J. Ellenberg. 2002. Nuclear envelope breakdown proceeds by microtubule-induced tearing of the lamina. *Cell,* 108:83-96.

Becker, J., F. Melchior, V. Gerke, F.R. Bischoff, H. Ponstingl, and A. Wittinghofer. 1995. RNA1 encodes a GTPase-activating protein specific for Gsp1p, the Ran/TC4 homologue of *Saccharomyces cerevisiae. J. Biol. Chem.,* 270:11860-5.

Belgareh, N., G. Rabut, S.W. Bai, M. van Overbeek, J. Beaudouin, N. Daigle, O.V. Zatsepina, F. Pasteau, V. Labas, M. Fromont-Racine, J. Ellenberg, and V. Doye. 2001. An evolutionarily conserved NPC subcomplex, which redistributes in part to kinetochores in mammalian cells. *J. Cell Biol.,* 154:1147-60.

Belgareh, N., C. Snay-Hodge, F. Pasteau, S. Dagher, C.N. Cole, and V. Doye. 1998. Functional characterization of a Nup159p-containing nuclear pore subcomplex. *Mol. Biol. Cell,* 9:3475-92.

Ben-Efraim, I., and L. Gerace. 2001. Gradient of increasing affinity of importin beta for nucleoporins along the pathway of nuclear import. *J. Cell Biol*., 152:411-7.

Bischoff, F.R., C. Klebe, J. Kretschmer, A. Wittinghofer, and H. Ponstingl. 1994. RanGAP1 induces GTPase activity of nuclear Ras-related Ran. *Proc. Natl. Acad. Sci. U S A,* 91:2587-91.

Bischoff, F.R., H. Krebber, E. Smirnova, W. Dong, and H. Ponstingl. 1995. Co-activation of RanGTPase and inhibition of GTP dissociation by Ran- GTP binding protein RanBP1. *EMBO J.,* 14:705-15.

Bischoff, F.R., and H. Ponstingl. 1991. Catalysis of guanine nucleotide exchange on Ran by the mitotic regulator RCC1. *Nature,* 354:80-2.

Blow, J.J., and R.A. Laskey. 1986. Initiation of DNA replication in nuclei and purified DNA by a cell-free extract of *Xenopus* eggs. *Cell,* 47:577-87.

Bodoor, K., S. Shaikh, D. Salina, W.H. Raharjo, R. Bastos, M. Lohka, and B. Burke. 1999. Sequential recruitment of NPC proteins to the nuclear periphery at the end of mitosis. *J. Cell Sci.,* 112:2253-64.

Borrow, J., A.M. Shearman, V.P. Stanton, Jr., R. Becher, T. Collins, A.J. Williams, I. Dube, F. Katz, Y.L. Kwong, C. Morris, K. Ohyashiki, K. Toyama, J. Rowley, and D.E. Housman. 1996. The t(7;11)(p15;p15) translocation in acute myeloid leukaemia fuses the genes for nucleoporin NUP98 and class I homeoprotein HOXA9. *Nat. Genet.,* 12:159-67.

Burke, B. 2001. The nuclear envelope: filling in gaps. *Nat. Cell Biol*., 3:E273-4.

Burke, B., and L. Gerace. 1986. A cell free system to study reassembly of the nuclear envelope at the end of mitosis. *Cell,* 44:639-52.

Cai, M., Y. Huang, R. Ghirlando, K.L. Wilson, R. Craigie, and G.M. Clore. 2001a. Solution structure of the constant region of nuclear envelope protein LAP2 reveals two LEM-domain structures: one binds BAF and the other binds DNA. *EMBO J.,* 20:4399-407.

Cai, S.T., F.L. Zhou, and J.Z. Zhang. 1997. Immunogold labeling electron microscopy showing vimentin filament anchored on nuclear pore complex. *Shi Yan Sheng Wu Xue Bao*, 30:193-9.

Cai, Y., B.B. Singh, A. Aslanukov, H. Zhao, and P.A. Ferreira. 2001b. The docking of kinesins, KIF5B and KIF5C, to Ran-binding protein 2 (RanBP2) is mediated via a novel RanBP2 domain. *J. Biol. Chem.,* 276:41594-602.

Carazo-Salas, R.E., O.J. Gruss, I.W. Mattaj, and E. Karsenti. 2001. Ran-GTP coordinates regulation of microtubule nucleation and dynamics during mitotic-spindle assembly. *Nat. Cell Biol.,* 3:228-34.

Carmo-Fonseca, M., L. Mendes-Soares, and I. Campos. 2000. To be or not to be in the nucleolus. *Nat. Cell Biol.,* 2:E107-12.

Chi, N.C., E.J. Adam, G.D. Visser, and S.A. Adam. 1996. RanBP1 stabilizes the interaction of Ran with p97 nuclear protein import. *J. Cell Biol.,* 135:559-69.

Chook, Y.M., and G. Blobel. 1999. Structure of the nuclear transport complex karyopherin-beta2-Ran x GppNHp. *Nature,* 399:230-7.

Cingolani, G., C. Petosa, K. Weis, and C.W. Müller. 1999. Structure of importin-beta bound to the IBB domain of importin-alpha. *Nature,* 399:221-9.

Clarke, P.R., and C. Zhang. 2001. Ran GTPase: a master regulator of nuclear structure and function during the eukaryotic cell division cycle? *Trends Cell Biol.,* 11:366-71.

Cole, C.N. 2000. mRNA export: the long and winding road. *Nat. Cell Biol.,* 2:E55-8.

Collas, P., and D. Poccia. 1998. Methods for studying *in vitro* assembly of male pronuclei using oocyte extracts from marine invertebrates: sea urchins and surf clams. *Methods Cell Biol.,* 53:417-52.

Conti, E., and E. Izaurralde. 2001. Nucleocytoplasmic transport enters the atomic age. *Curr. Opin. Cell Biol.,* 13:310-9.

Conti, E., M. Uy, L. Leighton, G. Blobel, and J. Kuriyan. 1998. Crystallographic analysis of the recognition of a nuclear localization signal by the nuclear import factor karyopherin alpha. *Cell,* 94:193-204.

Cordes, V.C., H.R. Rackwitz, and S. Reidenbach. 1997a. Mediators of nuclear protein import target karyophilic proteins to pore complexes of cytoplasmic annulate lamellae. *Exp. Cell Res.,* 237:419-33.

Cordes, V.C., S. Reidenbach, and W.W. Franke. 1995. High content of a nuclear pore complex protein in cytoplasmic annulate lamellae of *Xenopus* oocytes. *Eur. J. Cell Biol.,* 68:240-55.

Cordes, V.C., S. Reidenbach, A. Kohler, N. Stuurman, R. van Driel, and W.W. Franke. 1993. Intranuclear filaments containing a nuclear pore complex protein. *J. Cell Biol.,* 123:1333-44.

Cordes, V.C., S. Reidenbach, H.R. Rackwitz, and W.W. Franke. 1997b. Identification of protein p270/Tpr as a constitutive component of the nuclear pore complex-attached intranuclear filaments. *J. Cell Biol.,* 136:515-29.

Cremer, T., and C. Cremer. 2001. Chromosome territories, nuclear architecture and gene regulation in mammalian cells. *Nat. Rev. Genet.,* 2:292-301.

Dabauvalle, M.C., B. Schulz, U. Scheer, and R. Peters. 1988. Inhibition of nuclear accumulation of karyophilic proteins in living cells by microinjection of the lectin wheat germ agglutinin. *Exp. Cell Res.,* 174:291-6.

Daigle, N., J. Beaudouin, L. Hartnell, G. Imreh, E. Hallberg, J. Lippincott-Schwartz, and J. Ellenberg. 2001. Nuclear pore complexes form immobile networks and have a very low turnover in live mammalian cells. *J. Cell Biol.,* 154:71-84.

Davis, L.I., and G. Blobel. 1987. Nuclear pore complex contains a family of glycoproteins that includes p62: glycosylation through a previously unidentified cellular pathway. *Proc. Natl. Acad. Sci. U S A,* 84:7552-6.

de Noronha, C.M., M.P. Sherman, H.W. Lin, M.V. Cavrois, R.D. Moir, R.D. Goldman, and W.C. Greene. 2001. Dynamic disruptions in nuclear envelope architecture and integrity induced by HIV-1 Vpr. *Science,* 294:1105-8.

Del Priore, V., C. Heath, C. Snay, A. MacMillan, L. Gorsch, S. Dagher, and C. Cole. 1997. A structure/function analysis of Rat7p/Nup159p, an essential nucleoporin of Saccharomyces cerevisiae. *J. Cell Sci.,* 110:2987-99.

Delphin, C., T. Guan, F. Melchior, and L. Gerace. 1997. RanGTP targets p97 to RanBP2, a filamentous protein localized at the cytoplasmic periphery of the nuclear pore complex. *Mol. Biol. Cell,* 8:2379-90.

Desai, A., A. Murray, T.J. Mitchison, and C.E. Walczak. 1999. The use of *Xenopus* egg extracts to study mitotic spindle assembly and function *in vitro*. *Methods Cell Biol.,* 61:385-412.

Dimaano, C., J.R. Ball, A.J. Prunuske, and K.S. Ullman. 2001. RNA association defines a functionally conserved domain in the nuclear pore protein Nup153. *J. Biol. Chem.,* 276:45349-57.

Doye, V., and E. Hurt. 1997. From nucleoporins to nuclear pore complexes. *Curr. Opin. Cell Biol.,* 9:401-11.

Dreier, L., and T.A. Rapoport. 2000. *In vitro* formation of the endoplasmic reticulum occurs independently of microtubules by a controlled fusion reaction. *J. Cell Biol.,* 148:883-98.

Drummond, S., P. Ferrigno, C. Lyon, J. Murphy, M. Goldberg, T. Allen, C. Smythe, and C.J. Hutchison. 1999. Temporal differences in the appearance of NEP-B78 and an LBR-like protein during *Xenopus* nuclear envelope reassembly reflect the ordered recruitment of functionally discrete vesicle types. *J. Cell Biol.,* 144:225-40.

Dundr, M., and T. Misteli. 2001. Functional architecture in the cell nucleus. *Biochem. J.,* 356:297-310.

Ellenberg, J., E.D. Siggia, J.E. Moreira, C.L. Smith, J.F. Presley, H.J. Worman, and J. Lippincott-Schwartz. 1997. Nuclear membrane dynamics and reassembly in living cells: targeting of an inner nuclear membrane protein in interphase and mitosis. *J. Cell Biol.,* 138:1193-206.

Enarson, P., M. Enarson, R. Bastos, and B. Burke. 1998. Amino-terminal sequences that direct nucleoporin Nup153 to the inner surface of the nuclear envelope. *Chromosoma,* 107:228-36.

Englmeier, L., J.C. Olivo, and I.W. Mattaj. 1999. Receptor-mediated substrate translocation through the nuclear pore complex without nucleotide triphosphate hydrolysis. *Curr. Biol.,* 9:30-41.

Fabre, E., and E. Hurt. 1997. Yeast genetics to dissect the nuclear pore complex and nucleocytoplasmic trafficking. *Annu. Rev. Genet.,* 31:277-313.

Featherstone, C., M.K. Darby, and L. Gerace. 1988. A monoclonal antibody against the nuclear pore complex inhibits nucleocytoplasmic transport of protein and RNA *in vivo*. *J. Cell Biol.,* 107:1289-97.

Feldherr, C.M., E. Kallenbach, and N. Schultz. 1984. Movement of a karyophilic protein through the nuclear pores of oocytes. *J. Cell Biol.,* 99:2216-22.

Ferreira, P.A., T.A. Nakayama, W.L. Pak, and G.H. Travis. 1996. Cyclophilin-related protein RanBP2 acts as chaperone for red/green opsin. *Nature,* 383:637-40.

Ferreira, P.A., T.A. Nakayama, and G.H. Travis. 1997. Interconversion of red opsin isoforms by the cyclophilin-related chaperone protein Ran-binding protein 2. *Proc. Natl. Acad. Sci. U S A,* 94:1556-61.

Ferreira, P.A., C. Yunfei, D. Schick, and R. Roepman. 1998. The cyclophilin-like domain mediates the association of Ran-binding protein 2 with subunits of the 19 S regulatory complex of the proteasome. *J. Biol. Chem.,* 273:24676-82.

Finlay, D.R., and D.J. Forbes. 1990. Reconstitution of biochemically altered nuclear pores: transport can be eliminated and restored. *Cell,* 60:17-29.

Finlay, D.R., E. Meier, P. Bradley, J. Horecka, and D.J. Forbes. 1991. A complex of nuclear pore proteins required for pore function. *J. Cell Biol.,* 114:169-83.

Finlay, D.R., D.D. Newmeyer, T.M. Price, and D.J. Forbes. 1987. Inhibition of *in vitro* nuclear transport by a lectin that binds to nuclear pores. *J. Cell Biol.,* 104:189-200.

Fontoura, B.M., S. Dales, G. Blobel, and H. Zhong. 2001. The nucleoporin Nup98 associates with the intranuclear filamentous protein network of TPR. *Proc. Natl. Acad. Sci. U S A,* 98:3208-13.

Fornerod, M., J. Boer, S. van Baal, M. Jaegle, M. von Lindern, K.G. Murti, D. Davis, J. Bonten, A. Buijs, and G. Grosveld. 1995. Relocation of the carboxyterminal part of CAN from the nuclear envelope to the nucleus as a result of leukemia-specific chromosome rearrangements. *Oncogene,* 10:1739-48.

Fornerod, M., M. Ohno, M. Yoshida, and I.W. Mattaj. 1997a. CRM1 is an export receptor for leucine-rich nuclear export signals. *Cell,* 90:1051-60.

Fornerod, M., J. van Deursen, S. van Baal, A. Reynolds, D. Davis, K.G. Murti, J. Fransen, and G. Grosveld. 1997b. The human homologue of yeast CRM1 is in a dynamic subcomplex with CAN/Nup214 and a novel nuclear pore component Nup88. *EMBO J.,* 16:807-16.

Franke, W.W. 1974. Structure, biochemistry, and functions of the nuclear envelope. *Int. Rev. Cytol.*, Suppl:71-236.

Frosst, P., T. Guan, C. Subauste, K. Hahn, and L. Gerace. 2002. Tpr is localized within the nuclear basket of the pore complex and has a role in nuclear protein export. *J. Cell Biol.,* 156:617-30.

Gall, J.G. 2000. Cajal bodies: the first 100 years. *Annu. Rev. Cell Dev. Biol.,* 16:273-300.

Galy, V., J.C. Olivo-Marin, H. Scherthan, V. Doye, N. Rascalou, and U. Nehrbass. 2000. Nuclear pore complexes in the organization of silent telomeric chromatin. *Nature,* 403:108-12.

Gerace, L., and G. Blobel. 1980. The nuclear envelope lamina is reversibly depolymerized during mitosis. *Cell,* 19:277-87.

Goldberg, M.W., and T.D. Allen. 1993. The nuclear pore complex: three-dimensional surface structure revealed by field emission, in-lens scanning electron microscopy, with underlying structure uncovered by proteolysis. *J. Cell Sci.,* 106:261-74.

Goldberg, M.W., and T.D. Allen. 1996. The nuclear pore complex and lamina: three-dimensional structures and interactions determined by field emission in-lens scanning electron microscopy. *J. Mol. Biol.,* 257:848-65.

Goldberg, M.W., J.J. Blow, and T.D. Allen. 1992. The use of field emission in-lens scanning electron microscopy to study the steps of assembly of the nuclear envelope *in vitro*. *J. Struct. Biol.,* 108:257-68.

Görlich, D., S. Kostka, R. Kraft, C. Dingwall, R.A. Laskey, E. Hartmann, and S. Prehn. 1995a. Two different subunits of importin cooperate to recognize nuclear localization signals and bind them to the nuclear envelope. *Curr. Biol.,* 5:383-92.

Görlich, D., and U. Kutay. 1999. Transport between the cell nucleus and the cytoplasm. *Annu. Rev. Biochem.,* 15:607-60.

Görlich, D., and R.A. Laskey. 1995. Roles of importin in nuclear protein import. *Cold Spring Harb. Symp. Quant. Biol.,* 60:695-9.

Görlich, D., N. Pante, U. Kutay, U. Aebi, and F.R. Bischoff. 1996. Identification of different roles for RanGDP and RanGTP in nuclear protein import. *EMBO J.,* 15:5584-94.

Görlich, D., S. Prehn, R.A. Laskey, and E. Hartmann. 1994. Isolation of a protein that is essential for the first step of nuclear protein import. *Cell,* 79:767-78.

Görlich, D., F. Vogel, A.D. Mills, E. Hartmann, and R.A. Laskey. 1995b. Distinct functions for the two importin subunits in nuclear protein import. *Nature,* 377:246-8.

Grandi, P., T. Dang, N. Pane, A. Shevchenko, M. Mann, D. Forbes, and E. Hurt. 1997. Nup93, a vertebrate homologue of yeast Nic96p, forms a complex with a novel 205-kDa protein and is required for correct nuclear pore assembly. *Mol. Biol. Cell,* 8:2017-38.

Grandi, P., V. Doye, and E.C. Hurt. 1993. Purification of NSP1 reveals complex formation with 'GLFG' nucleoporins and a novel nuclear pore protein NIC96. *EMBO J.,* 12:3061-71.

Grandi, P., N. Schlaich, H. Tekotte, and E.C. Hurt. 1995. Functional interaction of Nic96p with a core nucleoporin complex consisting of Nsp1p, Nup49p and a novel protein Nup57p. *EMBO J.,* 14:76-87.

Griffis, E.R., N. Altan, J. Lippincott-Schwartz, and M.A. Powers. 2002. Nup98 is a mobile nucleoporin with transcription-dependent dynamics. *Mol. Biol. Cell,* 13:1282-97.

Grote, M., U. Kubitscheck, R. Reichelt, and R. Peters. 1995. Mapping of nucleoporins to the centre of the nuclear pore complex by post-embedding immunogold electron microscopy. *J. Cell Sci.,* 108:2963-72.

Gruss, O.J., R.E. Carazo-Salas, C.A. Schatz, G. Guarguaglini, J. Kast, M. Wilm, N. Le Bot, I. Vernos, E. Karsenti, and I.W. Mattaj. 2001. Ran induces spindle assembly by reversing the inhibitory effect of importin alpha on TPX2 activity. *Cell,* 104:83-93.

Gruter, P., C. Tabernero, C. von Kobbe, C. Schmitt, C. Saavedra, A. Bachi, M. Wilm, B.K. Felber, and E. Izaurralde. 1998. TAP, the human homolog of Mex67p, mediates CTE-dependent RNA export from the nucleus. *Mol. Cell,* 1:649-59.

Gurdon, J.B. 1976. Injected nuclei in frog oocytes: fate, enlargement, and chromatin dispersal. *J. Embryol. Exp. Morphol.,* 36:523-40.

Haraguchi, T., T. Koujin, T. Hayakawa, T. Kaneda, C. Tsutsumi, N. Imamoto, C. Akazawa, J. Sukegawa, Y. Yoneda, and Y. Hiraoka. 2000. Live fluorescence

imaging reveals early recruitment of emerin, LBR, RanBP2, and Nup153 to reforming functional nuclear envelopes. *J. Cell Sci.,* 113:779-94.

Hetzer, M., D. Bilbao-Cortes, T.C. Walther, O.J. Gruss, and I.W. Mattaj. 2000. GTP hydrolysis by Ran is required for nuclear envelope assembly. *Mol. Cell.,* 5:1013-24.

Hetzer, M., and I.W. Mattaj. 2000. An ATP-dependent, Ran-independent mechanism for nuclear import of the U1A and U2B" spliceosome proteins. *J. Cell Biol.,* 148:293-303.

Hetzer, M., H.H. Meyer, T.C. Walther, D. Bilbao-Cortes, G. Warren, and I.W. Mattaj. 2001. Distinct AAA-ATPase p97 complexes function in discrete steps of nuclear assembly. *Nat. Cell Biol.,* 3:1086-91.

Hinshaw, J.E. 1994. Architecture of the nuclear pore complex and its involvement in nucleocytoplasmic transport. *Biochem. Pharmacol.,* 47:15-20.

Ho, A.K., T.X. Shen, K.J. Ryan, E. Kiseleva, M.A. Levy, T.D. Allen, and S.R. Wente. 2000. Assembly and preferential localization of Nup116p on the cytoplasmic face of the nuclear pore complex by interaction with Nup82p. *Mol. Cell Biol.,* 20:5736-48.

Holmer, L., and H.J. Worman. 2001. Inner nuclear membrane proteins: functions and targeting. *Cell Mol. Life Sci.,* 58:1741-7.

Huber, J., U. Cronshagen, M. Kadokura, C. Marshallsay, T. Wada, M. Sekine, and R. Lührmann. 1998. Snurportin1, an m3G-cap-specific nuclear import receptor with a novel domain structure. *EMBO J.,* 17:4114-26.

Huber, J., A. Dickmanns, and R. Lührmann. 2002. The importin-beta binding domain of snurportin1 is responsible for the Ran- and energy-independent nuclear import of spliceosomal U snRNPs *in vitro. J. Cell Biol.,* 156:467-79.

Hurwitz, M.E., C. Strambio-de-Castillia, and G. Blobel. 1998. Two yeast nuclear pore complex proteins involved in mRNA export form a cytoplasmically oriented subcomplex. *Proc. Natl. Acad. Sci. U S A,* 95:11241-5.

Imai, N., S. Sasagawa, A. Yamamoto, F. Kikuchi, K. Sekiya, T. Ichimura, S. Omata, and T. Horigome. 1997. Characterization of the binding of nuclear envelope precursor vesicles and chromatin, and purification of the vesicles. *J/ Biochem. (Tokyo)*, 122:1024-33.

Jarmolowski, A., W.C. Boelens, E. Izaurralde, and I.W. Mattaj. 1994. Nuclear export of different classes of RNA is mediated by specific factors. *J. Cell Biol.,* 124:627-35.

Jarnik, M., and U. Aebi. 1991. Toward a more complete 3-D structure of the nuclear pore complex. *J. Struct. Biol.,* 107:291-308.

Jenkins, Y., M. McEntee, K. Weis, and W.C. Greene. 1998. Characterization of HIV-1 vpr nuclear import: analysis of signals and pathways. *J. Cell Biol.,* 143:875-85.

Kaffman, A., N.M. Rank, E.M. O'Neill, L.S. Huang, and E.K. O'Shea. 1998. The receptor Msn5 exports the phosphorylated transcription factor Pho4 out of the nucleus. *Nature,* 396:482-6.

Kalab, P., K. Weis, and R. Heald. 2002. Visualization of a Ran-GTP gradient in interphase and mitotic *Xenopus* egg extracts. *Science,* 295:2452-6.

Kasper, L.H., P.K. Brindle, C.A. Schnabel, C.E. Pritchard, M.L. Cleary, and J.M. van Deursen. 1999. CREB binding protein interacts with nucleoporin-specific FG

repeats that activate transcription and mediate NUP98-HOXA9 oncogenicity. *Mol. Cell Biol.,* 19:764-76.

Kiseleva, E., S. Rutherford, L.M. Cotter, T.D. Allen, and M.W. Goldberg. 2001. Steps of nuclear pore complex disassembly and reassembly during mitosis in early *Drosophila* embryos. *J. Cell Sci.,* 114:3607-18.

Kosova, B., N. Pante, C. Rollenhagen, A. Podtelejnikov, M. Mann, U. Aebi, and E. Hurt. 2000. Mlp2p, a component of nuclear pore attached intranuclear filaments, associates with Nic96p. *J. Biol. Chem.,* 275:343-50.

Kraemer, D., R.W. Wozniak, G. Blobel, and A. Radu. 1994. The human CAN protein, a putative oncogene product associated with myeloid leukemogenesis, is a nuclear pore complex protein that faces the cytoplasm. *Proc. Natl. Acad. Sci. U S A,* 91:1519-23.

Kraemer, D.M., C. Strambio-de-Castillia, G. Blobel, and M.P. Rout. 1995. The essential yeast nucleoporin NUP159 is located on the cytoplasmic side of the nuclear pore complex and serves in karyopherin-mediated binding of transport substrate. *J. Biol. Chem.,* 270:19017-21.

Kroon, E., U. Thorsteinsdottir, N. Mayotte, T. Nakamura, and G. Sauvageau. 2001. NUP98-HOXA9 expression in hemopoietic stem cells induces chronic and acute myeloid leukemias in mice. *EMBO J.,* 20:350-61.

Kuersten, S., M. Ohno, and I.W. Mattaj. 2001. Nucleocytoplasmic transport: Ran, beta and beyond. *Trends Cell Biol.,* 11:497-503.

Kurz, A., S. Lampel, J.E. Nickolenko, J. Bradl, A. Benner, R.M. Zirbel, T. Cremer, and P. Lichter. 1996. Active and inactive genes localize preferentially in the periphery of chromosome territories. *J. Cell Biol.,* 135:1195-205.

Kutay, U., E. Izaurralde, F.R. Bischoff, I.W. Mattaj, and D. Görlich. 1997. Dominant-negative mutants of importin-beta block multiple pathways of import and export through the nuclear pore complex. *EMBO J.,* 16:1153-63.

Kutay, U., G. Lipowsky, E. Izaurralde, F.R. Bischoff, P. Schwarzmaier, E. Hartmann, and D. Görlich. 1998. Identification of a tRNA-specific nuclear export receptor. *Mol. Cell,* 1:359-69.

Le Hir, H., D. Gatfield, E. Izaurralde, and M.J. Moore. 2001. The exon-exon junction complex provides a binding platform for factors involved in mRNA export and nonsense-mediated mRNA decay. *EMBO J.,* 20:4987-97.

Le Hir, H., E. Izaurralde, L.E. Maquat, and M.J. Moore. 2000. The spliceosome deposits multiple proteins 20-24 nucleotides upstream of mRNA exon-exon junctions. *EMBO J.,* 19:6860-9.

Lee, K.K., T. Haraguchi, R.S. Lee, T. Koujin, Y. Hiraoka, and K.L. Wilson. 2001. Distinct functional domains in emerin bind lamin A and DNA-bridging protein BAF. *J. Cell Sci.,* 114:4567-73.

Lenz-Böhme, B., J. Wismar, S. Fuchs, R. Reifegerste, E. Buchner, H. Betz, and B. Schmitt. 1997. Insertional mutation of the *Drosophila* nuclear lamin Dm0 gene results in defective nuclear envelopes, clustering of nuclear pore complexes, and accumulation of annulate lamellae. *J. Cell Biol.,* 137:1001-16.

Liu, J., T.R. Ben-Shahar, D. Riemer, M. Treinin, P. Spann, K. Weber, A. Fire, and Y. Gruenbaum. 2000. Essential roles for *Caenorhabditis elegans* lamin gene in

nuclear organization, cell cycle progression, and spatial organization of nuclear pore complexes. *Mol. Biol. Cell.,* 11:3937-47.

Lohka, M.J. 1988. The reconstitution of nuclear envelopes in cell-free extracts. *Cell Biol. Int. Rep.,* 12:833-48.

Lohka, M.J., and Y. Masui. 1983. Formation *in vitro* of sperm pronuclei and mitotic chromosomes induced by amphibian ooplasmic components. *Science,* 220:719-21.

Lourim, D., and G. Krohne. 1993. Membrane-associated lamins in *Xenopus* egg extracts: identification of two vesicle populations. *J. Cell Biol.,* 123:501-12.

Lourim, D., and G. Krohne. 1998. Chromatin binding and polymerization of the endogenous *Xenopus* egg lamins: the opposing effects of glycogen and ATP. *J. Cell Sci.,* 111:3675-86.

Luo, M.L., Z. Zhou, K. Magni, C. Christoforides, J. Rappsilber, M. Mann, and R. Reed. 2001. Pre-mRNA splicing and mRNA export linked by direct interactions between UAP56 and Aly. *Nature,* 413:644-7.

Macaulay, C., and D.J. Forbes. 1996. Assembly of the nuclear pore: biochemically distinct steps revealed with NEM, GTP gamma S, and BAPTA. *J. Cell Biol.,* 132:5-20.

Macaulay, C., E. Meier, and D.J. Forbes. 1995. Differential mitotic phosphorylation of proteins of the nuclear pore complex. *J. Biol. Chem.,* 270:254-62.

Mahajan, R., C. Delphin, T. Guan, L. Gerace, and F. Melchior. 1997. A small ubiquitin-related polypeptide involved in targeting RanGAP1 to nuclear pore complex protein RanBP2. *Cell,* 88:97-107.

Mansharamani, M., A. Hewetson, and B.S. Chilton. 2001. Cloning and characterization of an atypical Type IV P-type ATPase that binds to the RING motif of RUSH transcription factors. *J. Biol. Chem.,* 276:3641-9.

Matsuoka, Y., M. Takagi, T. Ban, M. Miyazaki, T. Yamamoto, Y. Kondo, and Y. Yoneda. 1999. Identification and characterization of nuclear pore subcomplexes in mitotic extract of human somatic cells. *Biochem. Biophys. Res. Commun.,* 254:417-23.

Mattaj, I.W., and L. Englmeier. 1998. Nucleocytoplasmic transport: the soluble phase. *Annu. Rev. Biochem.,* 67:265-306.

Matunis, M.J., E. Coutavas, and G. Blobel. 1996. A novel ubiquitin-like modification modulates the partitioning of the Ran-GTPase-activating protein RanGAP1 between the cytosol and the nuclear pore complex. *J. Cell Biol.,* 135:1457-70.

Matunis, M.J., J. Wu, and G. Blobel. 1998. SUMO-1 modification and its role in targeting the Ran GTPase-activating protein, RanGAP1, to the nuclear pore complex. *J. Cell Biol.,* 140:499-509.

Maul, G.G. 1977. The nuclear and the cytoplasmic pore complex: structure, dynamics, distribution, and evolution. *Int. Rev. Cytol. Suppl.,* 6:75-186.

Maul, G.G., H.M. Maul, J.E. Scogna, M.W. Lieberman, G.S. Stein, B.Y. Hsu, and T.W. Borun. 1972. Time sequence of nuclear pore formation in phytohemagglutinin-stimulated lymphocytes and in HeLa cells during the cell cycle. *J. Cell Biol.,* 55:433-47.

Maul, G.G., J.W. Price, and M.W. Lieberman. 1971. Formation and distribution of nuclear pore complexes in interphase. *J. Cell Biol.,* 51:405-18.

Meier, J., K.H. Campbell, C.C. Ford, R. Stick, and C.J. Hutchison. 1991. The role of lamin LIII in nuclear assembly and DNA replication, in cell- free extracts of *Xenopus* eggs. *J. Cell Sci.,* 98:271-9.

Melchior, F., and L. Gerace. 1998. Two-way trafficking with Ran. *Trends Cell Biol.,* 8:175-9.

Melchior, F., T. Guan, N. Yokoyama, T. Nishimoto, and L. Gerace. 1995. GTP hydrolysis by Ran occurs at the nuclear pore complex in an early step of protein import. *J. Cell Biol.,* 131:571-81.

Michael, W.M., P.S. Eder, and G. Dreyfuss. 1997. The K nuclear shuttling domain: a novel signal for nuclear import and nuclear export in the hnRNP K protein. *EMBO J.,* 16:3587-98.

Moore, M.S., and G. Blobel. 1992. The two steps of nuclear import, targeting to the nuclear envelope and translocation through the nuclear pore, require different cytosolic factors. *Cell,* 69:939-50.

Moroianu, J., G. Blobel, and A. Radu. 1997. RanGTP-mediated nuclear export of karyopherin alpha involves its interaction with the nucleoporin Nup153. *Proc. Natl. Acad. Sci. U S A,* 94:9699-704.

Müller, S., C. Hoege, G. Pyrowolakis, and S. Jentsch. 2001. SUMO, ubiquitin's mysterious cousin. *Nat. Rev. Mol. Cell Biol.,* 2:202-10.

Nachury, M.V., T.J. Maresca, W.C. Salmon, C.M. Waterman-Storer, R. Heald, and K. Weis. 2001. Importin beta is a mitotic target of the small GTPase Ran in spindle assembly. *Cell,* 104:95-106.

Nachury, M.V., and K. Weis. 1999. The direction of transport through the nuclear pore can be inverted. *Proc. Natl. Acad. Sci. U S A,* 96:9622-7.

Nakamura, T., D.A. Largaespada, M.P. Lee, L.A. Johnson, K. Ohyashiki, K. Toyama, S.J. Chen, C.L. Willman, I.M. Chen, A.P. Feinberg, N.A. Jenkins, N.G. Copeland, and J.D. Shaughnessy, Jr. 1996. Fusion of the nucleoporin gene NUP98 to HOXA9 by the chromosome translocation t(7;11)(p15;p15) in human myeloid leukaemia. *Nat. Genet.,* 12:154-8.

Nakielny, S., S. Shaikh, B. Burke, and G. Dreyfuss. 1999. Nup153 is an M9-containing mobile nucleoporin with a novel Ran-binding domain. *EMBO J.,* 18:1982-95.

Nehrbass, U., E. Fabre, S. Dihlmann, W. Herth, and E.C. Hurt. 1993. Analysis of nucleo-cytoplasmic transport in a thermosensitive mutant of nuclear pore protein NSP1. *Eur. J. Cell Biol.,* 62:1-12.

Newmeyer, D.D., D.R. Finlay, and D.J. Forbes. 1986. *In vitro* transport of a fluorescent nuclear protein and exclusion of non-nuclear proteins. *J. Cell Biol.,* 103:2091-102.

Newmeyer, D.D., and D.J. Forbes. 1988. Nuclear import can be separated into distinct steps *in vitro*: nuclear pore binding and translocation. *Cell,* 52:641-53.

Newmeyer, D.D., and K.L. Wilson. 1991. Egg extracts for nuclear import and nuclear assembly reactions. *Methods Cell Biol.,* 36:607-34.

Ohno, M., M. Fornerod, and I.W. Mattaj. 1998. Nucleocytoplasmic transport: the last 200 nanometers. *Cell,* 92:327-36.

Ohno, M., A. Segref, A. Bachi, M. Wilm, and I.W. Mattaj. 2000. PHAX, a mediator of U snRNA nuclear export whose activity is regulated by phosphorylation. *Cell,* 101:187-98.

Ohtsubo, M., H. Okazaki, and T. Nishimoto. 1989. The RCC1 protein, a regulator for the onset of chromosome condensation locates in the nucleus and binds to DNA. *J. Cell Biol.,* 109:1389-97.

Ottaviano, Y., and L. Gerace. 1985. Phosphorylation of the nuclear lamins during interphase and mitosis. *J. Biol. Chem.,* 260:624-32.

Palacios, I., K. Weis, C. Klebe, I.W. Mattaj, and C. Dingwall. 1996. RAN/TC4 mutants identify a common requirement for snRNP and protein import into the nucleus. *J. Cell Biol.,* 133:485-94.

Pante, N., and U. Aebi. 1996a. Sequential binding of import ligands to distinct nucleopore regions during their nuclear import. *Science,* 273:1729-32.

Pante, N., and U. Aebi. 1996b. Toward the molecular dissection of protein import into nuclei. *Curr. Opin. Cell Biol.,* 8:397-406.

Pante, N., R. Bastos, I. McMorrow, B. Burke, and U. Aebi. 1994. Interactions and three-dimensional localization of a group of nuclear pore complex proteins. *J. Cell Biol.,* 126:603-17.

Patel, S., and M. Latterich. 1998. The AAA team: related ATPases with diverse functions. *Trends Cell Biol.,* 8:65-71.

Philpott, A., G.H. Leno, and R.A. Laskey. 1991. Sperm decondensation in *Xenopus* egg cytoplasm is mediated by nucleoplasmin. *Cell,* 65:569-78.

Pichler, A., A. Gast, J.S. Seeler, A. Dejean, and F. Melchior. 2002. The nucleoporin RanBP2 has SUMO1 E3 ligase activity. *Cell,* 108:109-20.

Plato. 1899. Dialogues of Plato containing the applogyof Socrates, Crito, Phaedo and Protagoras. The Colonial Press, New York.

Pollard, V.W., W.M. Michael, S. Nakielny, M.C. Siomi, F. Wang, and G. Dreyfuss. 1996. A novel receptor-mediated nuclear protein import pathway. *Cell,* 86:985-94.

Powers, M.A., D.J. Forbes, J.E. Dahlberg, and E. Lund. 1997. The vertebrate GLFG nucleoporin, Nup98, is an essential component of multiple RNA export pathways. *J. Cell Biol.,* 136:241-50.

Powers, M.A., C. Macaulay, F.R. Masiarz, and D.J. Forbes. 1995. Reconstituted nuclei depleted of a vertebrate GLFG nuclear pore protein, p97, import but are defective in nuclear growth and replication. *J. Cell Biol.,* 128:721-36.

Pritchard, C.E., M. Fornerod, L.H. Kasper, and J.M. van Deursen. 1999. RAE1 is a shuttling mRNA export factor that binds to a GLEBS-like NUP98 motif at the nuclear pore complex through multiple domains. *J. Cell Biol.,* 145:237-54.

Pu, R.T., and M. Dasso. 1997. The balance of RanBP1 and RCC1 is critical for nuclear assembly and nuclear transport. *Mol. Biol. Cell,* 8:1955-70.

Radu, A., G. Blobel, and M.S. Moore. 1995. Identification of a protein complex that is required for nuclear protein import and mediates docking of import substrate to distinct nucleoporins. *Proc. Natl. Acad. Sci. U S A,* 92:1769-73.

Rakowska, A., T. Danker, S.W. Schneider, and H. Oberleithner. 1998. ATP-Induced shape change of nuclear pores visualized with the atomic force microscope. *J. Membr. Biol.,* 163:129-36.

Reed, R., and E. Hurt. 2002. A conserved mRNA export machinery coupled to pre-mRNA splicing. *Cell,* 108:523-31.

Reed, R., and K. Magni. 2001. A new view of mRNA export: separating the wheat from the chaff. *Nat. Cell Biol.,* 3:E201-4.

Reinsch, S., and P. Gönczy. 1998. Mechanisms of nuclear positioning. *J. Cell Sci.,* 111:2283-95.

Reinsch, S., and E. Karsenti. 1997. Movement of nuclei along microtubules in *Xenopus* egg extracts. *Curr. Biol.,* 7:211-4.

Renault, L., J. Kuhlmann, A. Henkel, and A. Wittinghofer. 2001. Structural basis for guanine nucleotide exchange on Ran by the regulator of chromosome condensation (RCC1). *Cell,* 105:245-55.

Renault, L., N. Nassar, I. Vetter, J. Becker, C. Klebe, M. Roth, and A. Wittinghofer. 1998. The 1.7 A crystal structure of the regulator of chromosome condensation (RCC1) reveals a seven-bladed propeller. *Nature,* 392:97-101.

Rexach, M., and G. Blobel. 1995. Protein import into nuclei: association and dissociation reactions involving transport substrate, transport factors, and nucleoporins. *Cell,* 83:683-92.

Ribbeck, K., and D. Görlich. 2001. Kinetic analysis of translocation through nuclear pore complexes. *EMBO J.,* 20:1320-30.

Ribbeck, K., and D. Görlich. 2002. The permeability barrier of nuclear pore complexes appears to operate via hydrophobic exclusion. *EMBO J.,* in press.

Ribbeck, K., G. Lipowsky, H.M. Kent, M. Stewart, and D. Görlich. 1998. NTF2 mediates nuclear import of Ran. *EMBO J.,* 17:6587-98.

Richardson, W.D., A.D. Mills, S.M. Dilworth, R.A. Laskey, and C. Dingwall. 1988. Nuclear protein migration involves two steps: rapid binding at the nuclear envelope followed by slower translocation through nuclear pores. *Cell,* 52:655-64.

Ris, H. 1991. The three-dimensional structure of the nuclear pore complex as seen by high voltage electron microscopy and high resolution low voltage scanning electron microscopy. *EMSA Bull.,* 21:54-56.

Ris, H. 1997. High-resolution field-emission scanning electron microscopy of nuclear pore complex. *Scanning,* 19:368-75.

Ris, H., and M. Malecki. 1993. High-resolution field emission scanning electron microscope imaging of internal cell structures after Epon extraction from sections: a new approach to correlative ultrastructural and immunocytochemical studies. *J. Struct. Biol.,* 111:148-57.

Rout, M.P., J.D. Aitchison, A. Suprapto, K. Hjertaas, Y. Zhao, and B.T. Chait. 2000. The yeast nuclear pore complex: composition, architecture, and transport mechanism. *J. Cell Biol.,* 148:635-51.

Rutherford, S.A., M.W. Goldberg, and T.D. Allen. 1997. Three-dimensional visualization of the route of protein import: the role of nuclear pore complex substructures. *Exp. Cell Res.,* 232:146-60.

Ryan, K.J., and S.R. Wente. 2000. The nuclear pore complex: a protein machine bridging the nucleus and cytoplasm. *Curr. Opin. Cell Biol.,* 12:361-71.

Saavedra, C., B. Felber, and E. Izaurralde. 1997. The simian retrovirus-1 constitutive transport element, unlike the HIV- 1 RRE, uses factors required for cellular mRNA export. *Curr. Biol.,* 7:619-28.

Saitoh, H., D.B. Sparrow, T. Shiomi, R.T. Pu, T. Nishimoto, T.J. Mohun, and M. Dasso. 1998. Ubc9p and the conjugation of SUMO-1 to RanGAP1 and RanBP2. *Curr. Biol.,* 8:121-4.

Salina, D., K. Bodoor, D.M. Eckley, T.A. Schroer, J.B. Rattner, and B. Burke. 2002. Cytoplasmic dynein as a facilitator of nuclear envelope breakdown. *Cell,* 108:97-107.

Sambrook, J., E.F. Frisch, and T. Maniatis. 1989. Molecular Cloning: A Laboratory Manual. Cold Spring Harbour Laboratory Press, New York.

Sasagawa, S., A. Yamamoto, T. Ichimura, S. Omata, and T. Horigome. 1999. *In vitro* nuclear assembly with affinity-purified nuclear envelope precursor vesicle fractions, PV1 and PV2. *Eur. J. Cell Biol.,* 78:593-600.

Schell, T., A.E. Kulozik, and M.W. Hentze. 2002. Integration of splicing, transport and translation to achieve mRNA quality control by the nonsense-mediated decay pathway. *Genome Biol.,* 3: 1006.1-1006.6.

Schmitt, C., C. von Kobbe, A. Bachi, N. Pante, J.P. Rodrigues, C. Boscheron, G. Rigaut, M. Wilm, B. Seraphin, M. Carmo-Fonseca, and E. Izaurralde. 1999. Dbp5, a DEAD-box protein required for mRNA export, is recruited to the cytoplasmic fibrils of nuclear pore complex via a conserved interaction with CAN/Nup159p. *EMBO J.,* 18:4332-47.

Schwoebel, E.D., B. Talcott, I. Cushman, and M.S. Moore. 1998. Ran-dependent signal-mediated nuclear import does not require GTP hydrolysis by Ran. *J. Biol. Chem.,* 273:35170-5.

Seewald, M.J., C. Korner, A. Wittinghofer, and I.R. Vetter. 2002. RanGAP mediates GTP hydrolysis without an arginine finger. *Nature,* 415:662-6.

Segref, A., K. Sharma, V. Doye, A. Hellwig, J. Huber, R. Lührmann, and E. Hurt. 1997. Mex67p, a novel factor for nuclear mRNA export, binds to both poly(A)+ RNA and nuclear pores. *EMBO J.,* 16:3256-71.

Shah, S., and D.J. Forbes. 1998. Separate nuclear import pathways converge on the nucleoporin Nup153 and can be dissected with dominant-negative inhibitors. *Curr. Biol.,* 8:1376-86.

Shah, S., S. Tugendreich, and D. Forbes. 1998. Major binding sites for the nuclear import receptor are the internal nucleoporin Nup153 and the adjacent nuclear filament protein Tpr. *J. Cell Biol.,* 141:31-49.

Sheehan, M.A., A.D. Mills, A.M. Sleeman, R.A. Laskey, and J.J. Blow. 1988. Steps in the assembly of replication-competent nuclei in a cell-free system from *Xenopus* eggs. *J. Cell Biol.,* 106:1-12.

Shumaker, D.K., K.K. Lee, Y.C. Tanhehco, R. Craigie, and K.L. Wilson. 2001. LAP2 binds to BAF.DNA complexes: requirement for the LEM domain and modulation by variable regions. *EMBO J.,* 20:1754-64.

Singh, B.B., H.H. Patel, R. Roepman, D. Schick, and P.A. Ferreira. 1999. The zinc finger cluster domain of RanBP2 is a specific docking site for the nuclear export factor, exportin-1. *J. Biol. Chem.,* 274:37370-8.

Slot, J.W., and H.J. Geuze. 1984. Goldmarkers for single and double immunolabelling of ultrathin cryosections. *In:* Immunolabelling for Electron Microscopy. J.M. Polak and I.M. Varndess, editors. Elsevier, New York.

Smythe, C., H.E. Jenkins, and C.J. Hutchison. 2000. Incorporation of the nuclear pore basket protein Nup153 into nuclear pore structures is dependent upon lamina assembly: evidence from cell-free extracts of *Xenopus* eggs. *EMBO J.,* 19:3918-31.

Snay-Hodge, C.A., H.V. Colot, A.L. Goldstein, and C.N. Cole. 1998. Dbp5p/Rat8p is a yeast nuclear pore-associated DEAD-box protein essential for RNA export. *EMBO J.,* 17:2663-76.

Spann, T.P., R.D. Moir, A.E. Goldman, R. Stick, and R.D. Goldman. 1997. Disruption of nuclear lamin organization alters the distribution of replication factors and inhibits DNA synthesis. *J. Cell Biol.,* 136:1201-12.

Stoffler, D., B. Fahrenkrog, and U. Aebi. 1999a. The nuclear pore complex: from molecular architecture to functional dynamics. *Curr. Opin. Cell Biol.,* 11:391-401.

Stoffler, D., K.N. Goldie, B. Feja, and U. Aebi. 1999b. Calcium-mediated structural changes of native nuclear pore complexes monitored by time-lapse atomic force microscopy. *J. Mol. Biol.,* 287:741-52.

Strambio-de-Castillia, C., G. Blobel, and M.P. Rout. 1999. Proteins connecting the nuclear pore complex with the nuclear interior. *J. Cell Biol.,* 144:839-55.

Strasser, K., and E. Hurt. 2001. Splicing factor Sub2p is required for nuclear mRNA export through its interaction with Yra1p. *Nature,* 413:648-52.

Sukegawa, J., and G. Blobel. 1993. A nuclear pore complex protein that contains zinc finger motifs, binds DNA, and faces the nucleoplasm. *Cell,* 72:29-38.

Tseng, S.S., P.L. Weaver, Y. Liu, M. Hitomi, A.M. Tartakoff, and T.H. Chang. 1998. Dbp5p, a cytosolic RNA helicase, is required for poly(A)+ RNA export. *EMBO J.,* 17:2651-62.

Ullman, K.S., S. Shah, M.A. Powers, and D.J. Forbes. 1999. The nucleoporin Nup153 plays a critical role in multiple types of nuclear export. *Mol. Biol. Cell,* 10:649-64.

Uv, A.E., P. Roth, N. Xylourgidis, A. Wickberg, R. Cantera, and C. Samakovlis. 2000. members only encodes a *Drosophila* nucleoporin required for rel protein import and immune response activation. *Genes Dev.,* 14:1945-57.

van Deursen, J., J. Boer, L. Kasper, and G. Grosveld. 1996. G2 arrest and impaired nucleocytoplasmic transport in mouse embryos lacking the proto-oncogene CAN/Nup214. *EMBO J.,* 15:5574-83.

Vasu, S., S. Shah, A. Orjalo, M. Park, W.H. Fischer, and D.J. Forbes. 2001. Novel vertebrate nucleoporins Nup133 and Nup160 play a role in mRNA export. *J. Cell Biol.,* 155:339-54.

Vetter, I.R., A. Arndt, U. Kutay, D. Görlich, and A. Wittinghofer. 1999a. Structural view of the Ran-Importin beta interaction at 2.3 A resolution. *Cell,* 97:635-46.

Vetter, I.R., C. Nowak, T. Nishimoto, J. Kuhlmann, and A. Wittinghofer. 1999b. Structure of a Ran-binding domain complexed with Ran bound to a GTP analogue: implications for nuclear transport. *Nature,* 398:39-46.

Walter, J., L. Sun, and J. Newport. 1998. Regulated chromosomal DNA replication in the absence of a nucleus. *Mol. Cell,* 1:519-29.

Wilde, A., S.B. Lizarraga, L. Zhang, C. Wiese, N.R. Gliksman, C.E. Walczak, and Y. Zheng. 2001. Ran stimulates spindle assembly by altering microtubule dynamics and the balance of motor activities. *Nat. Cell Biol.,* 3:221-7.

Wilken, N., J.L. Senecal, U. Scheer, and M.C. Dabauvalle. 1995. Localization of the Ran-GTP binding protein RanBP2 at the cytoplasmic side of the nuclear pore complex. *Eur. J. Cell Biol.,* 68:211-9.

Winey, M., D. Yarar, T.H. Giddings, Jr., and D.N. Mastronarde. 1997. Nuclear pore complex number and distribution throughout the *Saccharomyces cerevisiae* cell cycle by three-dimensional reconstruction from electron micrographs of nuclear envelopes. *Mol. Biol. Cell,* 8:2119-32.

Wong, K.F., C.C. So, and Y.L. Kwong. 1999. Chronic myelomonocytic leukemia with t(7;11)(p15;p15) and NUP98/HOXA9 fusion. *Cancer Genet. Cytogenet.,* 115:70-2.

Worman, H.J., J. Yuan, G. Blobel, and S.D. Georgatos. 1988. A lamin B receptor in the nuclear envelope. *Proc. Natl. Acad. Sci. U S A,* 85:8531-4.

Wu, J., M.J. Matunis, D. Kraemer, G. Blobel, and E. Coutavas. 1995. Nup358, a cytoplasmically exposed nucleoporin with peptide repeats, Ran- GTP binding sites, zinc fingers, a cyclophilin A homologous domain, and a leucine-rich region. *J. Biol. Chem.,* 270:14209-13.

Wu, X., L.H. Kasper, R.T. Mantcheva, G.T. Mantchev, M.J. Springett, and J.M. van Deursen. 2001. Disruption of the FG nucleoporin NUP98 causes selective changes in nuclear pore complex stoichiometry and function. *Proc. Natl. Acad. Sci. U S A,* 98:3191-6.

Yang, J., and S. Kornbluth. 1999. All aboard the cyclin train: subcellular trafficking of cyclins and their CDK partners. *Trends Cell Biol.,* 9:207-10.

Yang, L., T. Guan, and L. Gerace. 1997a. Integral membrane proteins of the nuclear envelope are dispersed throughout the endoplasmic reticulum during mitosis. *J. Cell Biol.,* 137:1199-210.

Yang, L., T. Guan, and L. Gerace. 1997b. Lamin-binding fragment of LAP2 inhibits increase in nuclear volume during the cell cycle and progression into S phase. *J. Cell Biol.,* 139:1077-87.

Yang, Q., M.P. Rout, and C.W. Akey. 1998. Three-dimensional architecture of the isolated yeast nuclear pore complex: functional and evolutionary implications. *Mol. Cell,* 1:223-34.

Yaseen, N.R., and G. Blobel. 1999a. GTP hydrolysis links initiation and termination of nuclear import on the nucleoporin Nup358. *J. Biol. Chem.,* 274:26493-502.

Yaseen, N.R., and G. Blobel. 1999b. Two distinct classes of Ran-binding sites on the nucleoporin Nup358. *Proc. Natl. Acad. Sci. U S A,* 96:5516-21.

Ye, Q., and H.J. Worman. 1996. Interaction between an integral protein of the nuclear envelope inner membrane and human chromodomain proteins homologous to *Drosophila* HP1. *J. Biol. Chem.,* 271:14653-6.

Yokoyama, N., N. Hayashi, T. Seki, N. Pante, T. Ohba, K. Nishii, K. Kuma, T. Hayashida, T. Miyata, U. Aebi, and et al. 1995. A giant nucleopore protein that binds Ran/TC4. *Nature,* 376:184-8.

Yoshida, K., and G. Blobel. 2001. The karyopherin Kap142p/Msn5p mediates nuclear import and nuclear export of different cargo proteins. *J. Cell Biol.,* 152:729-40.

Zhang, C., and P.R. Clarke. 2000. Chromatin-independent nuclear envelope assembly induced by Ran GTPase in *Xenopus* egg extracts. *Science,* 288:1429-32.

Zhang, C., and P.R. Clarke. 2001. Roles of Ran-GTP and Ran-GDP in precursor vesicle recruitment and fusion during nuclear envelope assembly in a human cell-free system. *Curr. Biol.,* 11:208-12.

Zimowska, G., J.P. Aris, and M.R. Paddy. 1997. A *Drosophila* Tpr protein homolog is localized both in the extrachromosomal channel network and to nuclear pore complexes. *J. Cell Sci.,* 110:927-44.

Zolotukhin, A.S., and B.K. Felber. 1999. Nucleoporins Nup98 and Nup214 participate in nuclear export of human immunodeficiency virus type 1 Rev. *J. Virol.,* 73:120-7.

7 <u>Acknowledgments</u>

Zuerst möchte ich meiner Familie, meinem Vater und ganz besonders meiner Mutter danken. Ohne Ihre Hilfe wäre mein Leben nicht so möglich wie es ist und es macht Spass dass es sie gibt. Speziell meine Mutter war und ist einer meiner besten Freunde und immer 100% da...vielen Dank!!

Iain Mattaj was a great supervisor and I am very happy that I had the opportunity to work in his lab. I like to thank him for the right combination of support, incentive, stimulation, challenge, critique and humor!! I thank him not only for the crucial ideas but also giving them at the right moment!

Regine Kahmann danke ich für Ihre Untertützung seit dem Begin meines Studiums. Sie hat mir immer geholfen ist mir mit guten Ratschlägen zur Seite gestanden. Sie hat mir geholfen Enthusiasmus für die Wissenschaft zu entwickeln - und zu behalten. Vielen Dank.

Terry Allen and Martin Goldberg tought me a lot about electron mictroscopy and I want to thank them a lot, also for continuing advice and suggestions. Many thanks also to the members of the Allen lab for their hospitality and help.

Thanks also to my advisors committee, Matthias Hentze and Jan Ellenberg. I also want to thank Jan Ellenberg and Elisa Izaurralde for their helpful discussions and suggestions.
I also want to acknowledge Volker Cordes, Jan van Deursen, Ed Hurt, Georg Krohne and Frauke Melchior who provided reagents and advice

Maarten Fornerod was a fantastic colleague and is a superb friend. I thank him for the time he devoted arguing with me about anything form CAN to Country music! Thanks a lot, it was a joy to work with you and made me enjoy the time in the lab!
Martin Hetzer, vielen Dank für unzählige Gespräche und dein offenes Ohr für " ..und wie schauts?"...einfach für die Österreichischen Momente im Labor. Ohne viele gute Martin tips wäre ich sehr oft noch viel frustrierter gewesen...und damit noch unausstehlicher.
I also want to thank the current and past members of the Mattaj laboratory. Especially Daniel Bilbao-Cortes was never tired to discuss, and always had very helpful advice....and a cigarette. The same is true for Sensai Hito Ohno who I thank for his amazing combination of knowledge and humour! Thanks to Gert-Jan Arts for his initial help with the extract system and later his hospitality. Vincent Galy, thank you for your patience with me my benchchaos the stolen tips, the music......was really fun working next to you!! Scott Kuersten, Thanx for the trips to the Netherlands, Italy, Munich and your great spirit in the lab. Kevin Czaplinski I want to thank for the good music and his bad mood. I want to also thank. Wolfram Antonin, Peter Askjaer, Attila Becksei, Virginie Hamel, Bastian Hülsmann, Puri Fortes, Cerstin Franz, Oliver Gruss, Margy Koffa and Alexandra Segref for the great athmosphere in the lab and the fun we had. A big "thank you" to Victoria Juarez and Pauli Persalmi for their help with animal work.

8 <u>Publications during the time of this thesis</u>

Hinkle, B., Rolls, M., **Walther, T. C**., Stein, P., Ellenberg, J. and M. Terasaki. 2002. Chromosomal association of Ran during meiotic and mitotic divisions, submitted.

*****Walther, T.C**., Pickersgill H., Cordes, V., Goldberg, M. W., Allen, T.D., Mattaj, I. W. and M. Fornerod. 2002. The cytoplasmic filaments of the nuclear pore complex are dispensable for selective nuclear protein import, *J. Cell Biol.,* in press.

Kuersten, S., Arts G.J.,**Walther, T.C**., Englmeier,L. and I.W. Mattaj. 2002. Steady State Nuclear Localization of Exportin-t involves RanGTP binding and two distinct NPC interaction domains, *Mol. Cell Bio.,* in press.

Hetzer, M., Meyer, H.M., **Walther, T.C**., Warren, G. and I.W. Mattaj. 2001. Distinct AAA-ATPase p97 complexes function in discrete steps of nuclear assembly, *Nat. Cell Biol.,* 3: 1086-1091.

*****Walther, T.C**., Fornerod, M., Pickersgill, H., Goldberg, M., Allen, T.D. and I.W. Mattaj. 2001. The nucleoporin Nup153 is required for in nuclear pore basket formation, nuclear pore complex anchoring and Import of a Subset of Nuclear proteins, *EMBO J.,* 20: 5703-5714.

Hetzer, M., Bilbao-Cortes, D., **Walther, T.C.**, Gruss, O.J., and I.W. Mattaj. 2000. GTP hydrolysis by Ran is required for membrane fusion in nuclear envelope assembly. *Mol. Cell.,* 5: 1013-1024.

Walther, T.C. and J. Kennell. 1999. Linear mitochondrial plasmids of F. oxysporum are novel, telomere-like retroelements. *Mol. Cell,* 4: 229-238.

Publications derived directly from this thesis are indicated by *****

9 **Curriculum vitae**

Particulars: Tobias C. Walther; born 16. 01 1973 in Munich, Germany; parents: Elfriede Walther-Kuffer and Ludwig Walther.

Education and scientific experience:

2000- collaboration with Prof. M. Terasaki (Univ. of Conneticut) on the dynamic localisation of the Ran GTPase during cell cycle.

1999- collaboration with Prof. T.D. Allen (Paterson Research Institute, Manchester) on the ultrastructure of the NPC; with Dr. V. Doye (Inst. Pasteur, Paris) and Dr. M. Fornerod (Netherlands Cancer Inst., Amsterdam) on the function of nucleoporins.

1998– PhD thesis in Dr. I.W. Mattaj's laboratory at the European Molecular Biology Laboratory (EMBL), Heidelberg.

1998 Diploma in biology, genetics, cell biology from Ludwig-Maximilians-Univ., Munich with distinction (1,0); Diploma thesis: *In-vivo* analyses of target sequences of the b-heterodimer of *Ustilago maydis* (1,0); done in the laboratory of Prof. R. Kahmann (Ludwig-Maximilians-Univ., Munich).

1997 internship with Prof. J. Kennell (Southern Methodist Univ., Dallas, Tx).

1995-8 diverse internships in the labs of Prof. R. Kahmann and at the Max Planck Inst. for Biochemistry (Martinsried).

1995 Prediploma in Chemistry and Biology.

1993 Prediploma in Political Science, Economics and Law.

1992 Abitur in Munich.

Scholarships:

2000 travel fellowships form Smith-Kline Beecham Foundation and the American Society for Cell Biology (ASCB).

1998- 3 year EMBL fellowship for the pursuit of Ph.D. studies.

1997 German academic exchange service fellowship for an internship in Prof. J. Kennell's laboratory.

1996-1998 Member of the Studienstiftung des dt. Volkes.

1994 German Ministry of Foreign Affairs, sponsorship for the 1994 Model United Nations in New York.